

Band 4

Göttinger Forstwissenschaften



Zhuo Feng

Partitioning of atmospheric nitrogen
under long-term reduced
atmospheric deposition conditions
in a Norway spruce forest ecosystem



Universitätsverlag Göttingen

Zhuo Feng

Partitioning of atmospheric nitrogen under long-term reduced atmospheric deposition conditions in a Norway spruce forest ecosystem

This work is licensed under the [Creative Commons](#) License 3.0 “by-nd”, allowing you to download, distribute and print the document in a few copies for private or educational use, given that the document stays unchanged and the creator is mentioned. Commercial use is not covered by the licence.



Erschienen als Band 4 in der Reihe „Göttinger Forstwissenschaften“ im
Universitätsverlag Göttingen 2010

Zhuo Feng

Partitioning of atmospheric
nitrogen under long-term
reduced atmospheric
deposition conditions in a
Norway spruce forest
ecosystem

Göttinger Forstwissenschaften
Band 4



Universitätsverlag Göttingen
2010

Bibliographische Information der Deutschen Nationalbibliothek

Die Deutsche Nationalbibliothek verzeichnet diese Publikation in der Deutschen Nationalbibliographie; detaillierte bibliographische Daten sind im Internet über <http://dnb.ddb.de> abrufbar.

Global Forest Decimal Classification: GFDC 114.52

Herausgeber der Reihe

Prof. Dr. Christian Ammer
Prof. Dr. Hermann Spellmann
Prof. Dr. Friedrich Beese
Prof. Dr. Stefan Schütz

Schriftleiter

Dr. Norbert Bartsch (n.bartsch@forst.uni-goettingen.de)

Anschrift der Autorin

Dr. Zhuo Feng
Georg-August-Universität
Abteilung Ökopedologie der gemäßigten Zonen
Büsgenweg 2, 37077 Göttingen

Dissertation Universität Göttingen 2010

Gutachter: Professor Dr. Norbert Lamersdorf

Professor Dr. Christian Ammer

Tag der mündlichen Prüfung: 10. Juni 2009

This work is protected by German Intellectual Property Right Law.

It is also available as an Open Access version through the publisher's homepage and the Online Catalogue of the State and University Library of Goettingen (<http://www.sub.uni-goettingen.de>). Users of the free online version are invited to read, download and distribute it. Users may also print a small number for educational or private use. However they may not sell print versions of the online book.

Satz und Layout: Zhuo Feng, Norbert Bartsch

Umschlaggestaltung: Wolfgang Tambour, Margo Bargheer

Titelabbildung: Ausschnitt der Dachkonstruktion des Dachprojektes im Solling

Rückenabbildung: Fichtenkronen oberhalb der Dachkonstruktion des Dachprojektes im Solling (Fotos: Forschungszentrum Waldökosysteme)

© 2010 Universitätsverlag Göttingen

<http://univerlag.uni-goettingen.de>

ISBN: 978-3-941875-81-4

ISSN: 1867-6731

Preface

I am greatly indebted to Prof. Dr. Norbert Lamersdorf for offering me the opportunity to work on this very interesting DFG project as a PhD student. He gave me strong support in many ways from sampling to analyse, to correction of grammatical errors and many more. I owe thanks to him from the bottom of my heart for his impressive kindness, great patience and continuous effort. I am grateful to Professor Dr. Christian Ammer for accepting to be co-referee and to Professor Dr. Gode Gravenhorst for accepting to be examiner.

I am full of gratitude to Dr. Rainer Brumme for his friendliness, guidance and considerate help. In particular, many constructive discussions based on his prolific knowledge are of great benefit to me.

My sincere and grateful thanks are given to Dr. Marife Corre for her trust and introducing me to this DFG project. I thank her also for generously allowing me to share her extensive experiences in ^{15}N diffusion method and for fruitful advices as well as motivational encouragement.

I appreciate Dr. Bettina John and Tamon Yamashita for the introduction of density fractionation procedure, Dr. Markus Lemeke for the cooperation in density fractionation experiment, Dr. Werne Borcken for the supply of fine root samples and Dr. Yijun Xu for the supply of seepage flow rate. I am grateful to Dr. Gabor Kovac, Dr. Seyed Mohammad Hojjati, especially to Dirk Böttger and Heinz Zimmer, for the help in the field work.

Special thanks are given to all technical assistance in the central laboratory as well as in the centre for stable isotope research and analysis for the measure of numerous probes. Thanks are also given to Dr. Jürgen Prenzel and Manfred Lindheim for the help in computer. Gratitude is extended to all other colleagues for the friendly atmosphere in the institute.

I appreciate deeply my family: my husband - Haijun Yang - for his love, encouragement, support and help during the study; my lovely son - Andi - for bringing me so much happiness; my parents and parents-in-law for looking after my son during the dissertation preparation.

Finally, sincere thanks are given to Deutsche Forschungsgesellschaft (DFG) for the financial support of the study.

Contents

Tables	IX
Figures	XI
Abbreviations and Acronyms.....	XIII
1 Introduction.....	1
1.1 N input to terrestrial ecosystem	1
1.2 Impact of elevated N input on temperate forest ecosystems	3
1.3 Distribution of N input among forest ecosystems	4
1.4 SOM	5
1.4.1 SOM stability	5
1.4.2 SOM pools	6
1.5 Application of N isotopes in forest ecosystem studies	7
1.5.1 Natural ¹⁵ N abundance	7
1.5.2 ¹⁵ N tracer.....	7
2 Objectives	11
3 Materials and Methods	13
3.1 Study site.....	13
3.2 Experimental design	13
3.3 ¹⁵ N tracer experiment.....	17
3.3.1 Sampling and analysis.....	17
3.3.1.1 Tree compartments	17
3.3.1.2 Soil.....	18
3.3.1.3 Soil solution	18
3.3.2 Natural ¹⁵ N abundance and N content in ecosystem compartments	20
3.3.3 N fluxes	20
3.3.4 Calculation of ¹⁵ N excess and recovery	21
3.4 Density fractionation experiment	22
3.4.1 Density fractionation procedure	22
3.4.2 Comparison of two aggregate-disrupting methods	24
3.4.3 Preparation of density solution	24
3.4.4 Analysis and calculation.....	24
3.5 Statistical analysis	25
4 Results	27
4.1 ¹⁵ N tracer experiment.....	27
4.1.1 The roof control plot	27
4.1.1.1 Natural ¹⁵ N abundance	27
4.1.1.2 N content in ecosystem compartments and N fluxes	28
4.1.1.3 ¹⁵ N enrichment in ecosystem compartments	29
4.1.1.4 ¹⁵ N recovery in ecosystem compartments	36

4.1.2	The clean rain plot.....	38
4.1.2.1	Natural ^{15}N abundance.....	38
4.1.2.2	N content in ecosystem compartments and N fluxes.....	38
4.1.2.3	^{15}N enrichment in ecosystem compartments.....	40
4.1.2.4	^{15}N recovery.....	45
4.2	Density fractionation.....	48
4.2.1	Preparation of density solution.....	48
4.2.2	Comparison of two aggregate-disrupting methods.....	48
4.2.3	Distribution of OC and N in soil density fractions.....	49
4.2.3.1	Organic layer.....	49
4.2.3.2	Mineral soil layers.....	49
4.2.4	Recovery of soil ^{15}N	50
5	Discussion.....	59
5.1	^{15}N tracer experiment.....	59
5.1.1	Natural ^{15}N abundance.....	59
5.1.2	^{15}N recoveries.....	60
5.1.2.1	Under ambient atmospheric deposition (the roof control plot).....	60
5.1.2.1.1	Soil.....	60
5.1.2.1.2	Tree.....	61
5.1.2.1.3	Leaching.....	62
5.1.2.2	Under long-term reduced atmospheric deposition (the clean rain plot).....	63
5.1.2.2.1	Soil.....	63
5.1.2.2.2	Tree.....	66
5.1.2.2.3	Leaching.....	68
5.2	Density fractionation experiment.....	69
5.2.1	Preparation of density solution.....	69
5.2.2	Comparison of two aggregate-disrupting methods.....	69
5.2.3	Distribution of OC and N in soil density fractions.....	71
5.2.4	Recovery of soil ^{15}N	73
6	Conclusion.....	77
7	Summary.....	79
8	Zusammenfassung.....	83
9	References.....	87
10	Appendix.....	97
	Lebenslauf.....	99

Tables

Table 1.1. ^{15}N recoveries in forest ecosystem compartments from some ^{15}N tracer studies	9
Table 3.1. Mean annual deposition of ammonium, nitrate, DON, sulphate and proton ($\text{kg ha}^{-1} \text{ yr}^{-1}$) in the clean rain and the roof control plot during 1992 and 2001	15
Table 4.1. Natural ^{15}N abundances (mean $\pm 1_{\text{SE}}$) of main tree compartments and soil of the 75-year-old spruce forest in the roof control plot	28
Table 4.2. Natural ^{15}N abundance (mean $\pm 1_{\text{SE}}$) of the throughfall water and the soil solution of the 75-year-old spruce forest in the roof control plot	29
Table 4.3. Masses, N concentration and contents of main tree compartments of the 75-year-old spruce forest in the roof control plot	30
Table 4.4. Masses, C-, N concentration and N contents of soil of the 75-year-old spruce forest in the roof control plot	31
Table 4.5. Annual N fluxes ($\text{kg ha}^{-1} \text{ yr}^{-1}$) (mean $\pm 1_{\text{SE}}$) in the roof control plot during Jan.02 and Jun.04.....	31
Table 4.6. Percent ^{15}N recoveries (mean $\pm 1_{\text{SE}}$) in main spruce forest ecosystem compartments in the roof control plot in 2004	37
Table 4.7. Natural ^{15}N abundances of main tree compartments and soil of the 75-year-old spruce forest in the clean rain plot.....	39
Table 4.8. Natural ^{15}N abundance of the throughfall water and the soil solution of the 75-year-old spruce forest in the clean rain plot.....	40
Table 4.9. Masses, N concentration and contents of main tree compartments of the 75-year-old spruce forest in the roof control and the clean rain plot.....	41
Table 4.10. Masses, C-, N concentration and N contents of soil of the 75-year-old spruce forest in the roof control and the clean rain plot.....	42
Table 4.11. Annual N fluxes ($\text{kg ha}^{-1} \text{ yr}^{-1}$) (mean $\pm 1_{\text{SE}}$) in the roof control and the clean rain plot during Jan.02 and Jun.04.....	43
Table 4.12. $\delta^{15}\text{N}$ excess (‰) (mean $\pm 1_{\text{SE}}$) of tree compartments and soil in the $^{15}\text{NH}_4^+$ - and $^{15}\text{NO}_3^-$ -labelled subplot of the clean rain plot.....	44

Table 4.13. $\delta^{15}\text{N}$ (‰) (mean \pm 1 _{SE}) of $\text{NO}_3\text{-N}$ and DON in soil solution in the $^{15}\text{NH}_4^+$ - and $^{15}\text{NO}_3^-$ -labelled subplot of the clean rain plot during Jan. 02 and Jun. 04.....	45
Table 4.14. Percent ^{15}N recoveries (mean \pm 1 _{SE}) in main spruce forest ecosystem compartments in the roof control and the clean rain plot in 2004.....	47
Table 4.15. Properties (mean \pm 1 _{SE}) of density fractions from the organic layer and the 0-5 cm mineral soil layer in the ambient control plot after using two different aggregate-disrupting methods (n = 5).....	52
Table 4.16. Natural ^{15}N abundances (mean \pm 1 _{SE}) of density fractions from the organic layer and the 0-5 cm mineral soil layer in the ambient control plot after using two different aggregate-disrupting methods (n = 5) ..	53
Table 4.17. Properties (mean \pm 1 _{SE}) of density fractions from the organic layer in the clean rain and the roof control plot (n = 5).....	54
Table 4.18. Properties (mean \pm 1 _{SE}) of density fractions from the 0-5 cm mineral soil layer in the clean rain and the roof control plot (n = 5).....	55
Table 4.19. Properties (mean \pm 1 _{SE}) of density fractions from the 5-10 cm mineral soil layer in the clean rain and the roof control plot (n = 5) ..	56
Table 4.20. Percent recovery (mean \pm 1 _{SE}) of soil ^{15}N in density fractions from the organic layer and the mineral soil layers in the clean rain and the roof control plot after $^{15}\text{NH}_4^+$ and $^{15}\text{NO}_3^-$ addition.....	57
Table 10.1. C and N concentration of the organic layer and mineral soil layers in the ambient control plot, the clean rain and the roof control plot based on oven-dried level.....	97
Table 10.2. The relationship between the amounts of SPT added to 150 g water and the volume change of solution.....	97
Table 10.3. $\delta^{15}\text{N}$ excess (‰) of density fractions from the organic layer and the mineral soil layers in the clean rain and the roof control plot after $^{15}\text{NH}_4^+$ and $^{15}\text{NO}_3^-$ addition	98

Figures

Fig. 1.1. Global N cycle among different environmental reservoirs (values estimated for 1990, Galloway and Cowling 2002).....	2
Fig. 1.2. N cycle in forest ecosystems.....	4
Fig. 3.1. Roof constructions in the 75-year-old Norway spruce forest at Solling (D1-clean rain plot, D2- roof control plot, D3- drought plot, drawn by R. Grote).....	14
Fig. 3.2. Separation of the clean rain and the roof control plot into ¹⁵ N-labelled subplots.	16
Fig. 3.3. Mixture of soil solution samples for ¹⁵ N analysis in each ¹⁵ N-labelled subplot of the clean rain and the roof control plot.....	19
Fig. 3.4. Diagram of density fractionation procedure.....	23
Fig. 4.1. δ ¹⁵ N excess (mean ± 1 _{SE}) of needles of different age classes in a) 2002; b) 2003; c) 2004 in the ¹⁵ NH ₄ ⁺ - and ¹⁵ NO ₃ ⁻ -labelled subplot of the roof control plot (n = 6). Arrow shows the time when ¹⁵ N tracer addition began.....	32
Fig. 4.2. δ ¹⁵ N excess (mean ± 1 _{SE}) of a) bark; b) wood of twigs and branches with different age classes in 2003 in the ¹⁵ NH ₄ ⁺ - and ¹⁵ NO ₃ ⁻ -labelled subplot of the roof control plot (n = 3). Arrow shows the time when ¹⁵ N tracer addition began.	32
Fig. 4.3. δ ¹⁵ N excess (mean ± 1 _{SE}) of bole bark and different increments of bole wood in the ¹⁵ NH ₄ ⁺ - and ¹⁵ NO ₃ ⁻ -labelled subplot of the roof control plot (n = 3) after over 3 year ¹⁵ N addition (2001-2004).....	33
Fig. 4.4. δ ¹⁵ N excess (mean ± 1 _{SE}) of a) live and dead fine roots (2002); b) live fine roots (2004) at different soil depths in the ¹⁵ NH ₄ ⁺ - and ¹⁵ NO ₃ ⁻ -labelled subplot of the roof control plot (n = 5 in 2002, n = 4 and 3 in 2004 in the ¹⁵ NH ₄ ⁺ and ¹⁵ NO ₃ ⁻ subplot, respectively).	34
Fig. 4.5. δ ¹⁵ N excess (mean ± 1 _{SE}) of soil at different depths in a) 2002; b) 2004 in the ¹⁵ NH ₄ ⁺ - and ¹⁵ NO ₃ ⁻ -labelled subplot of the roof control plot (n = 5). Soil samples taken in 2002 were only to 20 cm mineral soil.....	35

-
- Fig. 4.6. Gradient of ^{15}N abundance (mean $\pm 1_{\text{SE}}$) of a) NO_3^- ; b) DON in soil solution collected in selected months (Mai 2002, 2003, 2004, December 2002 and 2003) in the $^{15}\text{NH}_4^+$ - and $^{15}\text{NO}_3^-$ -labelled subplot of the roof control plot ($n = 5$).....35
- Fig. 4.7. The relationship between the amount of added SPT and the volume change of SPT solution.....48
- Fig. 5.1. Percent recovery of a) $^{15}\text{NH}_4^+$; b) $^{15}\text{NO}_3^-$ in the spruce forest ecosystem compartments in the clean rain and the roof control plot.....64
- Fig. 5.2. Percent recovery of soil ^{15}N in density fractions from a) the organic layer; b) the 0-5 cm mineral soil layer; c) the 5-10 cm mineral soil layer in the clean rain and the roof control plot after $^{15}\text{NH}_4^+$ and $^{15}\text{NO}_3^-$ addition.....74

Abbreviations and Acronyms

a.s.l.	above sea level
DF	dense fraction, density $> 2.0 \text{ g cm}^{-3}$
DON	dissolved organic nitrogen
FL	free light fraction, density $< 1.6 \text{ g cm}^{-3}$
fPOM	free particulated organic matter, density $< 1.6 \text{ g cm}^{-3}$
HF	heavy fraction
IRMS	isotope ratio mass spectrometer
LF	light fraction
min.	minute
Mineral-OM	mineral-associated organic matter, density $> 2.0 \text{ g cm}^{-3}$
N	nitrogen
NH_4^+	ammonium
NO_3^-	nitrate
OC	organic carbon
Ocl. I	occluded fraction I, density $< 1.6 \text{ g cm}^{-3}$
Ocl. II	occluded fraction II, density $= 1.6\text{-}1.8 \text{ g cm}^{-3}$
Ocl. III	occluded fraction III, density $= 1.8\text{-}2.0 \text{ g cm}^{-3}$
oPOM	occluded particulated organic matter
rpm	revolutions per minute
SOM	soil organic matter
SPT	sodium polytungstate, $\text{Na}_6(\text{H}_2\text{W}_{12}\text{O}_{40})$

1 Introduction

1.1 N input to terrestrial ecosystem

Under natural conditions N_2 fixation is the dominant process to provide reactive N to terrestrial ecosystems. Biologically unavailable N_2 in the atmosphere is transferred to reactive N forms such as ammonia (NH_3), ammonium (NH_4^+), nitrite (NO_2^-), nitrate (NO_3^-), nitrogen oxides (NO and NO_2), N_2O_5 and nitrous oxide (N_2O) through biological and oxidative fixation (Galloway and Cowling 2002, van Egmond et al. 2002). Biological N_2 fixation is accomplished by certain microorganisms, including a few free-living bacteria and blue-green algae as well as symbiotic bacteria, and contributed 89 Tg N yr^{-1} in 1990 (Galloway et al. 1995). Oxidative N_2 fixation is via lightning, and contributed 5 Tg N yr^{-1} in 1990 (Galloway et al. 1995).

Anthropogenic activities have increased N input drastically in the past century and become main contributor of N to terrestrial ecosystems. In 1890, fossil combustion contributed only about 0.6 Tg N yr^{-1} (van Aardenne et al. 2001). Cultivation contributed 15 Tg N yr^{-1} in 1900 (Smil 1999). In 1990, fertilizer consumption and other industry, cultivation, and fossil fuel combustion accounted for 85, 33 and 21 Tg N yr^{-1} , respectively (Levy et al. 1999, Smil 1999, 2002, FAO 2000, van Aardenne et al. 2001).

The drastically increased anthropogenic N input to terrestrial ecosystems influences the global N cycle (Fig. 1.1). Emission of reactive N to the atmosphere increases with increasing anthropogenic N input. Reactive N in the atmosphere spreads with air currents and increases deposition to terrestrial and marine ecosystems. NH_3 emission from agricultural land and livestock was 9 Tg N yr^{-1} in 1890 and increased to 43 Tg N yr^{-1} in 1990 (van Aardenne et al. 2001). NO_x emission from vegetation and fossil fuel combustion was 7 Tg N yr^{-1} in 1890 and increased to 33 Tg N yr^{-1} in 1990 (van Aardenne et al. 2001). Atmospheric N deposition to terrestrial ecosystems increased from 16 Tg N yr^{-1} in 1890 to 76 Tg N yr^{-1} in 1990, while atmospheric N deposition to the ocean surface increased from 17 Tg N yr^{-1} in 1890 to 27 Tg N yr^{-1} in 1990 (Lelieveld and Dentener 2000). Transfer of dissolved inorganic N to coastal ecosystems via rivers also increased, from 5 Tg N yr^{-1} in 1890 to 20 Tg N yr^{-1} in 1990 (Seitzinger and Kroeze 1998).

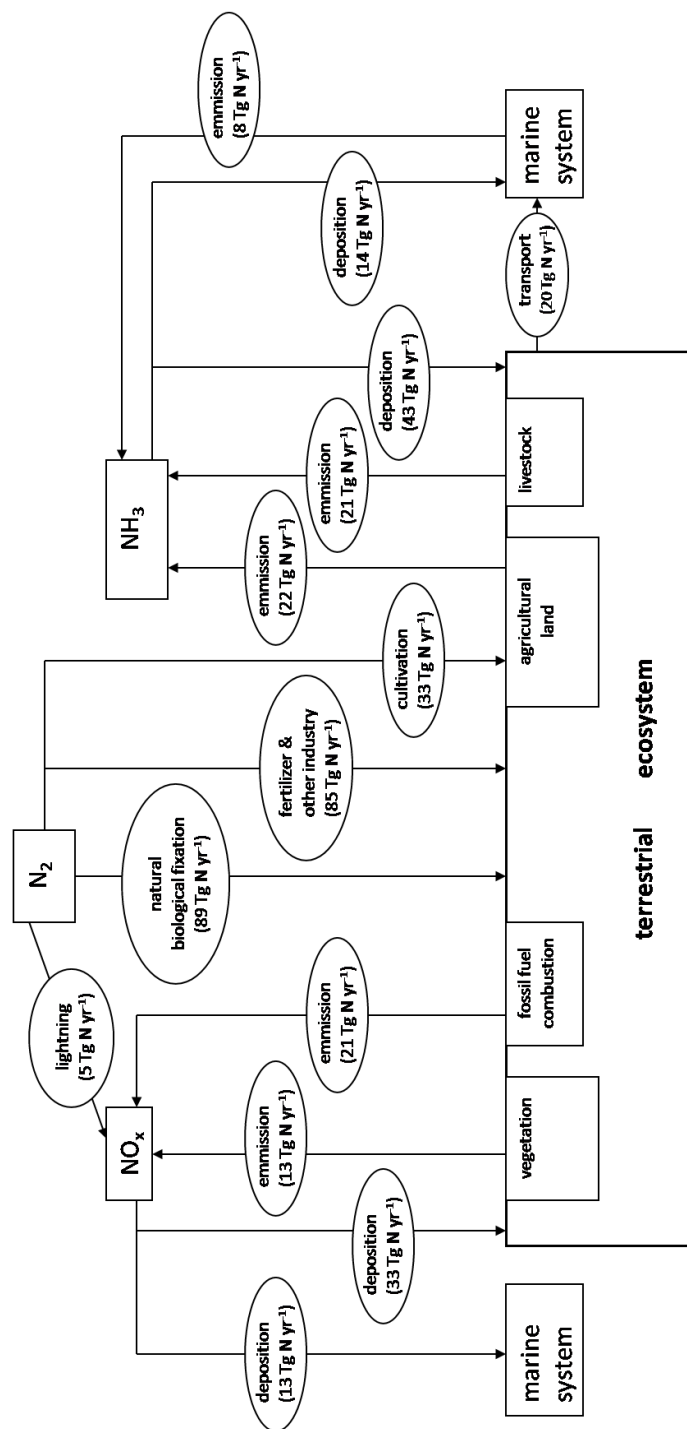


Fig. 1.1. Global N cycle among different environmental reservoirs (values estimated for 1990, Galloway and Cowling 2002).

1.2 Impact of elevated N input on temperate forest ecosystems

The increased anthropogenic N input influences not only the global N cycle, but also N cycle within terrestrial ecosystems. Temperate forest ecosystems are an important component of terrestrial ecosystems and their response to elevated N input has been documented.

In temperate forest ecosystems, soil organic matter (SOM) is mineralized to NH_4^+ (Fig. 1.2). A part of NH_4^+ is further nitrified to NO_3^- . NH_4^+ and NO_3^- can be immobilized by microorganisms and plants or react with SOM via an abiotic pathway. NH_4^+ can also be fixed on surfaces of clay minerals. NO_3^- can be leached to groundwater or denitrified. N_2 , N_2O and NO , which are produced during nitrification and denitrification, are released to the atmosphere. The increased anthropogenic N input participates in the N cycle and affects productivity, species composition, soil chemistry and water quality of temperate forest ecosystems (Nihlgård 1985, van Breemen and van Dijk 1988, Aber et al. 1989, Bobbink et al. 1998).

Temperate forest ecosystems are primary N-limited. The elevated N input increases N availability and stimulates initially forest growth (Tamm 1989, Kauppi et al. 1992, Spiecker 1999). When N input exceeds the biotic and abiotic demand of N within temperate forest ecosystems, N saturation is approached (Ågren and Bosatta 1988, Aber et al. 1989). Forest decline and mortality may occur (Schulze 1989, McNulty et al. 1996), due to element imbalance in foliage, increased plant susceptibility to other stress (frost, ozone, insect attack, etc.), soil acidification and depletion in base cation (see below, van Dijk and Roelofs 1988, Emmett 1999, Matson et al. 2002). Slow-growing and slow N-cycling coniferous stands may be replaced by fast-growing and fast N-cycling deciduous forests (McNulty et al. 1996).

The elevated N input can result in an initial increase, but ultimately a possible decrease in mineralization (McNulty et al. 1990, Aber et al. 1998). N accumulation in the soil has a consequent increase (Aber et al. 1998). The decreased mineralization and increased N accumulation are attributed to suppression of lignolytic enzymes in white rot fungi, and formation of stable nitrogenous compounds from lignin by-products (Berg and Matzner 1997).

Nitrification and nitrate leaching can increase with the elevated N input (Puhé and Ulrich 2001, Magill et al. 2004, Meesenburg et al. 2004). Increased release of proton (H^+), which occurs during nitrification and immobilization of NH_4^+ , can lead to soil acidification. Base cation in soil solution can become depleted with elevated N input (Federer et al. 1989, Lawrence et al. 1995), which is attributed to increased leaching of base cation as counterbalance ion for leached NO_3^- and reduced cation exchange site resulting from higher Al^{3+} availability and lower pH

(Matzner and Murach 1995, Likens et al. 1996). N gas losses can also increase as a result of the elevated N input (Schmidt et al. 1988, Butterbach-Bahl et al. 1998).

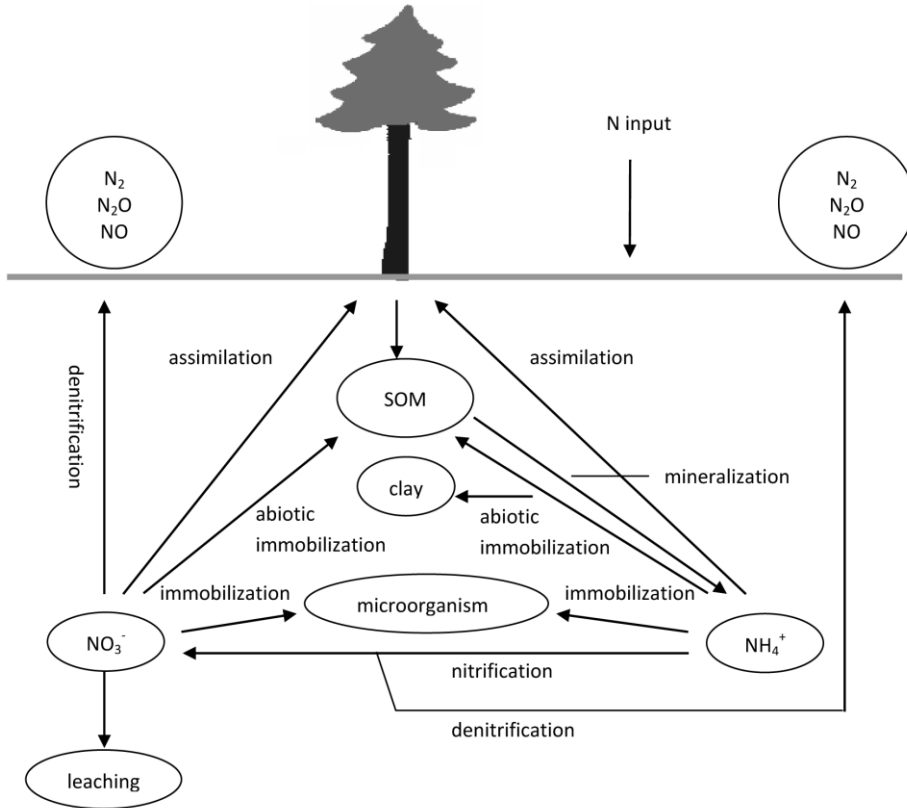


Fig. 1.2. N cycle in forest ecosystems.

1.3 Distribution of N input among forest ecosystems

N input to temperate forest ecosystems is distributed to different ecosystem compartments such as tree, soil and leachate. The distribution of N input among forest ecosystem compartments is an important basis to understand N cycling and functioning of temperate forest ecosystems.

Many studies have reported that forest ecosystems possess the ability to efficiently retain N input (Table 1.1). In forests with relative low N input ($\leq 20 \text{ kg ha}^{-1} \text{ yr}^{-1}$), the largest proportion of N input was found in soils, varying from 38% to 87% (Buchmann et al. 1996, Koopmans et al. 1996, Gundersen 1998, Nadel-

hoffer et al. 1999a). Trees and ground vegetations accounted for 3% to 44% of N input, while only up to 10% of N input was leach out. In forests with higher N input, soils retained 26% to 63% of N input (Melin et al. 1983, Koopmans et al. 1996, Tietema et al. 1998, Nadelhoffer et al. 1999a, b, Schleppei et al. 1999). 8% to 45% of N input was recovered in trees and vegetations, whereas leaching loss increased up to 50%. Among forest ecosystem compartments, soils are in most cases the largest sink for N input.

N is retained in the soil through microbial and abiotic immobilization. Abiotic immobilization includes fixation of NH_4^+ to clay mineral and reaction of N with SOM. Therefore, SOM can play an important role in the retention of N input.

1.4 SOM

1.4.1 SOM stability

The accumulation of N input in SOM is influenced by SOM stability. The amount of N accumulated in SOM is a balance between N input and N mineralization. N mineralization can be inhibited by stabilization mechanisms of SOM, leading to N accumulation in SOM. The stabilization mechanisms of SOM are proposed to be: 1) biochemical recalcitrance, 2) spatial inaccessibility to decomposer organisms, and 3) interaction of organic matter with minerals and metal ions (Sollins et al. 1996, von Lützow et al. 2006, Kögel-Knabner et al. 2008).

Recalcitrance refers to biodegradability of SOM due to its molecular-level characteristics, including elemental composition, presence of functional groups and molecular confirmation (Sollins et al. 1996, Kögel-Knabner et al. 2008). Recalcitrance of SOM includes that of plant litter, rhizodeposits, microbial products, humic polymers and charred organic matter (von Lützow et al. 2006).

Spatial inaccessibility refers to spatial location of SOM that influences the access to microbes and enzymes (Sollins et al. 1996). Spatial inaccessibility of SOM results from occlusion by aggregation, intercalation within phyllosilicates, hydrophobicity and encapsulation in organic macromolecules (von Lützow et al. 2006, Kögel-Knabner et al. 2008).

Interaction refers to inter-molecular interactions between SOM and mineral surfaces (Fe-, Al-, Mn-oxides and phyllosilicates) as well as between SOM and metal ions (Sollins et al. 1996, von Lützow et al. 2006). These interactions are accomplished through precipitation, sorption and complexation reaction and reduce availability of SOM to microorganisms and extracellular enzymes (Sollins et al. 1996).

1.4.2 SOM pools

SOM is composed of various pools, which differ in stability. These pools need to be identified to understand SOM dynamics in soil. Physical and chemical fractionation methods have been developed to separate the various SOM pools. Physical fractionation methods base on the association of SOM with soil particles, are less destructive than chemical fractionation methods and results are anticipated relative directly to the structure and function of SOM in situ (Christensen 1992, von Lützow et al. 2007). One of the usually used physical fractionation methods is density fractionation.

Density fractionation isolates SOM pools according to the degree of association between SOM and soil particles (Christensen 1992). These SOM pools are separated through floatation or sedimentation in a heavy solution with a specific density (Christensen 1992). SOM associated with fewer mineral particles, either as free OM or occluded OM, is separated into lighter density fraction. SOM adsorbed to mineral surfaces is separated into heavy density fraction. SOM in the lighter fraction is dominated by plant debris, while that in the heavy fraction is mainly of microbial origin. In the density fractionation method, the usually used density varies in the range of 1.6-2.2 g cm⁻³ and the preferred density agent in recent years is sodium polytungstate (SPT, Na₆(H₂W₁₂O₄₀)).

Golchin et al. (1994a, b) developed a hierarchical density fractionation scheme and proposed a conceptual model of SOM decomposition processes. They separated SOM into five pools: free particulate OM (fPOM, $d < 1.6 \text{ g cm}^{-3}$), three occluded particulate OM fractions (oPOM I, II, III, $d < 1.6 \text{ g cm}^{-3}$, $d = 1.6-1.8 \text{ g cm}^{-3}$, $d = 1.8-2.0 \text{ g cm}^{-3}$, respectively) and mineral-associated OM (Mineral-OM, $d > 2.0 \text{ g cm}^{-3}$). According to the model, carbonate-rich plant debris (fPOM) is attractive to microorganisms and establishes intimate association with mineral particles. With proceeding decomposition, the labile portion of plant debris is consumed; microbial biomass and products are adsorbed to surfaces of mineral particles. The association between SOM and mineral particles becomes looser. After disaggregation through ultrasonic treatment, SOM, which associates intimately with mineral particles, is accumulated in the fraction oPOM III. SOM, which has loose association with mineral particles, is released with fewer particles and accumulated in the fraction oPOM II or oPOM I. The remaining mineral particles with associated microbial biomass and products are accumulated in the fraction Mineral-OM. Generally, the stability of SOM pools follows the order: fPOM < oPOM < Mineral-OM (von Lützow et al. 2007). The higher stability of oPOM than fPOM is attributed to higher recalcitrance (Golchin et al. 1994a) and spatial inaccessibility caused by occlusion (Poirier et al. 2005).

1.5 Application of N isotopes in forest ecosystem studies

^{15}N and ^{14}N are two stable isotopes of nitrogen. ^{15}N is heavier and scarce in nature, while ^{14}N is lighter and abundant. ^{15}N abundance can be used to provide insight into N cycling within forest ecosystems. ^{15}N abundance is noted either as atom% or more commonly as $\delta^{15}\text{N}$, which is expressed as per mill deviation of the $^{15}\text{N}/^{14}\text{N}$ ratio from atmospheric standard (0.3663 atom%, eq. 1.1).

$$\delta^{15}\text{N} = \left(\frac{\left(\frac{^{15}\text{N}}{^{14}\text{N}} \right)_{\text{sample}}}{\left(\frac{^{15}\text{N}}{^{14}\text{N}} \right)_{\text{standard}}} - 1 \right) * 1000 \quad (1.1)$$

1.5.1 Natural ^{15}N abundance

In forest ecosystems, slight isotope fractionation occurs during N transformation processes, during which ^{14}N is preferentially transformed. As a result, natural ^{15}N abundances of forest ecosystems show systematic variation among and within ecosystem compartments. Plants are usually ^{15}N -depleted relative to soils. Soils are enriched in ^{15}N with depth. Natural ^{15}N abundances of plants and soils can be used to provide information on overall patterns of N cycling (Gebauer and Schulze 1991, Garten et al. 1994), contribution of N sources to plant uptake (Högberg 1997), change in N inputs and losses (Johannisson 1996, Nohrstedt et al. 1996, Emmett et al. 1998) and perturbations in nutrient cycles (Gebauer and Schulze 1991) over long timescales ranging from decades to centuries (Nadelhoffer and Fry 1994). For example, elevated N input could result in an increase in $\delta^{15}\text{N}$ of current needles, caused by increased nitrification and preferential uptake of NH_4^+ by trees (Johannisson 1996).

1.5.2 ^{15}N tracer

Application of ^{15}N tracers can provide a strong ^{15}N signal above natural background level (Nadelhoffer and Fry 1994), so that isotope fractionation during N transformation processes can be ignored. Usually, small amounts of highly ^{15}N -labelled tracers are applied to minimize priming effect (i.e. addition of ^{15}N tracers increases substrate pool, Jenkinson 1981). ^{15}N tracers are used in short-term incubation experiments (hours to days) to estimate gross N transformation rates such as mineralization, nitrification and immobilization rate with ^{15}N pool dilution technique (e.g. Davidson et al. 1991, Hart et al. 1994, Perakis and Hedin 2001, Compton and Boone 2002, Corre and Lamersdorf 2004). ^{15}N tracers can also be added to large scale forest ecosystems as a single pulse or periodically to estimate

distribution of N input in forest ecosystems (e.g. Melin et al. 1983, Vitousek and Matson 1984, Nõmmik 1990, Nadelhoffer et al. 1995, Buchmann et al. 1996, Gundersen 1998).

Table 1.1. ^{15}N recoveries in forest ecosystem compartments from some ^{15}N tracer studies

Study site	treatment	N input ($\text{kg ha}^{-1} \text{ yr}^{-1}$)	sampling after start of ^{15}N addition	tree		ground		organic layer		mineral soil		leaching
				$^{15}\text{NH}_4$	$^{15}\text{NO}_3$	$^{15}\text{NH}_4$	$^{15}\text{NO}_3$	$^{15}\text{NH}_4$	$^{15}\text{NO}_3$	$^{15}\text{NH}_4$	$^{15}\text{NO}_3$	
Fichtelgebirge ¹ Germany	control	12	8 months	4	10	9	15	63	46	24	33	mineral soil 0-65 cm
Alpial ² Switzerland	high N	42	1 year	21	5	5	42	42	21	21	10	labelled with $^{15}\text{NH}_4$, $^{15}\text{NO}_3$
Aber ³ UK	AN 35 SN 35 SN 50	50 50 90	1 year	32	32 20	47	47	17 11	1	15 15	25 35 50	labelled with $^{15}\text{NH}_4$, $^{15}\text{NO}_3$ labelled with $^{15}\text{NO}_3$ labelled with $^{15}\text{NO}_3$ mineral soil 0-25 cm
Klosterhede ^{3,4} Denmark	control high N	20 55	13 months	32 42	13 3	26 16	26 16	12 17	12 17	0 4	labelled with $^{15}\text{NH}_4$, $^{15}\text{NO}_3$ mineral soil 0-30 cm	
Speuld ⁵ the Netherlands	reduced control	4 44	21 months	33 29	22 15	22 15	22 15	2 33	2 33	2 33	mineral soil 0-70 cm	
Ysselsteyn ⁵ the Netherlands	reduced control	6 53	21 months	10 17	46 21	20 15	20 15	10 17	10 17	10 17	mineral soil 0-70 cm	
Ivantjärnsheden ⁶ Sweden	high N	100	2 years	23	28	8	9	22	13	30	26	mineral soil 0-30 cm

Table 1.1. (continued)

Study site	treatment	N input (kg ha ⁻¹ yr ⁻¹)	sampling after start of ¹⁵ N addition	tree		ground vegetation		organic layer		mineral soil		leaching
				¹⁵ NH ₄	¹⁵ NO ₃	¹⁵ NH ₄	¹⁵ NO ₃	¹⁵ NH ₄	¹⁵ NO ₃	¹⁵ NH ₄	¹⁵ NO ₃	
Harvard's Forest ⁷ USA	control	8	2 years	3	5	46	74	8	9	mineral soil 0-20 cm		
	fertilized	58		13	26	42	26	10	20			
Bear Brook ⁸ USA		30	17 months	8		32						

¹ Buchmann et al. (1996) Biogeochemistry 33, 1-23.² Schleppi et al. (1999) Water, Air, and Soil Pollution 116, 129-134.³ Tietema et al. (1998) Forest Ecology and Management 101, 19-27.⁴ Gundersen (1998) Forest Ecology and Management 101, 251-268.⁵ Koopmans et al. (1996) Biogeochemistry 34, 19-44.⁶ Melin et al. (1983) Plant and Soil 74, 249-263.⁷ Nadelhoffer et al. (1999a) Ecological Applications 9 (1), 72-86.⁸ Nadelhoffer et al. (1999b) Environmental Monitoring and Assessment 55, 187-210.

2 Objectives

Although temperate forest ecosystems are primary N limited, many forests in central Europe and North America have been subjected to N saturation, which increases concern about forest decline and nitrate leaching (Fenn et al. 1998, Matzner 2004). Of potential management strategies and practices to improve N-saturated forest ecosystems, reduction of atmospheric N emission is the only practical long-term solution in many areas (Fenn et al. 1998), especially in central Europe where atmospheric N deposition can be in excess of 60 kg N ha⁻¹ yr⁻¹ (MacDonald et al. 2002). To provide basis for policy, it is necessary to know how N-saturated forest ecosystems respond to reduced atmospheric N deposition. In a Europe-wide project, NITREX (NITrogen saturation EXperiment), responses of forest ecosystems to both N addition and reduced atmospheric N deposition have been investigated (Dise and Wright 1992, Wright and van Breemen 1995). Atmospheric N deposition in three sites (two in the Netherlands and one in Germany) was drastically reduced through roof construction below canopy of forests. Results from the NITREX project showed that reduced atmospheric N deposition led to rapid and drastic decrease of nitrate leaching as well as increased fine root growth (Boxman et al. 1995, Bredemeier et al. 1998a, Xu et al. 1998, Lamersdorf and Borken 2004). N transformation processes were influenced by reduced atmospheric N deposition: gross N mineralization rate showed a slight increase; microbial NH₄⁺ cycling was enhanced (i.e. higher microbial NH₄⁺ immobilization and faster turnover of NH₄⁺ and microbial N pools); gross nitrification was undetectable and abiotic nitrate immobilization increased (Corre and Lamersdorf 2004). In spite of these findings, some questions are still open: how atmospheric N is distributed among forest ecosystem compartments? Which forest ecosystem compartment is responsible for the decreased nitrate leaching? As inorganic N deposition has two N forms (NH₄⁺ and NO₃⁻), is there any difference in distribution of atmospheric ammonium and nitrate in forest ecosystems?

To answer such questions, a ¹⁵N tracer study has been conducted in coniferous forests at two Dutch sites (Koopmans et al. 1996). In this ¹⁵N tracer experiment, however, only ¹⁵NH₄⁺ was applied, because NH₄-N is the dominant N form in atmospheric N deposition at the two sites (Koopmans et al. 1996). In addition, the ¹⁵NH₄⁺ tracer had been added only for one year after three-years of reduction of atmospheric N deposition. Many forested sites have approximately equal deposition of atmospheric ammonium and nitrate (e.g. Buchmann et al. 1996, Nadelhoffer et al. 1999, Schleppi et al. 1999). In the present study, ¹⁵NH₄⁺ and ¹⁵NO₃⁻ have been separately added to a mature spruce forest for over three years, after a ten-year reduction of atmospheric N deposition. The main objective of the study was to evaluate how long-term reduced atmospheric N deposition influences the partitioning of atmospheric ammonium and nitrate in the spruce forest ecosystem.

Two main experiments were conducted in the study: a ^{15}N tracer experiment in the field and a density fractionation experiment in the laboratory. The aims were to:

1) *evaluate how long-term reduced atmospheric N deposition influences N retention in trees and soil as well as N loss by leaching*

Using a ^{15}N mass balance equation (Nadelhoffer and Fry 1994, see 3.3.4), the retention of atmospheric N in tree compartments (needle, twig and branch, bole and live fine root) and soil as well as leaching loss of atmospheric N were compared between under ambient atmospheric N deposition and under long-term reduced atmospheric N deposition. It was also determined whether the distribution of atmospheric NH_4^+ vs. NO_3^- in forest ecosystem compartments changes under long-term reduced atmospheric N deposition.

2) *evaluate how long-term reduced atmospheric N deposition influences the partitioning of atmospheric N retained in the soil in different SOM pools*

SOM was separated into five pools through a density fractionation procedure. The distribution of atmospheric N retained in the soil in different SOM pools was compared between under ambient atmospheric N deposition and under long-term reduced atmospheric N deposition. It was also determined whether the distribution of atmospheric ammonium retained in the soil in SOM pools is different from that of atmospheric nitrate under the two atmospheric N deposition conditions. In addition, equations were derived to prepare density solutions and two aggregate-disrupting methods were compared in a preliminary experiment.

3 Materials and Methods

3.1 Study site

The experimental site is a 75-year-old (2008) Norway spruce forest (*Picea abies* (L.) Karst.) on the Solling plateau in central Germany (51°31' N, 9° 34' E; 510 m a.s.l.). The area is characterized by a temperate sub-oceanic mountainous climate with prevailing southwest to west winds. The mean annual air temperature is 6.4 °C, varying from -2.2 °C in January to 14.7 °C in July. The annual precipitation is 1090 mm, distributed evenly throughout the year. N deposition in throughfall water was more than 30 kg ha⁻¹ yr⁻¹ (1973-2001) with an approximate ammonium-to-nitrate ratio of 1:1 (Manderscheid et al. 1995, Xu et al. 1998, Lamersdorf and Borken 2004).

The soil is classified as Typic Dystrachrept (USDA) or acidic Dystric Cambisol (FAO), developed from loess solifluction layer overlaying weathered sandstone (Heupel 1989). Depth of the loess solifluction layer is about 70-100 cm (Blanck et al. 1993). Soil texture is silty loam. pH (CaCl₂) value ranges from 3.2 at 0-10 cm mineral soil depth to 4.2 at 40-80 cm mineral soil depth and base saturation is up to 7% throughout the mineral soil profile (Bredemeier et al. 1998b). Soil solution is dominated by acid cations (Al, Mn and Fe), while sulfate and nitrate are the most important charge fraction among anions (Bredemeier et al. 1998b). The organic layer is 6-9 cm thick and classified as a moder humus form (Heupel 1989, Blanck et al. 1993).

The spruce forest is the second generation growing on previously European beech occupied area. The forest stand was thinned to about 845 trees ha⁻¹ in 1990 (Dohrenbusch et al. 1993). Ground vegetation is absent, due to high canopy density, thick organic layer and soil acidity (Bredemeier et al. 1995).

3.2 Experimental design

Three transparent roofs (each 300 m²) were constructed in 1991 with timber frames and polycarbonate ceiling 3.5 m above the forest floor (Fig. 3.1). One roofed plot was used to reduce the atmospheric inputs (D1, hereafter 'clean rain plot'). The second roofed plot served as a control (D2, hereafter 'roof control plot'). Another roofed plot was used for drought and rewetting experiment, whereby the intercepted throughfall water was held back to create artificial drought events (D3, 'drought plot', Lamersdorf et al. 1998). In this study, only two roofed plots (the clean rain and the roof control plot) were used. Besides the roofed plots, an adjacent non-roofed plot was selected in the same spruce stand to serve as a non-manipulated reference (D0, hereafter 'ambient control plot') and to investigate potential roof effects. The roof effects (reduction of photosynthetic

light, small change of soil temperature, etc.) were described by Gundersen et al. (1998) and Lamersdorf and Borken (2004). Prior to roof manipulation, soil type and soil chemistry were not different between the clean rain and the roof control plot (Blank et al. 1993). The basal area was slightly higher in 1998 in the clean rain plot ($61 \text{ m}^2 \text{ ha}^{-1}$) than in the roof control plot ($53 \text{ m}^2 \text{ ha}^{-1}$, Jaehne 2000).

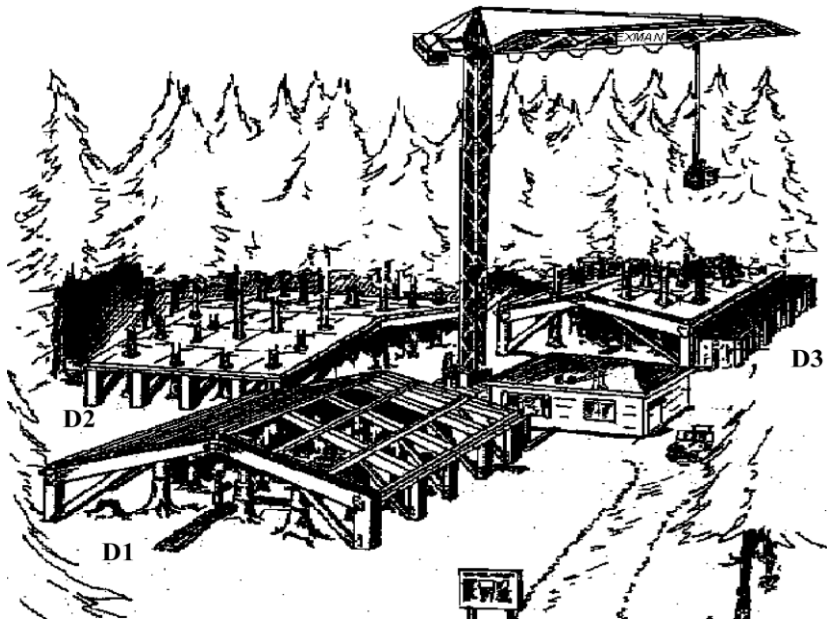


Fig. 3.1. Roof constructions in the 75-year-old Norway spruce forest at Solling (D1: clean rain plot, D2: roof control plot, D3: drought plot, drawn by R. Grote).

Throughfall water in the clean rain and the roof control plot was continuously collected from the roof surfaces and filtered ($350 \mu\text{m}$) to remove organic debris. In the clean rain plot, the throughfall water was subjected to further filtration ($50 \mu\text{m}$), ion exchange, addition of mineral solution and pH adjustment before its redistribution to soil surface by a sprinkler system (standard sprinkler system, Evers, Köln, Germany). In the roof control plot, the throughfall water was redistributed immediately to the soil surface without further treatment. Compared to the roof control plot, the annual atmospheric deposition of ammonium, nitrate, sulphate and proton in the clean rain plot was reduced by 86%, 49%, 53% and 77%, respectively, during 1992 and 2001; the annual deposition of dissolved or-

ganic nitrogen (DON) was reduced by 27% during 1998 and 2001 due to 50- μm filtration (Table 3.1).

Table 3.1. Mean annual deposition of ammonium, nitrate, DON, sulphate and proton ($\text{kg ha}^{-1} \text{ yr}^{-1}$) in the clean rain and the roof control plot during 1992 and 2001.

	$\text{NH}_4^+\text{-N}$	$\text{NO}_3^-\text{-N}$	DON*	$\text{SO}_4^{2-}\text{-S}$	H^+
roof control	15.0	15.0	2.5	26.0	0.5
clean rain	2.1	7.6	1.8	12.2	0.1
reduction	-86%	-49%	-27%	-53%	-77%

* Annual deposition of DON was the mean during 1998 and 2001.

In November 2001, each of the two roofed plots was separated into two approximately equal sections with a 1 m high polyethylene film above the ground and with steel panels in the upper mineral soil down to 30 cm soil depth (Fig. 3.2). Using another sprinkler systems installed at 80 cm above the ground, one half of each roofed plot was labelled with $^{15}\text{NH}_4\text{NO}_3$ (95 atom% ^{15}N), whereas the other half was labelled with $\text{NH}_4^{15}\text{NO}_3$ (98 atom% ^{15}N). The ^{15}N tracers were added homogeneously to the subplots as a 1 mm rain event after every 30-40 mm of regular throughfall water was re-sprinkled. The amount of added ^{15}N tracers, therefore, depended upon the amount of the collected throughfall water. In 2002, 2003 and 2004, ^{15}N tracers were added 34, 18, 22 times, respectively. In the clean rain plot, the $^{15}\text{NH}_4^+$ -labelled subplot yielded correspondingly 3.0, 1.6 and 2.0 $\text{mg }^{15}\text{N m}^{-2}$, which were equivalent to 0.3%, 0.1% and 0.2% of annual N deposition. The $^{15}\text{NO}_3^-$ -labelled subplot of the clean rain plot yielded correspondingly 12.0, 6.4 and 7.8 $\text{mg }^{15}\text{N m}^{-2}$, which were equivalent to 1.2%, 0.5% and 0.6% of annual N deposition. In the roof control plot, both the $^{15}\text{NH}_4^+$ - and $^{15}\text{NO}_3^-$ -labelled subplots received 21.3, 11.3 and 13.8 $\text{mg }^{15}\text{N m}^{-2}$ in 2002, 2003 and 2004 respectively, which were equivalent to 0.7%, 0.3% and 0.5% of annual N deposition. The ^{15}N abundance of the throughfall water in the clean rain plot increased from -6 to 534‰ (or from 0.3640 to 0.5604 atom‰) after the $^{15}\text{NH}_4^+$ addition and to 2179‰ (or to 1.1542 atom‰) after the $^{15}\text{NO}_3^-$ addition. In the roof control plot, the ^{15}N abundance of the throughfall water increased from 2 to 1332‰ (or from 0.3672 to 0.8493 atom‰) after the $^{15}\text{NH}_4^+$ addition and to 1347‰ (or to 0.8546 atom‰) after the $^{15}\text{NO}_3^-$ addition.

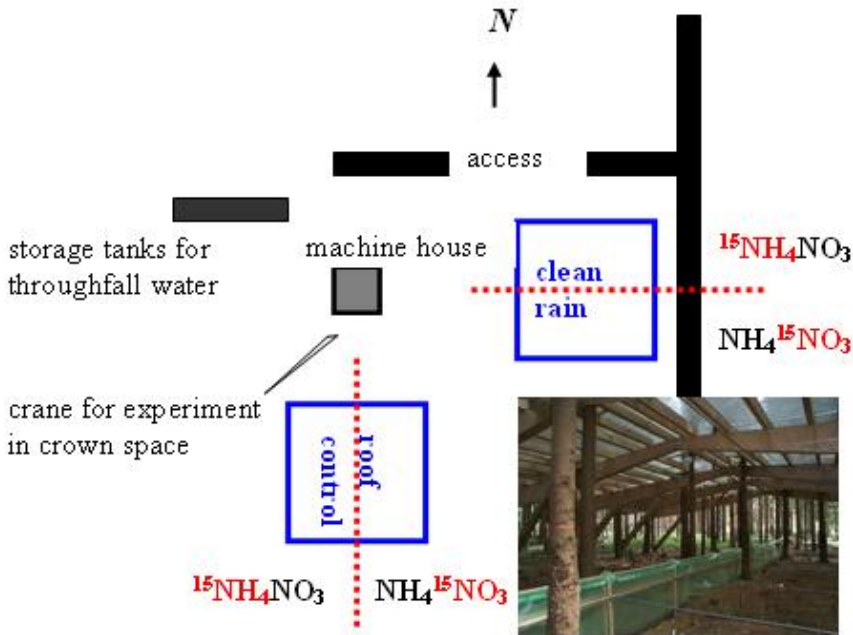


Fig. 3.2. Separation of the clean rain and the roof control plot into ^{15}N -labelled subplots.

To gain soil solution separately from the ^{15}N -labelled subplots, additional suction cup lysimeters were installed 4 weeks before the ^{15}N addition at the mineral soil depths of 0, 10, 40 and 100 cm with 10 single cups per depth in the $^{15}\text{NO}_3^-$ -labelled subplot of each roofed plot, whereas lysimeters had been installed in a previous study in the $^{15}\text{NH}_4^+$ -labelled subplots. The additional lysimeters were the same type of the previous lysimeters (*P-80* cups, 5 x 2 cm, CeramTec Ag, Marktredwitz, Germany) and were distributed in the same frequency (each two cups mixed to one replicate, i.e. $n = 5$ samples per depth). Although the additional lysimeters were installed with high caution to avoid contamination with organic particles and the collected first 0.5 to 1 L soil solution pro lysimeter was discarded, the NH_4^+ - but mainly the NO_3^- -N concentration and thus the N leaching rates were obviously higher in the $^{15}\text{NO}_3^-$ -labelled subplot than in the $^{15}\text{NH}_4^+$ -labelled subplot of each roofed plot (Table 4.11). We attribute differences in N-leaching between the two ^{15}N -labelled subplots of each roofed plot not to any treatment effect but mainly to stronger and local mineralization process induced by the installation of the additional lysimeters in the $^{15}\text{NO}_3^-$ -labelled subplots. The stronger mineralization in the $^{15}\text{NO}_3^-$ -labelled subplots caused higher NO_3^- -N fluxes, but simultaneously diluted ^{15}N concentration by enhanced ^{14}N release and thus might

not change ^{15}N fluxes. In the $^{15}\text{NO}_3^-$ -labelled subplot of the clean rain plot, one of the five replicates had much higher NO_3^- -N flux than the others (15.7 vs. 0.7 kg ha^{-1} yr^{-1}) at the 100 cm mineral soil depth. This replicate was treated as an outlier and not taken into consideration.

3.3 ^{15}N tracer experiment

3.3.1 Sampling and analysis

In this ^{15}N tracer experiment, samples were collected from different compartments (needle, twig and branch, bole, fine root, litter, soil and soil solution) in the $^{15}\text{NH}_4^+$ - and $^{15}\text{NO}_3^-$ -labelled subplot of each roofed plot to determine the allocation of ^{15}N within the spruce forest ecosystem. In the ambient control plot, ecosystem compartments were also sampled to provide reference values of natural ^{15}N abundance.

3.3.1.1 Tree compartments

Needle samples were collected each autumn from 2002 to 2004 with a crane from six trees at the 7th whorl within each ^{15}N -labelled subplot. The needles from each tree were separated into 2, 6 and 4 age classes in 2002, 2003 and 2004, respectively. More age classes were separated in the latter two years, because they reflected more completely ^{15}N allocation in the needles. Only in 2004, needle samples were collected from three trees in the ambient control plot.

Twig and branch samples were collected randomly in 2003 from three of the six trees per ^{15}N -labelled subplot, from which the needle samples were taken. The samples from each tree were divided into six age classes, whereby bark and wood were separated. Bole woods were sampled in April 2005 from the three trees from which branch samples were collected. In the ambient control plot, bole wood samples were taken from the three trees where the needles were sampled. Bole wood cores were taken at about 1.3 m height with a hollow punch (bark and outer wood samples) and an increment corer (inner wood samples). Cores from each tree were separated into outer bark, inner bark and six wood increments: wood produced before 1952, from 1952 to 1971, from 1972 to 1991, from 1992 to 1996, from 1997 to 2001 and from 2002 to 2004.

Litter was sampled seasonally from March 2003 to present in each ^{15}N -labelled subplot and the ambient control plot. Needles were separated from the litter samples that were collected during the spring (March to May) and autumn (August to October) of 2003.

Fine roots (≤ 2 mm) were collected in 2002 from the $\text{O}_{\text{F+H}}$, 0-5, 5-10, 10-20 cm mineral soil layers and in 2004 from the O_{H} , 0-10, 10-40 cm mineral soil layers (the samples in 2004 provided by Borke, personal communication,

BITÖK, Bayreuth, Germany, 2004). The fine root samples taken in 2002 were a mixture of live and dead fine roots, whereas the fine roots sampled in 2004 were separated into live and dead roots (according to their colour, elasticity and resiliency, Lamersdorf and Borken 2004) and the analysis was only done for the live fine roots.

All plant samples were oven-dried at 60 °C and grounded using either an ultra-centrifugal mill (0.25 mm sieve, Retsch ZM1, Haan, Germany) or a vibration mill (Retsch MM2, Haan, Germany). C and N concentrations were determined using elemental vario EL C/N analyser (Hanau, Germany). ^{15}N was measured with Finnigan MAT 251 (for natural ^{15}N abundance) or Finnigan Delta C (for ^{15}N enriched samples) isotope ratio mass spectrometer (IRMS, Bremen, Germany).

3.3.1.2 Soil

Soil samples were collected in December 2002 and June 2004 separately at five randomly selected locations in each ^{15}N -labelled subplot as well as in the ambient control plot, using stainless steel corers of 8 cm in diameter and 30 cm in length. The soil cores were divided into different layers: $\text{O}_{\text{F+H}}$, 0-5, 5-10, 10-20 cm mineral soil in 2002 and $\text{O}_{\text{L+F+H}}$, 0-5 cm mineral soil in 2004. Because the $\delta^{15}\text{N}$ values of the organic layer ($\text{O}_{\text{L+F+H}}$) sampled in 2004 in the $^{15}\text{NH}_4^+$ -labelled subplot of the clean rain plot showed strong variations, this layer in this subplot was resampled in July 2005 at six randomly selected locations and for further evaluation the average ^{15}N recovery of the both samplings was used. The soil was air dried, sieved (< 2 mm) and pulverized with a planetary mill (Retsch PM 4000, Haan, Germany) to measure total C, N concentrations and ^{15}N abundances. Soil samples from deeper layers were also taken in 2004 with a corer (3 cm in diameter and 1 m long) at the same sampling time and the same sampling locations as the upper soil layers in order to reveal completely ^{15}N allocation in the soil profile. These soil samples were separated into 5-10, 10-20, 20-30, 30-40, 40-60 cm mineral soil layers, oven-dried (40 °C), sieved and pulverized for C, N and ^{15}N analysis.

3.3.1.3 Soil solution

Soil solution samples for all mineral soil depths (0, 10, 40 and 100 cm) were collected monthly by the lysimeters between January 2002 and June 2004 in each ^{15}N -labelled subplot and the ambient control plot. The concentrations of NH_4^+ -, NO_3^- -N and total dissolved N in the samples were measured using continuous flow injection colorimetry (Cenco/Skalar Instruments, Breda, the Netherlands). ^{15}N was analysed either for the 100 cm mineral soil depth in quarterly mixed samples (i.e., 4 quarters per year with 5 replicates per quarter) or for all sampling depths only in two selected months per year (i.e., May 2002, 2003, 2004, December 2002 and 2003, Fig. 3.3).

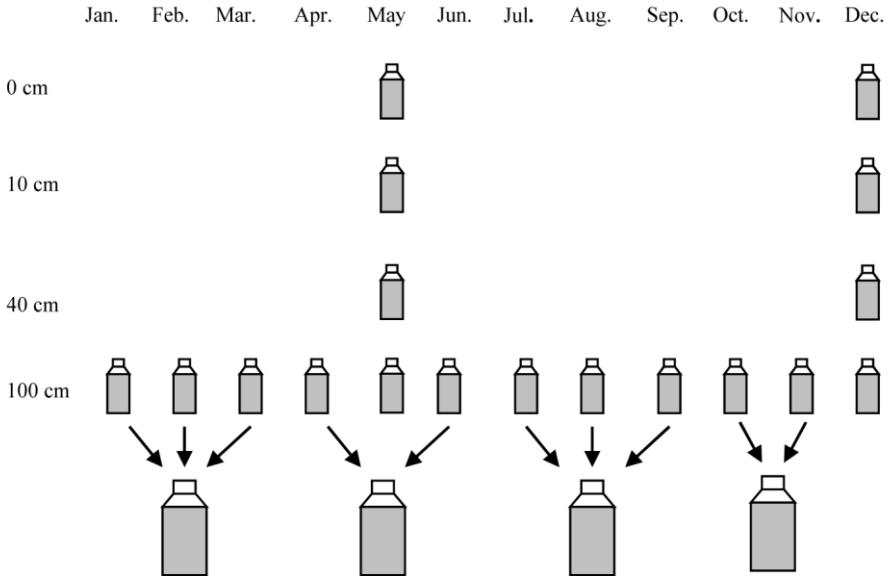


Fig. 3.3. Mixture of soil solution samples for ^{15}N analysis in each ^{15}N -labelled subplot of the clean rain and the roof control plot.

^{15}N abundance in the soil solution samples was determined using a diffusion method (Stark and Hart 1996) modified by Corre et al. (2003). In the $^{15}\text{NH}_4^+$ determination, appropriate amounts of the soil solution samples containing at least $20 \mu\text{g N}$ were put into 150 ml glass bottles. 0.2 g MgO was added to raise the pH value of the solution and to release NH_3 . Two glass fibre filter paper disks, each of which was acidified by $10 \mu\text{L}$ of $2.5 \text{ mol L}^{-1} \text{KHSO}_4$, were wrapped in Teflon traps and immediately placed on the mouths of the bottles before the lids were fastened. N diffusions were conducted at the room temperature (approximately $22 \text{ }^\circ\text{C}$) for 6 days, during which the bottles were swirled twice a day. In the $^{15}\text{NO}_3^-$ determination, MgO was added and the soil solution samples were then left open for 6 days in order to eliminate the influence of NH_4^+ . Subsequently 0.2 g MgO and 0.4 g Devard's alloy were added. The following procedures (placement of Teflon tapes and swirl of the bottles) were as same as those in the $^{15}\text{NH}_4^+$ determination. In the ^{15}N measurement of DON, the soil solution samples were digested with persulfate in order to convert all N forms to NO_3^- (Cabrera and Beare 1993, see also Stark and Hart 1996). The soil solution samples and oxidizing reagent (15 g NaOH L^{-1} , $30 \text{ g H}_3\text{BO}_3 \text{ L}^{-1}$, $50 \text{ g K}_2\text{S}_2\text{O}_8 \text{ L}^{-1}$) were mixed at a volume ratio of 1:1 in 150 ml glass bottles and placed in an autoclave. The samples were heated at $130 \text{ }^\circ\text{C}$ for 1 hour. The persulfate digestion of the soil solution samples were diffused similarly as in the $^{15}\text{NO}_3^-$ measurement, except for a shorter (3-day) open period and the use of $2 \text{ ml } 10 \text{ mol L}^{-1} \text{NaOH}$ instead of 0.2 g MgO. Because

of the low N concentration in many soil solution samples, additional $(\text{NH}_4)_2\text{SO}_4$ (0.366 atom% ^{15}N) or KNO_3 (0.365 atom% ^{15}N) was used to increase N content in the soil solution if necessary.

3.3.2 Natural ^{15}N abundance and N content in ecosystem compartments

Natural ^{15}N abundance in the ecosystem compartments was either obtained from Sah et al. (2008) in the clean rain and the roof control plot prior to the addition of the ^{15}N tracers (needle, needle litter, fine root, soil and NO_3^- in soil solution), respectively, or measured from the samples collected in the ambient control plot (bole bark, bole wood and DON in soil solution). N content in each compartment was calculated as the product of N concentration and mass of the compartment. N concentration was estimated using own measurement. Needle biomass in different age classes was obtained from Dohrenbusch et al. (2002). Biomass of branches, bole bark and bole wood were calculated from the breast height diameter obtained from Jaehne (2000) and the model provide by Müller-Using et al. (2004). Biomass of twig and branch bark was assumed to be 10% of twig and branch wood (Knigge and Schulz 1966). Fine root biomass was obtained from Borken (personal communication, BITÖK, Bayreuth, Germany, 2004). Soil mass for different depths was estimated based on bulk density.

3.3.3 N fluxes

Fluxes of NH_4^+ -, NO_3^- - and DON-N were calculated by multiplying their concentrations in the throughfall water and the soil solution at the 10 and 100 cm mineral soil depths with the respective cumulative throughfall amount and soil seepage. The soil seepage at different soil depths was estimated by Xu (personal communication, School of Renewable Natural Resources, Louisiana State University Agricultural Center, USA, 2005) from the throughfall amount and seepage flow rates at the corresponding soil depths. Daily seepage flow rates were estimated with a soil water balance model that was based on Richards' equation (Richards 1931) for vertical flow in unsaturated soil. The total amount of water available for infiltration at the soil surface was the amount of the throughfall water. Daily evapotranspiration was estimated using the Penman-Monteith equation (Monteith and Unsworth 1990). The estimated evapotranspiration rates were reduced with an empirical reduction function by Feddes et al. (1976) for the soil water uptake by roots. The modelled results on soil seepage for the clean rain and the roof control plot were verified through the comparison of the simulated soil matric potentials at the depths of 10 and 100 cm against the measurements over 4 years from 1998 through 2001.

3.3.4 Calculation of ^{15}N excess and recovery

$\delta^{15}\text{N}$ excess was calculated from enriched ^{15}N value subtracted by natural ^{15}N abundance. ^{15}N abundance in DON was calculated as follow:

$$at.\%^{15}\text{N}_{DON} = \frac{[N_t] * at.\%^{15}\text{N}_t - [NH_4^+ - N] * at.\%^{15}\text{N}_{NH_4^+} - [NO_3^- - N] * at.\%^{15}\text{N}_{NO_3^-}}{[DON]} \quad (3.1)$$

where $[N_t]$, $[NH_4^+ - N]$, $[NO_3^- - N]$ and $[DON]$ are N concentration of total N, NH_4^+ , NO_3^- and DON, respectively; $at.\%^{15}\text{N}_t$, $at.\%^{15}\text{N}_{NH_4^+}$, $at.\%^{15}\text{N}_{NO_3^-}$ and $at.\%^{15}\text{N}_{DON}$ are the values of atom percent ^{15}N in total N, NH_4^+ , NO_3^- and DON, respectively.

In this ^{15}N tracer experiment, $\delta^{15}\text{N}$ excess was used for all tree compartments and soil after ^{15}N addition, whereas absolute $\delta^{15}\text{N}$ value was given for the soil solution because natural ^{15}N abundance was not determined for NO_3^- and DON in the soil solution at all depths.

The mass of ^{15}N recovered in each ecosystem compartment was determined according to ^{15}N mass balance (Nadelhoffer and Fry 1994) as follow:

$$^{15}\text{N}_{comp.} = \frac{m_{comp.} * (at.\%^{15}\text{N}_{comp.} - at.\%^{15}\text{N}_{ref.})}{at.\%^{15}\text{N}_{tracer} - at.\%^{15}\text{N}_{ref.}} \quad (3.2)$$

where $^{15}\text{N}_{comp.}$ is ^{15}N mass recovered in a labelled ecosystem compartment (g m^{-2}); $m_{comp.}$ is the N mass of the labelled compartment (g m^{-2}); $at.\%^{15}\text{N}_{comp.}$, $at.\%^{15}\text{N}_{ref.}$ and $at.\%^{15}\text{N}_{tracer}$ are the atom percent ^{15}N of the labelled compartment, the reference compartment (natural ^{15}N abundance) and the applied ^{15}N tracer. ^{15}N recovery in the labelled compartment was expressed as percent of total applied ^{15}N tracer.

For soil solution, ^{15}N flux was determined for each quarter and selected month. These ^{15}N fluxes were summarized in the experiment period and ^{15}N recovery was calculated.

^{15}N recoveries in the ecosystem compartments were calculated for the samples taken in 2002 and 2004. ^{15}N allocation within the ecosystem compartments followed a similar pattern in the both sampling years. In 2004, more age classes (needles) and deeper layers (fine roots and soil) were sampled and analyzed with longer experiment duration. Therefore, only the ^{15}N recoveries calculated for the samples taken in 2004 were presented. Because all organic layers sampled in 2004 already included litter (O_1), no needle litter sample was used for the calculation of ^{15}N recovery.

3.4 Density fractionation experiment

A part of the soil samples collected in June 2004 from O_{L+F+H} , 0-5 cm and 5-10 cm mineral soil layer in each ^{15}N -labelled subplot and the ambient control plot were used in the density fractionation experiment. The soil samples from the 0-5 cm and the 5-10 cm mineral soil layer in the $^{15}\text{NH}_4^+$ -labelled subplot of the clean rain plot were not included due to undetectable ^{15}N signal (Table 4.12). The soil samples were air or oven (5-10 cm, 40 °C) dried, sieved (< 2 mm) and roots were removed before the density fractionation.

3.4.1 Density fractionation procedure

The density fractionation was conducted following the procedure described by Golchin et al. (1994a, b, Fig. 3.4), except that a 16-h shaking with glass beads was used to instead sonification to disrupt aggregates.

5 g (O_{L+F+H}) or 10 g (mineral soil) soil samples were placed in 50-ml centrifuge tubes and 25 to 40 ml SPT (Sometu, Berlin, Germany) with a density of 1.6 g cm^{-3} were added. The centrifuge tubes were inverted gently five times by hand and stood for 30 minutes. After 60-minute centrifugation at 4700 rpm (revolutions per minute), the supernatants were filtered through micro filter papers (0.45 μm) under vacuum. For the organic layer samples, the tubes stood 30 minutes after centrifugation to separate floating particles and sediments; the floating particles were then removed firstly with a small spoon and placed directly on the micro filter papers due to a large quantity of particles in the supernatants (Rovira and Vallejo 2003). The obtained particles from the organic layer and the mineral soil samples were washed several times with distilled water, transferred to pre-weighed evaporating dishes, dried at 40 °C and weighed. The separated fraction was free light fraction (FL, $d < 1.6 \text{ g cm}^{-3}$).

In the residual soils in the tubes, 40 ml SPT ($d = 1.6 \text{ g cm}^{-3}$) and 10 glass beads (5 mm in diameter) were added. The tubes were shaken for 16 hours at 60 rpm to disrupt aggregates (Balesdent et al. 1991, see also John et al. 2005), left to stand for 30 minutes and centrifuged. The floating particles were filtered, washed, dried and weighed. The separated fraction was occluded fraction I (Ocl. I, $d < 1.6 \text{ g cm}^{-3}$).

Subsequently, 40 ml SPT ($d = 1.8 \text{ g cm}^{-3}$) were added. The tubes stood overnight and were shaken for 10 minutes at 100 rpm. After standing and centrifugation, the particles were filtered, washed, dried and weighed. The separated fraction was occluded fraction II (Ocl. II, $d = 1.6\text{-}1.8 \text{ g cm}^{-3}$).

The procedure for the separation of the Ocl.II fraction was repeated with SPT ($d = 2.0 \text{ g cm}^{-3}$), the separated fraction was occluded fraction III (Ocl.III, $d = 1.8\text{-}2.0 \text{ g cm}^{-3}$).

Finally, distilled water was added and mixed with the residual soils in the tubes. The tubes were shaken for 10 minutes, centrifuged for 30 minutes and the supernatants were removed. The processes were repeated five times. The soils were then transferred to pre-weighed glass beakers, dried and weighed. The fraction was dense fraction (DF, $d > 2.0 \text{ g cm}^{-3}$).

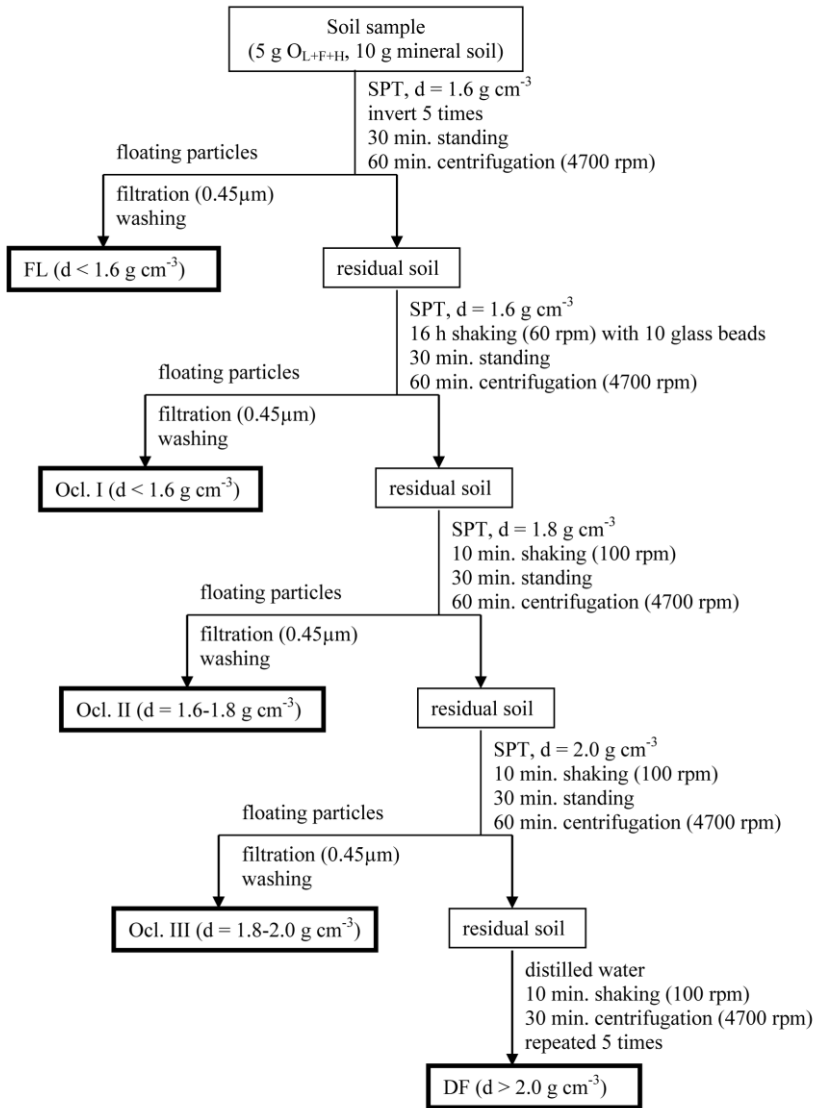


Fig. 3.4. Diagram of density fractionation procedure

3.4.2 Comparison of two aggregate-disrupting methods

For the samples taken from the organic layer and the 0-5 cm mineral soil layer in the ambient control plot, density fractionation was conducted using two different aggregate-disrupting methods. One method was 16-hour shaking with 10 glass beads, which was described as above. The other was sonification.

In the second method, the residual soils in the tubes were transferred to glass beakers with 40 ml SPT ($d = 1.6 \text{ g cm}^{-3}$) after the separation of the FL fraction. The beakers were placed into larger glass beakers with cool water and sonificated for 5 minutes using Branson 450-D. The soils were then transferred back to the tubes. The tubes stood for 30 minutes and were centrifuged. The following procedure was as same as that described above.

For the samples taken from the 5-10 cm mineral soil layer in the ambient control plot, aggregates were disrupted using sonification.

3.4.3 Preparation of density solution

150 g water was put into a 250-ml measuring cylinder and 25 g SPT was added. After SPT was completely dissolved, the solution was weighed and its volume was read from the cylinder. Subsequently, different amounts of SPT were gradually added, the procedure was repeated after each SPT addition.

3.4.4 Analysis and calculation

All separated fractions were grounded with a mortar and analyzed for C, N concentrations and ^{15}N abundances using IRMS. Because of the low pH value, inorganic C was absent in the soil. Total C concentration in the soil was equal to the concentration of soil organic C (OC).

The amount of soil ^{15}N recovered in each fraction was calculated according to ^{15}N mass balance (Nadelhoffer and Fry 1994). The recovery of soil ^{15}N in each fraction was expressed as the percentage of total soil ^{15}N and calculated as:

$$^{15}\text{N}_{\text{frac.}} (\%) = \frac{m_{\text{frac.}} * (\text{at.}\% ^{15}\text{N}_{\text{frac.}} - \text{at.}\% ^{15}\text{N}_{\text{ref.}})}{m_{\text{soil}} * (\text{at.}\% ^{15}\text{N}_{\text{soil}} - \text{at.}\% ^{15}\text{N}_{\text{ref.}})} * 100 \quad (3.3)$$

where $^{15}\text{N}_{\text{frac.}}$ is the percentage recovery of soil ^{15}N in a separated fraction; $m_{\text{frac.}}$ and m_{soil} are N mass of the separated fraction and the soil (g m^{-2}); $\text{at.}\% ^{15}\text{N}_{\text{frac.}}$, $\text{at.}\% ^{15}\text{N}_{\text{soil}}$ and $\text{at.}\% ^{15}\text{N}_{\text{ref.}}$ are atom percent ^{15}N of the separated fraction, the soil and the reference fraction (natural ^{15}N abundance).

For the soil samples taken from the organic layers and the 0-5 cm mineral soil layers, C and N concentrations of the soils were measured based on air-dried level, whereas those of the separated fractions were determined based on the oven-dried

level (40 °C). In order to reduce error caused by the temperature difference, sub-samples of the soils from the organic layers and the 0-5 cm mineral soil layers were taken, dried at 40 °C and water contents were calculated. C and N concentrations of these soil samples were recalculated based on the water contents.

With the assumption that the volume change of SPT solution is linearly correlated to the amount of added SPT (equation 3.4) and the density equation (equation 3.5), the amount of SPT and the volume of water needed for a SPT solution with an expected volume and density were calculated with equation 3.6 and 3.7:

$$V - V_{H_2O} = k * m_{SPT} \quad (3.4)$$

$$\rho = \frac{m_{SPT} + m_{H_2O}}{V} \quad (3.5)$$

$$m_{SPT} = \frac{V * (\rho - 1)}{(1 - k)} \quad (3.6)$$

$$V_{H_2O} = \frac{V * (1 - k \rho)}{(1 - k)} \quad (3.7)$$

where m_{SPT} and m_{H_2O} are the amount of SPT and H_2O in g, respectively; V and V_{H_2O} are the volume of SPT solution and water in ml, respectively; ρ is the density of SPT solution in $g\ cm^{-3}$; k is a constant.

3.5 Statistical analysis

In the study, both the two roofed plots and the ^{15}N applications had no replication. Statistical analyses were based on replicates within each ^{15}N -labelled subplot (i.e. pseudoreplicates). The nonparametric statistics (Mann-Whitney U Test) was used to test significant differences at $p \leq 0.05$ in N concentration, N fluxes and ^{15}N recovery for each ecosystem compartment (^{15}N tracer experiment) as well as in proportion of soil dry weight, of soil OC and N, in C and N concentration, the ratio of C/N and the recovery of soil ^{15}N for each fraction (density fractionation experiment) between the $^{15}NH_4^+$ - and $^{15}NO_3^-$ -labelled subplot within each roofed plot and between the clean rain and the roof control plot for each ^{15}N tracer. The difference was regarded as a tendency when the p-level was between 0.05 and 0.1. All statistical procedures were performed using the STATISTICA software package (StatSoft Europe GmbH, Hamburg, Germany).

4 Results

4.1 ^{15}N tracer experiment

4.1.1 The roof control plot

4.1.1.1 *Natural ^{15}N abundance*

In the roof control plot, all tree compartments showed negative natural ^{15}N abundance (Table 4.1). The mean $\delta^{15}\text{N}$ value of current year needles was -2.5‰ . The mean $\delta^{15}\text{N}$ value of bole bark, bole wood and needle litter samples were lower than that of green needles, except for the bole woods produced from 1972 to 1991. Compared with the bole bark, the bole wood showed a slightly higher average $\delta^{15}\text{N}$ value (-1.6‰ to -3.9‰). Natural ^{15}N abundance of the live fine roots increased with soil depth. The mean $\delta^{15}\text{N}$ value of the live fine roots increased from -4.2‰ in the O_H -layer to -0.6‰ in the 10-40 cm mineral soil layer. The natural ^{15}N abundance of the needles was within the range of the live fine roots in the upper and deeper soil layers. Compared to the live fine roots, a stronger increase of the mean $\delta^{15}\text{N}$ value was observed in the soil, from -2.2‰ in the organic layer to 7.2‰ in the 10-20 cm mineral soil layer. Since $\delta^{15}\text{N}$ value of the soil in each soil layer was not significantly different between the roof control plot and the clean rain plot (Table 4.1, 4.7), the averaged values of the two plots were used for calculation ($\delta^{15}\text{N}$ excess and ^{15}N recovery) and for extrapolation of natural ^{15}N abundances of deeper soil layers. In the same layer, the live fine roots had a lower $\delta^{15}\text{N}$ value than the soil. Generally, natural ^{15}N abundance in this Norway spruce forest ecosystem followed the pattern: tree compartments < organic layer < mineral soil.

Natural ^{15}N abundance of NH_4^+ was positive in the throughfall water (16.9‰ , Table 4.2) but could not be determined in the soil solution, since the concentration of $\text{NH}_4^+\text{-N}$ in the soil solution was below the detection limit of 0.15 mg L^{-1} . Natural ^{15}N abundances of NO_3^- in both the throughfall water and the soil solution were negative. The mean $\delta^{15}\text{N}$ value of NO_3^- was -11.5‰ in the throughfall water and varied from -4.3‰ to -3.2‰ in leachate at the different soil depths. Natural ^{15}N abundance of DON in the soil solution was positive, ranging from 6.4‰ at the 10 cm mineral soil depth to 5.6‰ at the 100 cm mineral soil depth.

Table 4.1. Natural ^{15}N abundances (mean \pm 1_{SE}) of main tree compartments and soil of the 75-year-old spruce forest in the roof control plot.

Compartment	$\delta^{15}\text{N}$ (‰)	SE
Needle		
current year	-2.5	0.2
Bole bark		
outer	-4.8	0.5
inner	-4.1	0.2
Bole wood produced in		
2002-2004	-3.9	0.1
1997-2001	-3.3	0.6
1992-1996	-3.0	0.1
1972-1991	-1.6	0.6
1952-1971	-2.9	0.5
< 1952	-2.6	0.9
Needle litter	-4.3	0.2
Live fine roots in		
O _H	-4.2	1.3
0-10 cm mineral soil	-3.5	0.9
10-40 cm mineral soil	-0.6	1.8
Soil		
O _{L+F+H}	-2.2	0.4
0-5 cm	2.9	0.4
5-10 cm	5.0	0.1
10-20 cm	7.2	0.6
20-30 cm	*8.4	
30-40 cm	*9.1	
40-60 cm	*9.7	
60-100 cm	*9.7	

*Natural ^{15}N abundance was estimated using extrapolation based on average values of the upper soil in the clean rain and the roof control plot.

4.1.1.2 N content in ecosystem compartments and N fluxes

Total N content in the trees amounted to 880 kg ha⁻¹ in the roof control plot (Table 4.3). Much of the total N content was found in the bole and needle biomass. The bole bark and bole wood contained 504 kg N ha⁻¹, accounting for 57% of the total N in the trees. The needles contained 276 kg N ha⁻¹, accounting for 31% of the total N in the trees. About 100 kg N ha⁻¹ were contained in the twigs, branches, needle litter and live fine roots. Soil was the largest N pool in the spruce forest ecosystem (Table 4.4). In total 9089 kg N ha⁻¹ were accumulated in the or-

ganic layer and the top 100 cm mineral soil. The organic layer alone contained 1585 kg N ha⁻¹, accounting for 17% of the total soil N content.

Table 4.2. Natural ¹⁵N abundance (mean ± 1_{SE}) of the throughfall water and the soil solution of the 75-year-old spruce forest in the roof control plot.

Compartment	$\delta^{15}\text{N-NH}_4^+$ (‰)	$\delta^{15}\text{N-NO}_3^-$ (‰)	$\delta^{15}\text{N-DON}$ (‰)
Throughfall	16.9 (2.2)	-11.5 (2.4)	n.d.
Soil solution			
10 cm mineral soil depth	n.d.	-4.3 (2.4)	6.4 (2.3)
100 cm mineral soil depth	n.d.	-3.2 (3.6)	5.6 (5.6)

n.d. = not determined.

In the ¹⁵NH₄⁺- and ¹⁵NO₃⁻-labelled subplot of the roof control plot, annual N fluxes in the soil solution at the 100 cm mineral soil depth were lower than those at the 10 cm mineral soil depth (Table 4.5). In the soil solution at the 10 cm mineral soil depth, the annual N fluxes were not significantly different between the ¹⁵NH₄⁺- and ¹⁵NO₃⁻-labelled subplot of the roof control plot. In the soil solution at the 100 cm mineral soil depth, however, the difference in annual N fluxes between the two ¹⁵N-labelled subplots of the roof control plot was significant. NH₄⁺- and NO₃⁻-N flux at the 100 cm mineral soil depth were obviously lower in the ¹⁵NH₄⁺-labelled subplot (0 and 4.6 kg ha⁻¹ yr⁻¹, respectively) than those in the ¹⁵NO₃⁻-labelled subplot (0.8 and 10.1 kg ha⁻¹ yr⁻¹, respectively).

4.1.1.3 ¹⁵N enrichment in ecosystem compartments

In the ¹⁵NH₄⁺- and ¹⁵NO₃⁻-labelled subplot of the roof control plot, $\delta^{15}\text{N}$ excess of the needles declined with increased age classes (Fig. 4.1). A clear ¹⁵N signal was shown in both the young needles that grew after ¹⁵N tracer addition (42-92‰ $\delta^{15}\text{N}$ excess) and the needles of older age classes (15-41‰ $\delta^{15}\text{N}$ excess). For the needles of each age class, the $\delta^{15}\text{N}$ excess was similar between the two ¹⁵N-labelled subplots.

Table 4.3. Masses, N concentration and contents of main tree compartments of the 75-year-old spruce forest in the roof control plot.

Compartment	Masse (kg ha ⁻¹)	N (mg g ⁻¹)	C/N	N content (kg ha ⁻¹)
Needle				
current year	7229	13.4	38	97
1-year-old	5622	14.7	35	83
2-year-old	4076	13.8	37	56
3-year-old	2249	13.2	39	30
4-year-old	884	11.6	43	10
5-year-old	10	11.0	45	0
subtotal	20100			276
Twig and branch				
bark				
current year	41	6.2	82	0.3
1-year-old	41	7.1	71	0.3
2-year-old	41	7.1	72	0.3
3-year-old	41	8.5	59	0.4
4-year-old	41	8.4	58	0.3
>4-year-old	41	7.2	68	0.3
wood				
current year	413	10.5	45	4.3
1-year-old	413	9.1	55	3.7
2-year-old	413	6.9	75	2.8
3-year-old	413	4.5	112	1.9
4-year-old	413	3.5	143	1.5
>4-year-old	413	2.9	167	1.2
subtotal	2723			17.3
Bole bark				
outer	9557	4.7	103	45
inner	10671	5.6	85	59
Bole wood produced in				
2002-2004	15459	2.6	176	40
1997-2001	25765	1.3	385	33
1992-1996	25765	1.2	363	31
1972-1991	103059	1.1	354	116
1952-1971	103059	0.9	459	93
<1952	92753	0.9	511	86
subtotal (bark+wood)	386088			504
Needle litter	2077	12.1	38	25
Live fine roots in				
O _H	1816	13.2	37	24
0-10 cm mineral soil	967	11.9	35	11
10-40 cm mineral soil	1957	11.1	35	22
subtotal	4740			57
Total tree	413651			880

Table 4.4. Masses, C-, N concentration and N contents of soil of the 75-year-old spruce forest in the roof control plot.

Depth	Masse (kg ha ⁻¹)	C (mg g ⁻¹)	N (mg g ⁻¹)	C/N	N pool (kg ha ⁻¹)
O _{L+F+H}	114031	352	13.9	25	1585
0-5 cm	356212	57	2.6	22	932
5-10 cm	389500	39	1.7	22	676
10-20 cm	790000	28	1.3	21	1037
20-30 cm	856000	16	0.9	18	777
30-40 cm	856000	11	0.7	14	634
40-60 cm	2308800	5	0.5	10	1149
60-100 cm	4617600	5	0.5	10	2298
total	10288143				9089

Table 4.5. Annual N fluxes (kg ha⁻¹ yr⁻¹) (mean ± 1_{SE}) in the roof control plot during Jan.02 and Jun.04.

	NH ₄ ⁺ -N	NO ₃ ⁻ -N	DON	N _t
10 cm mineral soil depth				
¹⁵ NH ₄ ⁺ subplot	0.0 (0.0)	12.4 (3.0)	3.0 (0.3)	15.5 (3.0)
¹⁵ NO ₃ ⁻ subplot	1.2 (0.6)	18.1 (2.5)	3.1 (0.3)	22.4 (3.0)
100 cm mineral soil depth				
¹⁵ NH ₄ ⁺ subplot	0.0 ^a (0.0)	4.6 ^a (1.3)	0.9 (0.2)	5.4 ^a (1.2)
¹⁵ NO ₃ ⁻ subplot	0.8 ^b (0.4)	10.1 ^b (0.6)	1.5 (0.2)	12.4 ^b (0.7)

Different letters show the significant difference between the ¹⁵NH₄⁺- and ¹⁵NO₃⁻-labelled subplot of the roof control plot (Mann-Whitney U Test, p ≤ 0.05).

The δ¹⁵N excess of the bark and wood of the twig and branch samples followed similar pattern as the needle samples in the roof control plot (Fig. 4.2). The mean δ¹⁵N excess declined from 42.6‰ in current year bark to 20.6‰ in > 4-year-old bark after ¹⁵NH₄⁺ addition and from 55.5‰ to 27.0‰ after ¹⁵NO₃⁻ addition. Between the two ¹⁵N tracers, the δ¹⁵N excess of the bark and wood of the twig and branch samples were not different.

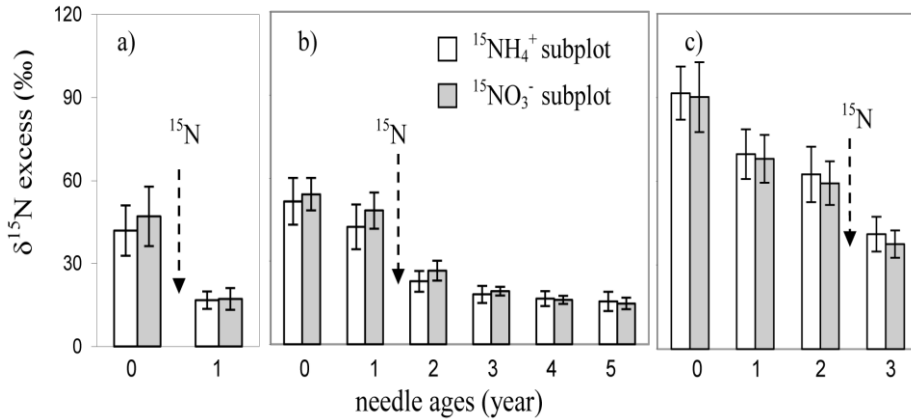


Fig. 4.1. $\delta^{15}\text{N}$ excess (mean $\pm 1\text{SE}$) of needles of different age classes in a) 2002; b) 2003; c) 2004 in the $^{15}\text{NH}_4^+$ - and $^{15}\text{NO}_3^-$ -labelled subplot of the roof control plot ($n = 6$). Arrow shows the time when ^{15}N tracer addition began.

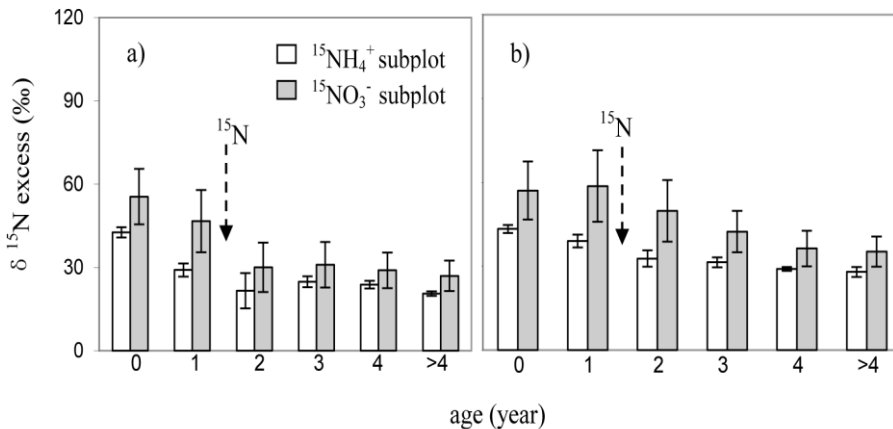


Fig. 4.2. $\delta^{15}\text{N}$ excess (mean $\pm 1\text{SE}$) of a) bark; b) wood of twigs and branches with different age classes in 2003 in the $^{15}\text{NH}_4^+$ - and $^{15}\text{NO}_3^-$ -labelled subplot of the roof control plot ($n = 3$). Arrow shows the time when ^{15}N tracer addition began.

In the tree boles, the same tendencies were observed in the two ^{15}N -labelled subplots of the roof control plot (Fig. 4.3). The mean $\delta^{15}\text{N}$ excess of the inner bark was 29.6‰ in the $^{15}\text{NH}_4^+$ -labelled subplot and 50.9‰ in the $^{15}\text{NO}_3^-$ -labelled subplot. These values were higher than those of the outer bark (11.5‰ and 7.7‰, respectively). The $\delta^{15}\text{N}$ excess of the bole wood decreased with wood age. A noticeable ^{15}N signal was detected also in the bole wood produced decades ago. The

mean $\delta^{15}\text{N}$ excess of the bole wood produced from 1972 to 1991 was 26.4‰ in the $^{15}\text{NH}_4^+$ -labelled subplot and 41.5‰ in the $^{15}\text{NO}_3^-$ -labelled subplot. In the bole wood produced before 1972, the mean $\delta^{15}\text{N}$ excess was smaller than 1.8‰.

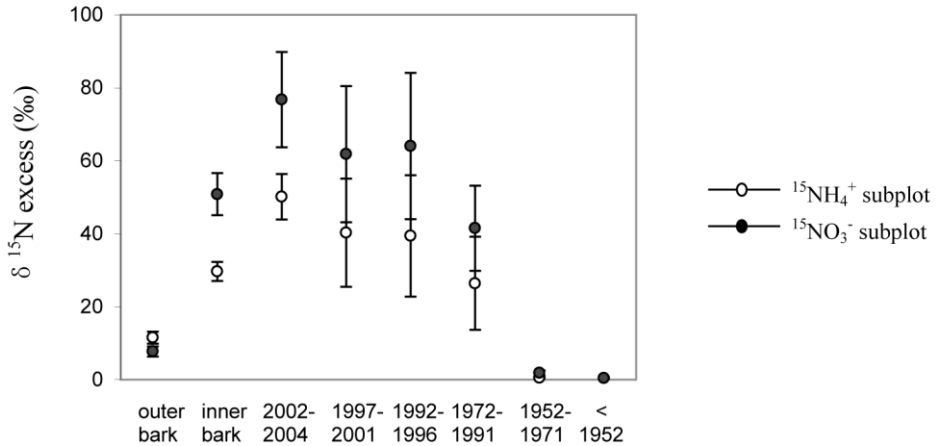


Fig. 4.3. $\delta^{15}\text{N}$ excess (mean \pm 1SE) of bole bark and different increments of bole wood in the $^{15}\text{NH}_4^+$ - and $^{15}\text{NO}_3^-$ -labelled subplot of the roof control plot ($n = 3$) after over 3 year ^{15}N addition (2001-2004).

In spring 2003, the mean $\delta^{15}\text{N}$ excess of the needle litter was 10.2‰ in the $^{15}\text{NH}_4^+$ -labelled subplot and 11.1‰ in the $^{15}\text{NO}_3^-$ -labelled subplot. The values were similar to those in autumn 2003 and did not differ significantly from those of ≥ 5 -year-old needles, which varied from 14.7‰ to 16.5‰.

In 2002, the mean $\delta^{15}\text{N}$ excess of the live and dead fine roots in the organic layer was not significantly different between in the $^{15}\text{NH}_4^+$ -labelled subplot (133‰) and in the $^{15}\text{NO}_3^-$ -labelled subplot (52‰) of the roof control plot (Fig. 4.4). The $\delta^{15}\text{N}$ excess declined with soil depth in the $^{15}\text{NH}_4^+$ -labelled subplot, whereas the value rose in the $^{15}\text{NO}_3^-$ -labelled subplot. In 2004, the live fine roots had the same pattern as in 2002. The mean $\delta^{15}\text{N}$ excess of the live fine roots in the organic layer was 213‰ in the $^{15}\text{NH}_4^+$ -labelled subplot and 93‰ in the $^{15}\text{NO}_3^-$ -labelled subplot. In the 10-40 cm mineral soil layer, the mean $\delta^{15}\text{N}$ excess of the live fine roots declined to 102‰ in the $^{15}\text{NH}_4^+$ -labelled subplot, whereas it increased to 239‰ in the $^{15}\text{NO}_3^-$ -labelled subplot.

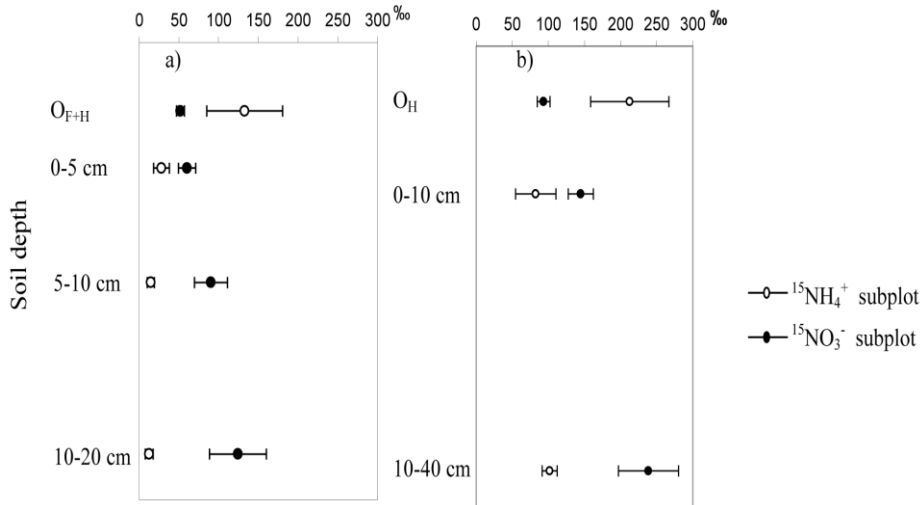


Fig. 4.4. $\delta^{15}\text{N}$ excess (mean \pm 1SE) of a) live and dead fine roots (2002); b) live fine roots (2004) at different soil depths in the $^{15}\text{NH}_4^+$ - and $^{15}\text{NO}_3^-$ -labelled subplot of the roof control plot ($n = 5$ in 2002, $n = 4$ and 3 in 2004 in the $^{15}\text{NH}_4^+$ and $^{15}\text{NO}_3^-$ subplot, respectively).

The $\delta^{15}\text{N}$ excess of the organic layer was higher in the $^{15}\text{NH}_4^+$ -labelled subplot than in the $^{15}\text{NO}_3^-$ -labelled subplot of the roof control plot (Fig. 4.5). In 2002, the mean $\delta^{15}\text{N}$ excess was 12‰ in the $^{15}\text{NH}_4^+$ -labelled subplot and 4‰ in the $^{15}\text{NO}_3^-$ -labelled subplot. In 2004, the mean $\delta^{15}\text{N}$ excess of the organic layer increased to 43‰ in the $^{15}\text{NH}_4^+$ -labelled subplot, whereas the value kept low (6‰) in the $^{15}\text{NO}_3^-$ -labelled subplot. In the $^{15}\text{NH}_4^+$ -labelled subplot, the $\delta^{15}\text{N}$ excess decreased drastically from the organic layer to the mineral soil. The ^{15}N signal was hardly detectable in the mineral soil below the 5 cm (2002) or 20 cm (2004). In the $^{15}\text{NO}_3^-$ -labelled subplot, the $\delta^{15}\text{N}$ excess was relative stable throughout all measured soil depths. A detectable ^{15}N signal was still shown in 2004 at the 40-60 cm mineral soil depth with 2‰ $\delta^{15}\text{N}$ excess.

The mean $\delta^{15}\text{N-NO}_3^-$ in the soil solution collected in the selected months was higher in the $^{15}\text{NO}_3^-$ -labelled subplot than in the $^{15}\text{NH}_4^+$ -labelled subplot of the roof control plot at the 0, 10 and 40 cm mineral soil depths, whereas no difference was found at the 100 cm mineral soil depth (Fig. 4.6). Based on the quarterly mixed samples for the output calculation at the 100 cm mineral soil depth (January 2002 to June 2004), the average $\delta^{15}\text{N-NO}_3^-$ was 493‰ in the $^{15}\text{NH}_4^+$ -labelled subplot and 728‰ in the $^{15}\text{NO}_3^-$ -labelled subplot.

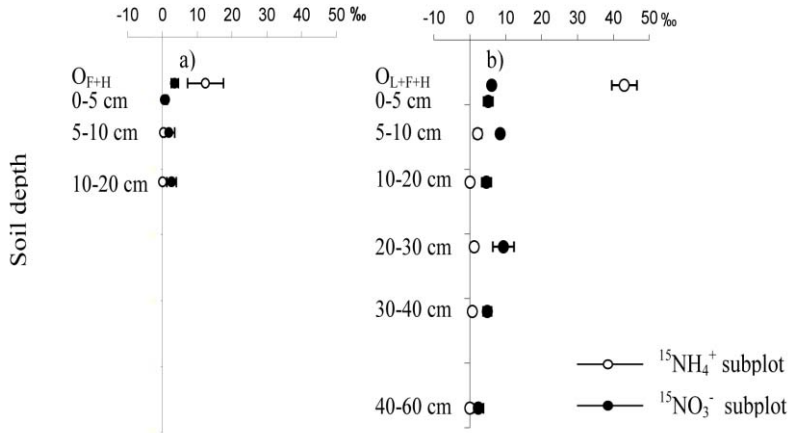


Fig. 4.5. $\delta^{15}\text{N}$ excess (mean \pm 1SE) of soil at different depths in a) 2002; b) 2004 in the $^{15}\text{NH}_4^+$ - and $^{15}\text{NO}_3^-$ -labelled subplot of the roof control plot ($n = 5$). Soil samples taken in 2002 were only to 20 cm mineral soil.

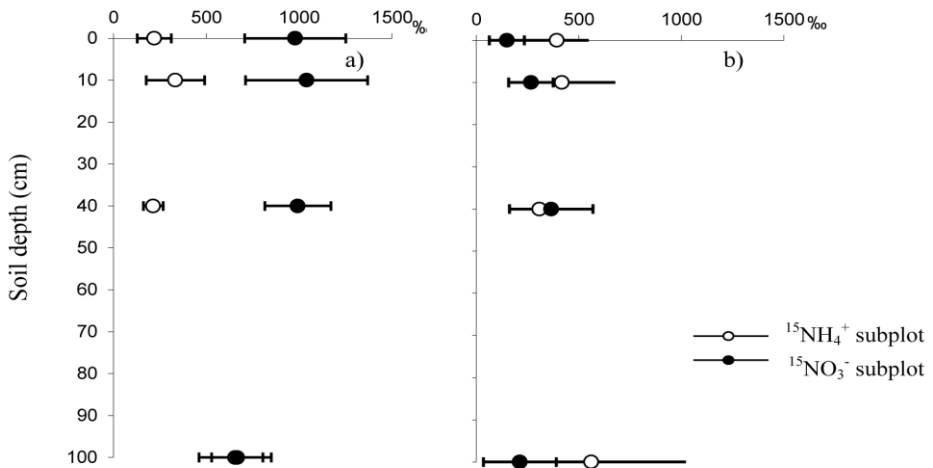


Fig. 4.6. Gradient of ^{15}N abundance (mean \pm 1SE) of a) NO_3^- ; b) DON in soil solution collected in selected months (Mai 2002, 2003, 2004, December 2002 and 2003) in the $^{15}\text{NH}_4^+$ - and $^{15}\text{NO}_3^-$ -labelled subplot of the roof control plot ($n = 5$).

The ^{15}N abundance of DON in the soil solution showed similar values at all measured soil depths and did not differ between the two ^{15}N -labelled subplots of the roof control plot (Fig. 4.6). In the quarterly mixed samples at the 100 cm min-

eral soil depth (January 2002 to June 2004), the mean $\delta^{15}\text{N}$ -DON was 351‰ in the $^{15}\text{NH}_4^+$ -labelled subplot and 317‰ in the $^{15}\text{NO}_3^-$ -labelled subplot.

4.1.1.4 ^{15}N recovery in ecosystem compartments

In the roof control plot, about 15% of added ^{15}N were found in the needles for the both ^{15}N tracers (Table 4.6). ^{15}N recovery was highest in the current year needles (7%) and declined with increased age classes. In the 3-year-old needles, ^{15}N recovery was only 1%.

Woody tissues (twigs, branches and boles) retained a large proportion of the added ^{15}N in the roof control plot. ^{15}N recovery in the boles was higher than that in the twigs and branches. In the $^{15}\text{NH}_4^+$ -labelled subplot, 0.7% of ^{15}N was found in the twigs and branches and 6.7% in the boles. ^{15}N recovery was 1.1% in the twigs and branches and 12.2% in the boles in the $^{15}\text{NO}_3^-$ -labelled subplot. In the two ^{15}N -labelled subplots of the roof control plot, ^{15}N recovery in the inner bark was higher than that in the outer bark. ^{15}N in the bole wood was concentrated in the wood produced between 1972 and 2004. Less than 0.2% of ^{15}N was found in the bole wood produced before 1972.

In the roof control plot, 6.8% of added $^{15}\text{NH}_4^+$ and 7.1% of added $^{15}\text{NO}_3^-$ were recovered in the live fine roots. The recovery of $^{15}\text{NH}_4^+$ tended to be higher in the live fine roots in the organic layer (O_H horizon, 4.2%) than in those in the 0-10 cm mineral soil layer (0.9%, $p = 0.06$). In the live fine roots in the organic layer, the recovery of $^{15}\text{NH}_4^+$ seemed to be higher (4.2%) than that of $^{15}\text{NO}_3^-$ (1.8%), although this difference was not statistically significant. In the live fine roots in the 10-40 cm mineral soil layer, the recovery of $^{15}\text{NO}_3^-$ was conversely higher (4.1%) than that of $^{15}\text{NH}_4^+$ (1.8%, $p = 0.06$).

In total, 30.0% of the added $^{15}\text{NH}_4^+$ and 35.6% of the added $^{15}\text{NO}_3^-$ were found in the tree compartments (needles, twigs, branches, boles and live fine roots) in the roof control plot. As ^{15}N recovery in each tree compartment was not statistically different between the two ^{15}N -labelled subplots of the roof control plot, the total recoveries of the two ^{15}N tracers in the tree compartments should not differ from each other in the roof control plot.

Soil retained the largest proportion of ^{15}N tracers in the roof control plot. 71.1% of the added $^{15}\text{NH}_4^+$ and 42.2% of the added $^{15}\text{NO}_3^-$ were found in the organic layer and the top 100 cm mineral soil. In the $^{15}\text{NH}_4^+$ -labelled subplot, most ^{15}N was accumulated in the organic layer (64.6%). ^{15}N recovery in the mineral soil was low (6.4%) and decreased with soil depth. Only < 1.2% of the added $^{15}\text{NH}_4^+$ was found in the mineral soil below the 10 cm soil depth. In the $^{15}\text{NO}_3^-$ -labelled subplot, only 8.0% of the added ^{15}N was recovered in the organic layer, whereas 34.2% of the applied ^{15}N was distributed evenly across the analysed mineral soil depths.

Table 4.6. Percent ^{15}N recoveries (mean \pm 1SE) in main spruce forest ecosystem compartments in the roof control plot in 2004.

Compartment	$^{15}\text{NH}_4^+$ subplot	$^{15}\text{NO}_3^-$ subplot
Needle		
current year	7.1 (0.9)	7.2 (1.0)
1-year-old	4.6 (0.6)	4.5 (0.5)
2-year-old	2.9 (0.5)	2.6 (0.3)
3-year-old	1.0 (0.2)	0.9 (0.1)
subtotal	15.7	15.2
Twig and branch		
bark	0.1 (0.0)	0.1 (0.0)
wood	0.7 (0.1)	1.1 (0.2)
subtotal	0.7	1.1
Bole bark		
outer	0.4 (0.1)	0.2 (0.0)
inner	1.2 (0.1)	2.3 (0.3)
Bole wood formed in		
2002-2004	1.6 (0.1)	1.9 (0.2)
1997-2001	0.8 (0.3)	1.9 (0.9)
1992-1996	0.7 (0.3)	1.6 (0.4)
1972-1991	1.9 (0.9)	4.2 (1.3)
1952-1971	0.0 (0.0)	0.1 (0.0)
<1952	0.0 (0.0)	0.0 (0.0)
subtotal (bark+wood)	6.7	12.2
Live fine roots in		
O ₁₁	4.2 (1.2)	1.8 (0.2)
0-10 cm	0.9 (0.3)	1.2 (0.2)
10-40 cm	1.8 (0.3)	4.1 (0.7)
subtotal	6.8	7.1
subtotal (tree)	30.0	35.6
Soil		
O _{L+F+H}	64.6 (5.5) a	8.0 (1.2) b
0-5 cm	4.2 (1.1)	4.3 (0.8)
5-10 cm	1.1 (0.4) a	4.5 (0.2) b
10-20 cm	0.1 (0.1) a	3.9 (0.7) b
20-30 cm	0.8 (0.3) a	6.9 (2.5) b
30-40 cm	0.3 (0.2) a	2.8 (0.7) b
40-60 cm	0.0 (0.0)	3.9 (2.6)
60-100 cm	0.0 (0.0)	7.9 (5.2)
subtotal (mineral soil)	6.4 a	34.2 b
subtotal (organic layer + mineral soil)	71.1	42.2
Leaching at 100 cm mineral soil depth		
NO ₃ ⁻	3.4 (1.3)	19.2
DON	0.4 (0.0)	0.6 (0.2)
subtotal	3.7	19.8
Total	104.8	97.6

Different letters show the significant difference between the $^{15}\text{NH}_4^+$ - and $^{15}\text{NO}_3^-$ -labelled subplot of the roof control plot (Mann-Whitney U Test, $p \leq 0.05$).

The ^{15}N tracers appeared also in nitrate and DON leachate in the two ^{15}N -labelled subplots of the roof control plot. At the 100 cm mineral soil depth, the ^{15}N recovery in the nitrate leachate was higher in the $^{15}\text{NO}_3^-$ -labelled subplot (19.2%) than in the $^{15}\text{NH}_4^+$ -labelled subplot (3.4%). Mean ^{15}N recovery in the DON leachate was lower than 0.8% in the two ^{15}N -labelled subplots.

4.1.2 The clean rain plot

4.1.2.1 Natural ^{15}N abundance

Natural ^{15}N abundances of the spruce forest ecosystem compartments in the clean rain plot showed similar patterns as those in the roof control plot. The natural ^{15}N abundances of the tree compartments were negative in the clean rain plot, except for the live fine roots in the 10-40 cm mineral soil layer (Table 4.7). The mean $\delta^{15}\text{N}$ value of the current year needles was -3.5‰ and slightly higher than that of the needle litter (-4.4‰). The natural ^{15}N abundance of the live fine roots increased with soil depth. The mean $\delta^{15}\text{N}$ value of the live fine roots was -2.4‰ in the organic layer and increased to 1.6‰ in the 10-40 cm mineral soil layer. Compared to the live fine roots, soil showed a stronger increase of $\delta^{15}\text{N}$ value with soil depth, from -1.4‰ in the organic layer to 6.0‰ in the 10-20 cm mineral soil layer. In the same layer, the natural ^{15}N abundance of the soil was always higher than that of the live fine roots.

In the clean rain plot, the natural ^{15}N abundance of NH_4^+ in the throughfall water and the soil solution could not be determined as the ^{15}N signal was below the detection limit of IRMS (Sah et al. 2008, Table 4.8). The natural ^{15}N abundance of NO_3^- in the throughfall water and the soil solution were negative in the clean rain plot. The mean $\delta^{15}\text{N}$ value of NO_3^- was -9.3‰ in the throughfall water and varied from -6.3‰ to -2.0‰ in the soil solution at different soil depth.

4.1.2.2 N content in ecosystem compartments and N fluxes

N concentration of the tree compartments was generally lower in the clean rain plot than that in the roof control plot (Table 4.9). However, trees in the clean rain plot contained 947 kg N ha^{-1} and the value was higher than that in the roof control plot, mainly due to the higher basal area in the clean rain plot. As in the roof control plot, most of tree N in the clean rain plot was found in the boles and the needles, containing 554 kg N ha^{-1} and 292 kg N ha^{-1} , respectively. The twigs, the branches, the needle litter and the live fine roots together contained about 100 kg N ha^{-1} . N concentration and contents of the soil in the clean rain plot did not differ from those in the roof control plot (Table 4.10). The organic layer and the top 100 cm mineral soil contained $9161 \text{ kg N ha}^{-1}$ in the clean rain plot.

Table 4.7. Natural ^{15}N abundances of main tree compartments and soil of the 75-year-old spruce forest in the clean rain plot.

Compartment	$\delta^{15}\text{N}$ (‰)	SE
Needle		
current year	-3.5	0.2
Bole bark		
outer	-4.8	0.5
inner	-4.1	0.2
Bole wood produced in		
2002-2004	-3.9	0.1
1997-2001	-3.3	0.6
1992-1996	-3.0	0.1
1972-1991	-1.6	0.6
1952-1971	-2.9	0.5
< 1952	-2.6	0.9
Needle litter	-4.4	0.2
Live fine roots in		
O_H	-2.4	0.6
0-10 cm mineral soil	-1.9	0.6
10-40 cm mineral soil	1.6	1.0
Soil		
$\text{O}_{\text{L}+\text{F}+\text{H}}$	-1.4	0.1
0-5 cm	2.8	0.1
5-10 cm	5.5	0.6
10-20 cm	6.0	0.4
20-30 cm	*8.4	
30-40 cm	*9.1	
40-60 cm	*9.7	
60-100 cm	*9.7	

*Natural ^{15}N abundance was estimated using extrapolation based on average values of the upper soil in the clean rain and the roof control plot.

Table 4.8. Natural ^{15}N abundance (mean $\pm 1\text{s.e.}$) of the throughfall water and the soil solution of the 75-year-old spruce forest in the clean rain plot.

Compartment	$\delta^{15}\text{N-NH}_4^+$ (‰)	$\delta^{15}\text{N-NO}_3^-$ (‰)	$\delta^{15}\text{N-DON}$ (‰)
Throughfall	n.d.	-9.3 (1.7)	n.d.
Soil solution			
10 cm mineral soil depth	n.d.	-6.3 (3.7)	6.4 (2.3)
100 cm mineral soil depth	n.d.	-2.0 (3.5)	5.6 (5.6)

n.d. = not determined.

In the soil solution at the 10 cm and the 100 cm mineral soil depth, NO_3^- -N and total dissolved N fluxes were obviously lower in the clean rain plot than in the roof control plot, while NH_4^+ -N and DON fluxes in the soil solution at the both mineral soil depths were either not significantly different between the two plots or slightly lower in the clean rain plot (Table 4.11). In the clean rain plot, NH_4^+ - and NO_3^- -N fluxes in the soil solution at the 10 cm mineral soil depth were significantly higher in the $^{15}\text{NO}_3^-$ -labelled subplot than in the $^{15}\text{NH}_4^+$ -labelled subplot, while the differences in N fluxes between the two ^{15}N -labelled subplots were not significant in the soil solution at the 100 cm mineral soil depth.

4.1.2.3 ^{15}N enrichment in ecosystem compartments

Evaluating ^{15}N abundances of the spruce forest ecosystem compartments, it should be noticed that the clean rain plot yielded different amount of $^{15}\text{N-NH}_4^+$ and $^{15}\text{N-NO}_3^-$. Moreover, the amounts of the two ^{15}N tracers yielded in the clean rain plot were different from those yielded in the roof control plot, respectively. Therefore, the direct comparison of ^{15}N abundance for each forest ecosystem compartment was not possible between the $^{15}\text{NH}_4^+$ - and $^{15}\text{NO}_3^-$ -labelled subplot within the clean rain plot as well as between the clean rain and the roof control plot for each ^{15}N tracer.

$\delta^{15}\text{N}$ excess of tree compartments in the clean rain plot showed similar patterns as in the roof control plot. In the $^{15}\text{NH}_4^+$ - and $^{15}\text{NO}_3^-$ -labelled subplot of the clean rain plot, $\delta^{15}\text{N}$ excess of aboveground tree tissues (needle, twig, branch and bole) decreased with increased tissue age (Table 4.12). $\delta^{15}\text{N}$ excess of the fine roots declined with soil depth in the $^{15}\text{NH}_4^+$ -labelled subplot, whereas the value rose in the $^{15}\text{NO}_3^-$ -labelled subplot, except for the samples take in 2002.

Table 4.9. Masses, N concentration and contents of main tree compartments of the 75-year-old spruce forest in the roof control and the clean rain plot.

Compartment	Masse (kg ha ⁻¹)		N (mg g ⁻¹)			C/N		N content (kg ha ⁻¹)		
	roof control	clean rain	roof control	clean rain		roof control	clean rain	roof control	clean rain	
Needle										
current year	7229	8392	13.4	12.7	*	38	39	97	106	
1-year-old	5622	6527	14.7	12.9	***	35	39	83	84	
2-year-old	4076	4732	13.8	12.3	**	37	41	56	58	
3-year-old	2249	2611	13.2	11.9	***	39	42	30	31	
4-year-old	884	1026	11.6	11.2		43	45	10	12	
5-year-old	10	47	11.0	9.8	**	45	51	0	0	
subtotal	20100	23333						276	292	
Twig and branch										
bark										
current year	41	52	6.2	7.2		82	71	0.3	0.4	
1-year-old	41	52	7.1	7.1		71	72	0.3	0.4	
2-year-old	41	52	7.1	7.0		72	72	0.3	0.4	
3-year-old	41	52	8.5	7.0	**	59	72	0.4	0.4	
4-year-old	41	52	8.4	6.6	***	58	76	0.3	0.3	
>4-year-old	41	52	7.2	6.7		68	75	0.3	0.3	
wood										
current year	413	519	10.5	8.0	**	45	60	4.3	4.1	
1-year-old	413	519	9.1	6.3	*	55	76	3.7	3.3	
2-year-old	413	519	6.9	4.0	**	75	125	2.8	2.1	
3-year-old	413	519	4.5	3.3	*	112	145	1.9	1.7	
4-year-old	413	519	3.5	2.6	**	143	181	1.5	1.4	
>4-year-old	413	519	2.9	2.8		167	176	1.2	1.4	
subtotal	2723	3427						17.3	16.1	
Bole bark										
outer	9557	11336	4.7	4.6		103	111	45	52	
inner	10671	12208	5.6	5.4		85	90	59	66	
Bole wood produced in										
2002-2004	15459	19429	2.6	1.5	***	176	327	40	29	
1997-2001	25765	32381	1.3	1.0		385	468	33	32	
1992-1996	25765	32381	1.2	0.9	**	363	503	31	30	
1972-1991	103059	129524	1.1	1.1		354	448	116	139	
1952-1971	103059	129524	0.9	0.8		459	502	93	110	
<1952	92753	116571	0.9			511	569	86	96	
subtotal (bark+wood)	386088	483352						504	554	
Needle litter										
	2077	2172	12.1	9.2	***	38	50	25	20	
Live fine roots in										
O _H	1816	3017	13.2	12.1		37	41	24	37	
0-10 cm mineral soil	967	1149	11.9	11.8		35	35	11	14	
10-40 cm mineral soil	1957	1667	11.1	8.9	***	35	50	22	15	
subtotal	4740	5833						57	65	
Total tree	413651	515945						880	947	

* showed difference in N concentration of main tree compartments between the clean rain and the roof control plot (Mann-Whitney U Test, * $p \leq 0.1$, ** $p \leq 0.05$, *** $p \leq 0.01$).

Table 4.10. Masses, C-, N concentration and N contents of soil of the 75-year-old spruce forest in the roof control and the clean rain plot.

Depth	Masse (kg ha ⁻¹)	C (mg g ⁻¹)		N (mg g ⁻¹)		C/N		N pool (kg ha ⁻¹)	
	clean rain roof control	roof control	clean rain	roof control	clean rain	roof control	clean rain	roof control	clean rain
O _{L+F+H}	114031	352 (15)	389 (10)	13.9 (0.4)	13.8 (0.5)	25	28	1585	1573
0-5 cm	356212	57 (2)	81 (7)	2.6 (0.1)	3.1 (0.3)	22	26	932	1110
5-10 cm	389500	39 (7)	33 (2)	1.7 (0.2)	1.6 (0.1)	22	20	676	640
10-20 cm	790000	28 (3)	21 (2)	1.3 (0.1)	1.1 (0.1)	21	18	1037	901
20-30 cm	856000	16 (1)	14 (1)	0.9 (0.0)	0.9 (0.1)	18	15	777	744
30-40 cm	856000	11 (1)	10 (1)	0.7 (0.05)	0.8 (0.03)	14	13	634	664
40-60 cm	2308800	5 (1)	6 (1)	0.5 (0.06)	0.5 (0.04)	10	11	1149	1176
60-100 cm	4617600	5	6	0.5	0.5	10	11	2298	2352
total	10288143							9089	9161

Table 4.11. Annual N fluxes ($\text{kg ha}^{-1} \text{ yr}^{-1}$) (mean \pm 1SE) in the roof control and the clean rain plot during Jan.02 and Jun.04.

	$\text{NH}_4^+\text{-N}$		$\text{NO}_3^-\text{-N}$		DON		N_t	
	roof control	clean rain	roof control	clean rain	roof control	clean rain	roof control	clean rain
10 cm mineral soil depth								
$^{15}\text{NH}_4^+$ subplot	0.0 ^a (0.0)	0.0 ^b (0.0)	12.4 ^a (3.0)	0.0 ^b (0.0)	3.0 (0.3)	2.6 (0.1)	15.5 ^a (3.0)	2.6 ^b (0.1)
$^{15}\text{NO}_3^-$ subplot	1.2 ^{ac} (0.6)	0.9 ^c (0.4)	18.1 ^a (2.5)	4.1 ^c (1.9)	3.1 (0.3)	2.5 (0.6)	22.4 ^a (3.0)	7.6 ^b (2.4)
100 cm mineral soil depth								
$^{15}\text{NH}_4^+$ subplot	0.0 ^a (0.0)	0.0 ^a (0.0)	4.6 ^a (1.3)	0.0 ^c (0.0)	0.9 ^a (0.2)	0.2 ^b (0.1)	5.4 ^a (1.2)	0.2 ^c (0.1)
$^{15}\text{NO}_3^-$ subplot	0.8 ^b (0.4)	0.0 ^a (0.0)	10.1 ^b (0.6)	0.7 ^c (0.5)	1.5 (0.2)	0.6 (0.4)	12.4 ^b (0.7)	1.3 ^c (0.7)

Different letters show the significant difference between the clean rain and the roof control plot for $^{15}\text{NH}_4^+$ - or $^{15}\text{NO}_3^-$ -labelled subplot as well as between the $^{15}\text{NH}_4^+$ - and $^{15}\text{NO}_3^-$ -labelled subplot within each plot (Mann-Whitney U Test, $p \leq 0.05$).

In the $^{15}\text{NH}_4^+$ -labelled subplot of the clean rain plot, ^{15}N signal was only detectable in the organic layer. The mean $\delta^{15}\text{N}$ excess of the organic layer was 1.7‰ in 2002 and 4.0‰ in 2004. In the $^{15}\text{NO}_3^-$ -labelled subplot of the clean rain plot, the mean $\delta^{15}\text{N}$ excess was highest in the organic layer (14.9‰ in 2002 and 16.0‰ in 2004) and stable $\delta^{15}\text{N}$ excess was observed in the mineral soil, varying from 1.0‰ to 4.9‰.

The mean $\delta^{15}\text{N-NO}_3^-$ in the soil solution was undetectable in the $^{15}\text{NH}_4^+$ -labelled subplot of the clean rain plot due to the very low NO_3^- -N concentration (Table 4.13). In the $^{15}\text{NO}_3^-$ -labelled subplot of the clean rain plot, the mean $\delta^{15}\text{N-NO}_3^-$ in the soil solution was similar at all measured soil depth with the value of more than 2000‰. The mean $\delta^{15}\text{N-NO}_3^-$ in the quarterly mixed soil solution samples at the 100 cm mineral soil depth (Jan. 2002 to Jun. 2004) was 2281‰ in the $^{15}\text{NO}_3^-$ -labelled subplot.

The mean $\delta^{15}\text{N-DON}$ in the soil solution did not differ significantly among soil depths in the $^{15}\text{NH}_4^+$ - and $^{15}\text{NO}_3^-$ -labelled subplot of the clean rain plot, respectively. Based on the quarterly mixed soil solution samples at the 100 cm mineral soil depth (Jan. 2002 to Jun. 2004), the mean $\delta^{15}\text{N-DON}$ was 1146‰ in the $^{15}\text{NH}_4^+$ -labelled subplot and 413‰ in the $^{15}\text{NO}_3^-$ -labelled subplot.

Table 4.12. $\delta^{15}\text{N}$ excess (‰) (mean \pm 1_{SE}) of tree compartments and soil in the $^{15}\text{NH}_4^+$ - and $^{15}\text{NO}_3^-$ -labelled subplot of the clean rain plot.

Compartment	$^{15}\text{NH}_4^+$ subplot			$^{15}\text{NO}_3^-$ subplot		
	2002	2003	2004	2002	2003	2004
Needle						
current year	5.7 (1.0)	11.2 (4.5)	14.9 (5.4)	24.5 (4.9)	30.5 (4.3)	58.6 (8.2)
1-year-old	2.6 (0.5)	9.9 (5.1)	11.0 (4.0)	11.0 (2.4)	25.6 (3.9)	46.6 (6.4)
2-year-old		5.1 (2.6)	9.9 (4.2)		14.6 (2.4)	39.3 (5.8)
3-year-old		4.2 (2.4)	5.7 (3.0)		11.2 (1.8)	24.1 (3.6)
4-year-old		3.6 (2.0)			11.0 (2.6)	
5-year-old		1.4 (0.8)			9.8 (2.7)	
Twig and branch						
bark						
current year		7.3 (1.0)			28.2 (6.3)	
1-year-old		5.7 (1.0)			15.6 (4.4)	
2-year-old		3.0 (0.8)			10.8 (1.9)	
3-year-old		3.3 (1.0)			11.4 (2.5)	
4-year-old		2.2 (0.6)			10.4 (3.0)	
>4-year-old		0.9 (0.7)			10.5 (5.6)	
wood						
current year		7.2 (0.9)			27.7 (5.7)	
1-year-old		6.4 (1.0)			25.9 (5.6)	
2-year-old		5.3 (1.2)			21.5 (4.9)	
3-year-old		4.5 (1.1)			19.7 (4.1)	
4-year-old		4.3 (0.7)			18.2 (4.0)	
>4-year-old		4.4 (1.1)			17.9 (7.9)	
Bole bark						
outer			1.6 (0.6)			4.4 (1.4)
inner			5.7 (1.9)			25.1 (8.0)
Bole wood produced in						
2002-2004			8.6 (2.5)			35.1 (9.3)
1997-2001			6.4 (2.8)			25.8 (5.8)
1992-1996			6.7 (1.7)			19.4 (6.2)
1972-1991			2.5 (0.7)			5.0 (0.3)
1952-1971			1.2 (0.2)			1.6 (0.1)
Fine roots in*						
$\text{O}_{\text{F+H}}/\text{O}_{\text{H}}$	19.4 (3.7)		20.4 (3.7)	50.1 (4.3)		86.0 (21.6)
0-5 cm	6.1 (3.5)		9.7 (1.3)	26.6 (2.8)		132.2 (61.3)
5-10 cm	2.1 (0.8)			17.2 (2.6)		
10-20 cm/10-40 cm	0.6 (0.4)		6.1 (0.3)	21.7 (6.1)		128.8 (61.3)
Soil						
$\text{O}_{\text{F+H}}/\text{O}_{\text{L+F+H}}$ **	1.7 (0.5)		4.0 (1.5)	14.9 (4.0)		16.0 (3.3)
0-5 cm	0.0 (0.0)		0.0 (0.0)	2.4 (0.9)		4.9 (1.8)
5-10 cm	0.0 (0.0)		0.0 (0.0)	1.2 (0.7)		3.5 (1.3)
10-20 cm	0.0 (0.0)		0.0 (0.0)	1.7 (1.1)		4.3 (1.3)
20-30 cm			0.1 (0.1)			4.0 (2.1)
30-40 cm			0.0 (0.0)			1.8 (1.6)
40-60 cm			0.0 (0.0)			1.0 (0.7)

* Fine roots collected in 2002 were from $\text{O}_{\text{F+H}}$, 0-5, 5-10, 10-20 cm soil layer and not separated between live and dead fine roots; those collected in 2004 were from O_{H} , 0-10, 10-40 cm soil layer and live fine roots were separated and analyzed..

** $\text{O}_{\text{F+H}}$ was sampled in 2002 and $\text{O}_{\text{L+F+H}}$ in 2004.

Table 4.13. $\delta^{15}\text{N}$ (‰) (mean \pm 1_{SE}) of NO_3^- -N and DON in soil solution in the $^{15}\text{NH}_4^+$ - and $^{15}\text{NO}_3^-$ -labelled subplot of the clean rain plot during Jan. 02 and Jun. 04.

Depth	NO_3^-		DON	
	$^{15}\text{NH}_4^+$ subplot	$^{15}\text{NO}_3^-$ subplot	$^{15}\text{NH}_4^+$ subplot	$^{15}\text{NO}_3^-$ subplot
0 cm	n.d.	2896 (302)	98 (45)	192 (34)
10 cm	n.d.	2231 (878)	512 (188)	269 (53)
40 cm	n.d.	2042 (252)	324 (122)	523 (70)
100 cm	n.d.	2425	447 (119)	341 (86)

n.d. = not determined. The $\delta^{15}\text{N}$ of NO_3^- in soil solution in the $^{15}\text{NH}_4^+$ -labelled subplot was not determined due to the concentration below the detection limit (0.15 mg L⁻¹).

4.1.2.4 ^{15}N recovery

In the clean rain plot, 17.9% of added $^{15}\text{NH}_4^+$ and 18.9% of added $^{15}\text{NO}_3^-$ were found in the needles (Table 4.14). ^{15}N recovery in the needles declined with increased age classes from 9% in the current-year needles to 1% in the 3-year-old needles in the two ^{15}N -labelled subplots.

Among woody tissues, ^{15}N recovery in the boles was higher than that in the twigs and branches in the clean rain plot. ^{15}N recovery in the boles was 8.2% in the $^{15}\text{NH}_4^+$ -labelled subplot and 6.4% in the $^{15}\text{NO}_3^-$ -labelled subplot. In the twigs and branches, ^{15}N recovery was 0.7% and 0.8%, respectively. ^{15}N in the bole wood was retained mostly in the wood produced between 1972 and 2004. In the wood produced before 1972, ^{15}N recovery was less than 0.5% in the two ^{15}N -labelled subplots.

The live fine roots retained 5.7% of added $^{15}\text{NH}_4^+$ and 9.2% of added $^{15}\text{NO}_3^-$ in the clean rain plot. In the $^{15}\text{NH}_4^+$ -labelled subplot, the live fine roots in the organic layer (O_H) alone retained 4.3% of added ^{15}N , while those in the mineral soil layers together retained only 1.4% of added ^{15}N . In the $^{15}\text{NO}_3^-$ -labelled subplot, ^{15}N recovery in the live fine roots in the organic layer (4.4%) was approximately equal to that in the live fine roots in the mineral soil layers (4.8%). Within the clean rain plot, ^{15}N recovery in the live fine roots in the 10-40 cm mineral soil layer tended to be lower in the $^{15}\text{NH}_4^+$ -labelled subplot (0.6%) than in the $^{15}\text{NO}_3^-$ -labelled subplot (2.4%, $p = 0.06$). ^{15}N recovery in the live fine roots was in total not different between the clean rain and the roof control plot for each ^{15}N tracer. However, ^{15}N recovery in the live fine roots in different soil layers showed differences between the two plots. The recovery of $^{15}\text{NH}_4^+$ in the live fine roots in the 10-40 cm mineral soil layer tended to be lower in the clean rain plot than in the roof control ($p = 0.06$), whereas the recovery of $^{15}\text{NO}_3^-$ in the live fine roots in

the organic layer tended to be higher in the clean rain plot than in the roof control ($p = 0.06$).

In total, 32.4% of added $^{15}\text{NH}_4^+$ and 35.3% of added $^{15}\text{NO}_3^-$ were found in the tree compartments in the clean rain plot. The ^{15}N recovery in each tree compartment was not significantly different between the $^{15}\text{NH}_4^+$ - and the $^{15}\text{NO}_3^-$ -labelled subplot of the clean rain plot. Therefore, the total recoveries of the two ^{15}N tracers in the tree compartments did not differ from each other in the clean rain plot. For each ^{15}N tracer, the ^{15}N recovery in each tree compartment was also not significantly different between the clean rain and the roof control plot. The total recovery of each ^{15}N tracer in the tree compartments was thus not different between the two roofed plots.

The organic layer and the top 100 cm mineral soil retained 71.0% of added $^{15}\text{NH}_4^+$ and 67.6% of added $^{15}\text{NO}_3^-$ in the clean rain plot. In the $^{15}\text{NH}_4^+$ -labelled subplot, the largest proportion of added ^{15}N was found in the organic layer (70.3%) and only 0.7% of added ^{15}N was recovered in the mineral soil. In the $^{15}\text{NO}_3^-$ -labelled subplot, 37.0% of added ^{15}N was found in the organic layer and 30.7% was distributed evenly throughout the mineral soil. The ^{15}N recovery in the organic layer was higher in the $^{15}\text{NH}_4^+$ -labelled subplot than in the $^{15}\text{NO}_3^-$ -labelled subplot, although the difference was not significant. Conversely, the ^{15}N recovery in the mineral soil was obviously lower in the $^{15}\text{NH}_4^+$ -labelled subplot than in the $^{15}\text{NO}_3^-$ -labelled subplot. In the clean rain plot, the recovery of added $^{15}\text{NH}_4^+$ in the total soil profile was not significantly different from that in the roof control plot. However, the distribution of added $^{15}\text{NH}_4^+$ in the soil layers was different between the clean rain and the roof control plot. The recovery of added $^{15}\text{NH}_4^+$ in the organic layer had a slight increase in the clean rain plot, while that in the mineral soil was significantly lower in the clean rain plot than in the roof control plot (0.7% vs. 6.4%). Compared to the roof control plot, the recovery of added $^{15}\text{NO}_3^-$ in the soil had a significant increase in the clean rain plot. The increased recovery of added $^{15}\text{NO}_3^-$ in the soil in the clean rain plot was caused by an obviously increased ^{15}N recovery in the organic layer. The recovery of added $^{15}\text{NO}_3^-$ in the mineral soil was not different between the two roofed plots.

The NO_3^- leachate at the 100 cm mineral soil depth accounted for 0% of added $^{15}\text{NH}_4^+$ and 2.0% of added $^{15}\text{NO}_3^-$ in the clean rain plot. The recoveries of both added $^{15}\text{NH}_4^+$ and $^{15}\text{NO}_3^-$ in the NO_3^- leachate at the 100 cm mineral soil depth were obviously lower in the clean rain plot than in the roof control plot. The ^{15}N recovery in the DON leachate at the 100 cm mineral soil depth was not different between the $^{15}\text{NH}_4^+$ -labelled subplot (1.3%) and the $^{15}\text{NO}_3^-$ -labelled subplot (0.5%) of the clean rain plot. For each ^{15}N tracer, the ^{15}N recovery in the DON leachate at the 100 cm mineral soil depth was also not different between the clean rain and the roof control plot.

Table 4.14. Percent ^{15}N recoveries (mean \pm 1SE) in main spruce forest ecosystem compartments in the roof control and the clean rain plot in 2004.

Compartment	roof control		clean rain	
	$^{15}\text{NH}_4^+$ subplot	$^{15}\text{NO}_3^-$ subplot	$^{15}\text{NH}_4^+$ subplot	$^{15}\text{NO}_3^-$ subplot
Needle				
current year	7.1 (0.9)	7.2 (1.0)	9.0 (3.5)	8.8 (1.2)
1-year-old	4.6 (0.6)	4.5 (0.5)	4.9 (1.7)	5.7 (0.8)
2-year-old	2.9 (0.5)	2.6 (0.3)	3.1 (1.2)	3.2 (0.5)
3-year-old	1.0 (0.2)	0.9 (0.1)	0.9 (0.4)	1.1 (0.2)
subtotal	15.7	15.2	17.9	18.9
Twig and branch				
bark	0.1 (0.0)	0.1 (0.0)	0.1 (0.0)	0.1 (0.0)
wood	0.7 (0.1)	1.1 (0.2)	0.7 (0.1)	0.7 (0.1)
subtotal	0.7	1.1	0.7	0.8
Bole bark				
outer	0.4 (0.1)	0.2 (0.0)	0.4 (0.2)	0.3 (0.1)
inner	1.2 (0.1)	2.3 (0.3)	1.8 (0.7)	2.1 (0.6)
Bole wood formed in				
2002-2004	1.6 (0.1)	1.9 (0.2)	1.3 (0.5)	1.2 (0.2)
1997-2001	0.8 (0.3)	1.9 (0.9)	1.0 (0.4)	1.1 (0.2)
1992-1996	0.7 (0.3)	1.6 (0.4)	0.9 (0.2)	0.8 (0.3)
1972-1991	1.9 (0.9)	4.2 (1.3)	2.2 (0.9)	0.7 (0.0)
1952-1971	0.0 (0.0)	0.1 (0.0)	0.5 (0.1)	0.2 (0.0)
<1952	0.0 (0.0)	0.0 (0.0)		
subtotal (bark+wood)	6.7	12.2	8.2	6.4
Live fine roots in				
O _H	4.2 (1.2)	1.8 (0.2)	4.3 (1.0)	4.4 (1.1)
0-10 cm	0.9 (0.3)	1.2 (0.2)	0.8 (0.1)	2.4 (1.1)
10-40 cm	1.8 (0.3)	4.1 (0.7)	0.6 (0.0)	2.4 (1.2)
subtotal	6.8	7.1	5.7	9.2
subtotal (tree)	29.9	35.6	32.4	35.3
Soil				
O _{L+F+H}	64.6 (5.5) ^a	8.0 (1.2) ^b	70.3 (12.9) ^a	37.0 (7.1) ^a
0-5 cm	4.2 (1.1) ^a	4.3 (0.8) ^{ac}	0.0 (0.0) ^b	7.1 (2.7) ^c
5-10 cm	1.1 (0.4) ^a	4.5 (0.2) ^b	0.0 (0.0) ^c	3.5 (1.4) ^b
10-20 cm	0.1 (0.1) ^a	3.9 (0.7) ^b	0.1 (0.1) ^a	6.1 (1.8) ^b
20-30 cm	0.8 (0.3) ^a	6.9 (2.5) ^b	0.6 (0.6) ^a	4.6 (2.2) ^{ab}
30-40 cm	0.3 (0.2) ^a	2.8 (0.7) ^b	0.0 (0.0) ^a	1.9 (1.6) ^b
40-60 cm	0.0 (0.0)	3.9 (2.6)	0.0 (0.0)	2.5 (1.9)
60-100 cm	0.0 (0.0)	7.9 (5.2)	0.0 (0.0)	5.0 (3.7)
subtotal (mineral soil)	6.4 ^a	34.2 ^b	0.7 ^c	30.7 ^b
subtotal (organic layer + mineral soil)	71.1	42.2	71.0	67.6
Leaching at 100 cm mineral soil depth				
NO ₃ ⁻	3.4 (1.3) ^a	19.2	0.0 (0.0) ^b	2.0 (2.0) ^b
DON	0.4 (0.0)	0.6 (0.2)	1.3 (0.7)	0.5 (0.2)
subtotal	3.7	19.8	1.3	2.5
Total	104.8	97.6	104.7	105.4

Different letters show the significant difference for each plot between ^{15}N tracers as well as for each ^{15}N tracer between the clean rain and the roof control plot (Mann-Whitney U Test, $p \leq 0.05$).

4.2 Density fractionation

4.2.1 Preparation of density solution

The relationship between the amount of added SPT and the volume change of SPT solution was shown in Table 10.2. The volume of 150 g H₂O was 152 ml and slightly higher than the theoretical value (150 ml). It may be partly attributed to the room temperature (> 30 °C), at which the solution was prepared, since the measuring cylinder is calibrated at 20 °C. The volume of SPT solution was thus corrected in the proportion, in which 152 ml H₂O was corrected to 150 ml. The volume change of SPT solution was closely correlated with the amount of added SPT ($y = 0.1863x$, $r^2 = 0.9993$, Fig. 4.7).

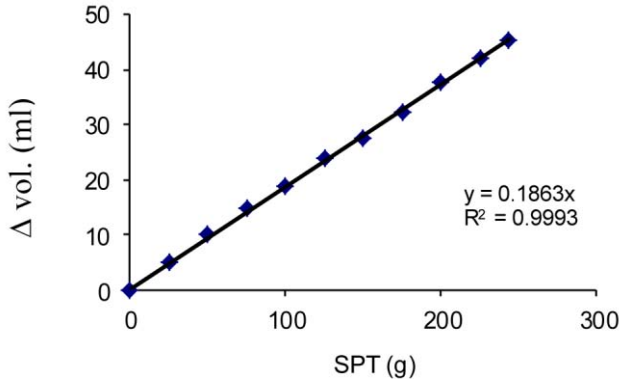


Fig. 4.7. The relationship between the amount of added SPT and the volume change of SPT solution.

4.2.2 Comparison of two aggregate-disrupting methods

The properties of separated soil density fractions from the ambient control plot after the use of two different aggregate-disrupting methods were shown in Table 4.15. The proportion of soil dry weight, soil OC and total soil N in the Ocl. I fraction was higher after sonification than after shaking, although the difference was not significant in the Ocl. I fraction from the organic layer. C and N concentration of the Ocl. II fraction from the organic layer was higher after sonification than after shaking, whereas lower C concentration after sonification than after shaking was observed in the Ocl. II fraction from the 0-5 cm mineral soil layer. The proportion of total soil N in the Ocl. II fraction from the 0-5 cm mineral soil layer tended to be higher after sonification than after shaking. The properties of

the Ocl. III fraction from both soil layers were not different after using the two aggregate-disrupting methods, except that lower C/N ratios were found after sonification than after shaking. The DF from the organic layer had lower C and N concentration, a lower C/N ratio and proportion of soil OC after sonification than after shaking. In both soil layers, 59-92% of soil OC and 81-98% of total soil N were recovered in the separated density fractions after using the two aggregate-disrupting methods, respectively.

Natural ^{15}N abundances of the soil density fractions increased generally with increased density in the organic layer and the 0-5 cm mineral soil layer after using the two aggregate-disrupting methods (Table 4.16). In the organic layer, natural ^{15}N abundances of the occluded fractions and the DF were higher after sonification than after shaking, although the difference was not significant in the Ocl. II fraction. In the 0-5 cm mineral soil layer, natural ^{15}N abundances of these fractions were not different after using the two aggregate-disrupting methods, except that the $\delta^{15}\text{N}$ value of the Ocl. I fraction tended to be lower after sonification than after shaking.

4.2.3 Distribution of OC and N in soil density fractions

4.2.3.1 Organic layer

In the organic layer, the FL fraction accounted for the largest proportion of soil dry weight (72-95%) in the clean rain and the roof control plot, followed by the DF (4-14%, Table 4.17). C and N concentration of the density fractions decreased generally with increased density. C and N concentration of the DF were about 3% and 0.2%, respectively, which were much lower than those of other fractions (17-43% and 1-2%, respectively). The highest C/N ratio was found in the FL fraction and the lowest in the DF. The FL fraction contained most of soil OC and total soil N with more than 84%.

The soil OC and N distribution in the occluded fractions from the organic layer were different between the clean rain and the roof control plot. Compared to the roof control plot, C and N concentration of the occluded fractions as well as the proportion of soil dry weight, soil OC and total soil N in these fractions were lower in the clean rain plot.

4.2.3.2 Mineral soil layers

In the clean rain and the roof control plot, the density fractions separated from the mineral soil layers had different OC and N distribution from those separated from the organic layer (Table 4.18, Table 4.19). The DF accounted for the largest proportion of soil dry weight (88-94%), followed by the Ocl. III and the FL fractions (1-6%, respectively). C and N concentrations of the density fractions decreased with increased density. The FL and the Ocl. I fractions had the same den-

sity (1.6 g cm^{-3}), but C and N concentrations of the Ocl. I fractions were higher than those of the FL fractions, respectively. The largest proportion of soil OC and total soil N were found in the DF (29-58% and 34-81%, respectively). The Ocl. I fractions accounted for the lowest proportion of soil OC and total soil N (1-2%, respectively).

The density fractions from different mineral soil layers showed little differences in properties. The DF from the 5-10 cm mineral soil layer comprised higher proportions of soil dry weight, soil OC and total soil N than those from the 0-5 cm mineral soil layer in the two roofed plots. C and N concentration of each fraction from the 5-10 cm mineral soil layer were lower than those from the 0-5 cm mineral soil layer.

Compared to the roof control plot, the FL fractions from the mineral soil layers accounted for higher proportion of soil dry weight, soil OC and total soil N in the clean rain plot, although the differences were not always significant. C and N concentrations of the FL fractions were lower in the clean rain plot than in the roof control plot. Conversely, the occluded fractions comprised lower proportions of soil dry weight, soil OC and total soil N in the clean rain plot than in the roof control plot. C concentrations of the occluded fractions were higher in the clean rain plot than in the roof control plot.

4.2.4 Recovery of soil ^{15}N

In the organic layer, most of soil $^{15}\text{NH}_4^+$ and $^{15}\text{NO}_3^-$ were recovered in the FL fractions in the clean rain and the roof control plot (Table 4.20). The recoveries of soil $^{15}\text{NH}_4^+$ and $^{15}\text{NO}_3^-$ in the FL fraction were 89.8% and 81.4% in the clean rain plot, respectively. The FL fraction in the roof control plot retained 78.7% of soil $^{15}\text{NH}_4^+$ and 72.9% of soil $^{15}\text{NO}_3^-$, respectively. In the clean rain plot, no soil $^{15}\text{NH}_4^+$ was recovered in the Ocl. III fraction and the DF from the organic layer, while the recovery of soil $^{15}\text{NO}_3^-$ in the two fractions was 1.5%. In the roof control plot, the recoveries of soil $^{15}\text{NH}_4^+$ in the Ocl. I and Ocl. II fraction from the organic layer were lower than those of soil $^{15}\text{NO}_3^-$. The recovery of soil $^{15}\text{NH}_4^+$ in the DF was conversely higher than that of soil $^{15}\text{NO}_3^-$.

Compared to the roof control plot, the recoveries of soil $^{15}\text{NH}_4^+$ in the Ocl. III fraction and the DF from the organic layer were lower in the clean rain plot. The recovery of soil $^{15}\text{NO}_3^-$ in the Ocl. I fraction was significantly lower in the clean rain plot than in the roof control plot. A tendency to a lower recovery of soil $^{15}\text{NO}_3^-$ in the clean rain plot than in the roof control plot was also observed in the Ocl. II fraction ($p = 0.09$). The DF from the organic layer retained 0.4% of soil $^{15}\text{NO}_3^-$ in the clean rain plot and the value was higher than that in the roof control plot (0%).

In the 0-5 cm mineral soil layer, the recovery of soil $^{15}\text{NO}_3^-$ was highest (35.5%) in the DF in the clean rain plot. The FL fraction and the occluded frac-

tions in the clean rain plot accounted for 20.1% and 19.8% of soil $^{15}\text{NO}_3^-$, respectively. In the roof control plot, the recovery of soil $^{15}\text{NH}_4^+$ in the FL fraction from the 0-5 cm mineral soil layer tended to be lower (20.8%) than that of soil $^{15}\text{NO}_3^-$ (35.8%, $p = 0.09$). Conversely, the Ocl. II fraction retained significantly larger proportion of soil $^{15}\text{NH}_4^+$ (14.9%) than soil $^{15}\text{NO}_3^-$ (7.1%) and the same tendencies were found in the Ocl. I fraction and the DF ($p = 0.09$). Compared to the roof control plot, the recovery of soil $^{15}\text{NO}_3^-$ in the DF from the 0-5 cm mineral soil layer tended to be higher in the clean rain plot ($p = 0.09$).

In the 5-10 cm mineral soil layer, most of soil $^{15}\text{NO}_3^-$ in the clean rain plot was found in the DF (63.7%), followed by the FL fraction (22.9%). The occluded fractions retained 17.6% of soil $^{15}\text{NO}_3^-$. In the roof control plot, the FL fraction, the occluded fractions and the DF accounted for 33.2%, 21.9% and 34.9% of soil $^{15}\text{NH}_4^+$, respectively. The recovery of soil $^{15}\text{NO}_3^-$ in these fractions was 27.9%, 16.8% and 38.3% in the roof control plot, respectively. The recoveries of soil $^{15}\text{NH}_4^+$ and $^{15}\text{NO}_3^-$ in each fraction from the 5-10 cm mineral soil layer did not differ from each other in the roof control plot. The recovery of soil $^{15}\text{NO}_3^-$ in each fraction from the 5-10 cm mineral soil layer was also not different between the clean rain and the roof control plot.

Table 4.15. Properties (mean \pm 1SE) of density fractions from the organic layer and the 0-5 cm mineral soil layer in the ambient control plot after using two different aggregate-disrupting methods (n = 5).

Soil layer fraction	% of soil weight		C%		N%		C/N		% of soil OC		% of total soil N	
	sonifi- cation	shak- ing	sonifi- cation	shak- ing	sonifi- cation	shak- ing	sonifi- cation	shak- ing	sonifi- cation	shak- ing	sonifi- cation	shak- ing
O _{L+FH}	81.3 (4.9)	85.6 (3.9)	40.4 (1.8)	41.4 (0.9)	1.8 (0.1)	1.7 (0.0)	23	24	78.2 (3.8)	82.2 (2.5)	85.8 (4.1)	87.7 (2.8)
Ocl.I	4.3 (1.5)	1.0 (0.1)	39.4 (5.0)	37.8 (3.2)	1.9 (0.2)	1.7 (0.1)	20	22	4.6 (1.8)	0.9 (0.1)	5.5 (2.1)	1.0* (0.1)
Ocl.II	4.2 (1.2)	8.1 (2.2)	38.0 (0.5)	33.9* (1.8)	1.8 (0.0)	1.5** (0.1)	21	22	4.1 (1.3)	6.9 (2.1)	4.9 (1.6)	7.8 (2.3)
Ocl.III	1.2 (0.3)	2.3 (0.7)	23.1 (1.6)	21.8 (1.5)	1.2 (0.1)	1.0 (0.1)	19	22*	0.8 (0.2)	1.3 (0.4)	1.1 (0.2)	1.5 (0.5)
DF	7.2 (1.9)	4.1 (1.1)	0.8 (0.2)	3.6** (0.7)	0.1 (0.0)	0.2*** (0.1)	10	19**	0.1 (0.0)	0.5** (0.2)	0.3 (0.1)	0.5 (0.2)
total	98.3	101.1							87.7	91.6	97.2	98.5
0-5 cm	4.3 (1.5)	2.9 (0.7)	17.9 (2.1)	21.8 (3.5)	0.8 (0.1)	0.9 (0.1)	23	23	7.9 (1.9)	6.7 (1.1)	10.7 (2.7)	8.6 (1.0)
Ocl.I	2.1 (0.5)	0.5** (0.2)	40.4 (1.9)	37.9 (1.5)	1.5 (0.2)	1.3 (0.2)	30	25	9.5 (1.7)	2.1** (0.5)	9.6 (1.4)	2.1*** (0.7)
Ocl.II	2.9 (0.7)	2.1 (0.7)	30.4 (0.9)	33.9*** (0.4)	1.3 (0.1)	1.3 (0.1)	25	27	10.1 (1.7)	7.3 (1.1)	12.3 (1.6)	8.6* (1.9)
Ocl.III	5.8 (1.2)	6.5 (1.9)	21.3 (0.9)	23.1 (0.1)	1.1 (0.0)	1.0 (0.1)	19	24***	14.4 (2.0)	16.0 (1.5)	22.3 (1.5)	20.9 (2.9)
DF	82.9 (2.5)	86.9* (3.1)	2.0 (0.3)	2.4 (0.2)	0.1 (0.0)	0.1 (0.0)	17	19	21.6 (5.1)	27.2 (6.5)	38.0 (7.5)	40.5 (6.3)
total	97.9	98.9							63.6	59.2	92.9	80.7

FL = free light fraction ($d < 1.6$ g cm⁻³), Ocl. = occluded fraction (Ocl. I $d < 1.6$ g cm⁻³, Ocl. II $d = 1.6-1.8$ g cm⁻³, Ocl. III $d = 1.8-2.0$ g cm⁻³), DF = dense fraction ($d > 2.0$ g cm⁻³).

* show difference between two methods (Mann-Whitney U Test, * $p \leq 0.1$, ** $p \leq 0.05$, *** $p \leq 0.01$)

Table 4.16. Natural ^{15}N abundances (mean \pm 1_{SE}) of density fractions from the organic layer and the 0-5 cm mineral soil layer in the ambient control plot after using two different aggregate-disrupting methods (n = 5).

Soil layer	fraction	$\delta^{15}\text{N}$ (‰)		
		sonification	shaking	
$\text{O}_{\text{L+F+H}}$	FL	-2.5 (0.4)	-2.5 (0.4)	
	Ocl.I	1.3 (1.4)	-1.1 (0.2)	**
	Ocl.II	0.4 (0.2)	-0.1 (0.2)	
	Ocl.III	8.4 (1.3)	3.6 (0.6)	**
	DF	18.4 (1.6)	6.3 (1.1)	***
0-5 cm	FL	1.8 (0.4)	2.0 (0.4)	
	Ocl.I	2.4 (0.6)	4.1 (0.9)	*
	Ocl.II	3.0 (0.4)	2.8 (0.6)	
	Ocl.III	3.7 (0.6)	3.1 (0.4)	
	DF	4.7 (0.6)	4.8 (0.5)	

FL = free light fraction ($d < 1.6 \text{ g cm}^{-3}$), Ocl.=occluded fraction (Ocl. I $d < 1.6 \text{ g cm}^{-3}$, Ocl. II $d = 1.6\text{-}1.8 \text{ g cm}^{-3}$, Ocl. III $d = 1.8\text{-}2.0 \text{ g cm}^{-3}$), DF = dense fraction ($d > 2.0 \text{ g cm}^{-3}$).

* show difference in natural ^{15}N abundance between two methods (Mann-Whitney U Test, * $p \leq 0.1$, ** $p \leq 0.05$, *** $p \leq 0.01$).

Table 4.17. Properties (mean \pm 1_{SE}) of density fractions from the organic layer in the clean rain and the roof control plot (n = 5).

treatment fraction	% of soil weight				C%				N%				C/N				% of soil OC				% of total soil N										
	clean		roof		clean		roof		clean		roof		clean		roof		clean		rain		roof		clean		rain		roof				
	rain	control	rain	control	rain	control	rain	control	rain	control	rain	control	rain	control	rain	control	rain	control	rain	control	rain	control	rain	control	rain	control	rain	control			
¹⁵ NH ₄ ⁺ subplot	FL	95.0 (2.3)	90.4 (0.9)	42.0 (1.1)	43.2 (0.5)	1.7 (0.0)	1.8 (0.1)	25	24	89.4 (2.5)	97.4 (1.4)	102.3 (3.3)	103.0 (2.8)																		
	Ocl.I	0.7 (0.2)	0.5 (0.1)	20.7 (5.1)	39.6 (1.1)	1.2 (0.2)	1.7 (0.0)	20	23 *	0.4 (0.1)	0.5 (0.1)	0.4 (0.1)	0.5 (0.1)																		
	Ocl.II	1.0 (0.2)	2.8 (0.6)	28.6 (5.1)	36.6 (3.3)	1.3 (0.1)	1.6 (0.0)	22	23 *	0.7 (0.1)	2.6 (0.5)	0.8 (0.2)	2.9 (0.6)																		
	Ocl.III	0.8 (0.2)	1.3 (0.1)	21.9 (0.7)	25.6 (0.5)	1.1 (0.1)	1.1 (0.0)	21	23 *	0.4 (0.1)	0.8 (0.0)	0.6 (0.2)	0.9 (0.1)																		
	DF	5.1 (2.5)	3.9 (0.7)	2.5 (0.4)	3.3 (0.3)	0.1 (0.0)	0.2 (0.0)	17	19	0.3 (0.1)	0.3 (0.1)	0.4 (0.2)	0.4 (0.1)																		
¹⁵ NO ₃ ⁻ subplot	FL	88.1 (5.5)	72.3 (8.0)	42.5 (1.3)	40.6 (1.3)	1.7 (0.0)	1.6 (0.0)	25	24	89.3 (3.9)	84.8 (4.9)	100.1 (3.7)	86.4 (5.5)																		
	Ocl.I	0.6 (0.1)	1.2 (0.2)	32.4 (2.9)	41.0 (1.1)	1.4 (0.2)	1.9 (0.1)	23	21	0.5 (0.1)	1.4 (0.2)	0.6 (0.2)	1.6 (0.2)																		
	Ocl.II	2.2 (0.9)	4.3 (0.8)	30.1 (1.3)	35.7 (0.3)	1.4 (0.1)	1.6 (0.1)	22	23	1.8 (0.8)	4.8 (1.2)	2.2 (1.0)	5.3 (1.4)																		
	Ocl.III	3.5 (2.1)	7.5 (3.6)	17.2 (3.2)	23.6 (3.8)	0.8 (0.1)	1.1 (0.1)	22	21	2.0 (1.4)	5.2 (2.2)	2.4 (1.6)	7.1 (3.6)																		
	DF	6.9 (2.8)	13.6 (4.3)	2.9 (0.3)	2.6 (0.2)	0.2 (0.0)	0.1 (0.0)	17	19	0.6 (0.3)	1.2 (0.5)	0.9 (0.4)	1.4 (0.5)																		

FL = free light fraction ($d < 1.6 \text{ g cm}^{-3}$), Ocl. = occluded fraction (Ocl. I $d < 1.6 \text{ g cm}^{-3}$, Ocl. II $d = 1.6\text{-}1.8 \text{ g cm}^{-3}$, Ocl. III $d = 1.8\text{-}2.0 \text{ g cm}^{-3}$), DF = dense fraction ($d > 2.0 \text{ g cm}^{-3}$).

* show differences in properties between the clean rain and the roof control plot (Mann-Whitney U Test, * $p \leq 0.1$, ** $p \leq 0.05$, *** $p \leq 0.01$)

Table 4.18. Properties (mean \pm 1_{SE}) of density fractions from the 0-5 cm mineral soil layer in the clean rain and the roof control plot (n = 5).

treatment	fraction	% of soil weight				C%				N%				C/N				% of soil OC				% of soil N			
		clean		roof		clean		roof		clean		roof		clean		roof		clean		roof		clean		roof	
		rain	control	rain	control	rain	control	rain	control	rain	control	rain	control	rain	control	rain	control	rain	control	rain	control	rain	control	rain	control
¹⁵ NH ₄ ⁺ subplot	FL	4.9 (1.1)	1.5 ** (0.2)	28.3 (1.7)	34.3 ** (0.6)	1.2 (0.1)	1.4 (0.0)	25 (0.0)	25	15.6 (3.6)	9.3 * (0.9)	16.6 (3.0)	8.2 ** (0.6)												
	Ocl.I	0.6 (0.2)	0.2 ** (0.0)	35.3 (3.4)	36.3 (0.6)	1.6 (0.2)	1.6 (0.0)	24 (0.0)	23	2.0 (0.4)	1.6 (0.1)	2.2 (0.3)	1.5 ** (0.1)												
	Ocl.II	1.6 (0.1)	1.9 * (0.2)	33.3 (0.9)	33.0 (0.3)	1.4 (0.0)	1.4 (0.0)	23 (0.0)	23	6.1 (0.5)	11.4 *** (0.6)	7.0 (0.5)	10.7 *** (0.6)												
	Ocl.III	4.9 (0.8)	5.9 (0.7)	25.2 (0.4)	23.2 *** (0.3)	1.2 (0.0)	1.1 * (0.0)	21 (0.0)	21	13.8 (1.8)	24.2 *** (1.6)	17.3 (1.9)	25.5 * (2.1)												
	DF	87.8 (1.1)	88.8 (0.8)	3.9 (0.6)	3.0 (0.3)	0.2 (0.0)	0.2 (0.0)	19 (0.0)	19	38.5 (5.4)	48.8 (7.6)	53.4 (3.9)	57.2 (8.8)												
¹⁵ NO ₃ ⁻ subplot	FL	4.5 (1.4)	1.8 (0.2)	30.4 (0.9)	33.6 (1.8)	1.2 (0.1)	1.5 ** (0.1)	25 (0.1)	23	16.5 (3.2)	10.4 (1.3)	16.8 (3.4)	10.1 (1.1)												
	Ocl.I	0.2 (0.0)	0.7 *** (0.3)	41.3 (1.0)	33.3 ** (2.2)	1.7 (0.1)	1.6 (0.1)	25 (0.1)	20	1.0 (0.1)	2.0 ** (0.3)	1.0 (0.0)	2.2 *** (0.2)												
	Ocl.II	1.2 (0.5)	1.8 (0.1)	34.4 (0.7)	32.5 * (0.2)	1.4 (0.0)	1.4 (0.1)	24 (0.1)	23	5.1 (1.1)	10.0 ** (0.5)	5.3 (1.2)	9.7 ** (0.6)												
	Ocl.III	4.2 (0.8)	6.3 (0.8)	24.8 (0.4)	22.8 (2.1)	1.1 (0.0)	1.1 (0.1)	23 (0.1)	21	14.1 (1.7)	23.8 *** (2.2)	15.7 (2.1)	24.7 *** (1.5)												
	DF	88.5 (2.5)	88.8 (0.9)	3.4 (0.6)	1.9 * (0.7)	0.2 (0.0)	0.1 (0.0)	19 (0.0)	18	40.6 (4.1)	28.7 (9.7)	53.9 (5.5)	33.8 (10.7)												

FL = free light fraction ($d < 1.6 \text{ g cm}^{-3}$), Ocl. = occluded fraction (Ocl. I $d < 1.6 \text{ g cm}^{-3}$, Ocl. II $d = 1.6\text{-}1.8 \text{ g cm}^{-3}$, Ocl. III $d = 1.8\text{-}2.0 \text{ g cm}^{-3}$), DF = dense fraction ($d > 2.0 \text{ g cm}^{-3}$).

* show differences in properties between the clean rain and the roof control plot (Mann-Whitney U Test, * $p \leq 0.1$, ** $p \leq 0.05$, *** $p \leq 0.01$)

Table 4.19. Properties (mean \pm 1_{SE}) of density fractions from the 5-10 cm mineral soil layer in the clean rain and the roof control plot (n = 5).

treatment	fraction	% of soil weight				C%				N%				C/N				% of soil OC				% of soil N				
		rain	roof	rain	roof	rain	roof	rain	roof	rain	roof	rain	roof	rain	roof	rain	roof	rain	roof	rain	roof	rain	roof	rain	roof	
¹⁵ NH ₄ ⁺ subplot	FL	1.3 (0.3)	2.8 (1.4)	25.0 (1.0)	30.2 (3.5)	1.0 (0.0)	1.1 (0.2)	25	29	10.2 (2.0)	15.0 (5.1)	8.0 (1.3)	12.8 (5.3)													
	Ocl.I	0.2 (0.0)	0.2 (0.1)	29.4 (2.0)	33.9 (6.6)	1.2 (0.1)	1.2 (0.2)	25	27	2.3 (0.2)	1.8 (0.0)	1.8 (0.1)	1.4 (0.2)													
	Ocl.II	0.7 (0.1)	2.6 (1.7)	28.6 (2.8)	28.4 (2.8)	1.0 (0.1)	1.0 (0.1)	29	29	7.0 (0.6)	12.4 (5.0)	5.0 (0.5)	11.2 (5.8)													
	Ocl.III	1.6 (0.1)	3.0** (1.0)	20.4 (0.8)	21.2 (1.2)	0.8 (0.1)	0.9 (0.1)	25	24	11.4 (1.1)	14.5* (1.0)	9.3 (0.6)	13.7*** (1.7)													
	DF	93.8 (0.4)	90.5 (3.6)	1.7 (0.1)	2.3* (0.3)	0.1 (0.0)	0.1 (0.0)	15	16	55.4 (4.1)	57.0 (8.9)	73.5 (2.9)	81.2 (12.4)													
¹⁵ NO ₃ ⁻ subplot	FL	2.7 (0.6)	1.2* (0.2)	17.3 (1.7)	28.2*** (1.0)	0.7 (0.1)	1.1*** (0.1)	25	27	12.9 (2.1)	9.9 (1.7)	10.0 (1.3)	8.1 (1.5)													
	Ocl.I	0.1 (0.0)	0.1*** (0.0)	37.6 (0.7)	34.6** (0.1)	1.6 (0.1)	1.4 (0.0)	23	25	0.6 (0.2)	1.4** (0.1)	0.6 (0.2)	1.2 (0.1)													
	Ocl.II	0.3 (0.0)	1.3*** (0.3)	32.5 (0.7)	24.4** (3.5)	1.2 (0.1)	0.8*** (0.1)	27	35*	3.2 (0.1)	8.2*** (0.8)	2.4 (0.2)	5.2*** (0.6)													
	Ocl.III	1.4 (0.1)	2.1** (0.2)	23.0 (0.3)	21.7* (0.6)	0.9 (0.0)	0.8 (0.0)	26	26	9.5 (1.0)	13.1** (0.8)	7.3 (1.0)	11.0* (0.8)													
	DF	93.6 (0.6)	94.3 (0.5)	2.1 (0.2)	2.0 (0.2)	0.1 (0.0)	0.1 (0.0)	17	16	58.3 (7.2)	55.6 (6.6)	68.8 (12.4)	78.7 (11.6)													

FL = free light fraction ($d < 1.6 \text{ g cm}^{-3}$), Ocl. = occluded fraction (Ocl. I $d < 1.6 \text{ g cm}^{-3}$, Ocl. II $d = 1.6\text{-}1.8 \text{ g cm}^{-3}$, Ocl. III $d = 1.8\text{-}2.0 \text{ g cm}^{-3}$), DF=dense fraction ($d > 2.0 \text{ g cm}^{-3}$).

* show differences in properties between the clean rain and the roof control plot (Mann-Whitney U Test, * $p \leq 0.1$, ** $p \leq 0.05$, *** $p \leq 0.01$)

Table 4.20. Percent recovery (mean $\pm 1_{SE}$) of soil ^{15}N in density fractions from the organic layer and the mineral soil layers in the clean rain and the roof control plot after $^{15}\text{NH}_4^+$ and $^{15}\text{NO}_3^-$ addition

Soil layer	fraction	clean rain		roof control	
		$^{15}\text{NH}_4^+$ subplot	$^{15}\text{NO}_3^-$ subplot	$^{15}\text{NH}_4^+$ subplot	$^{15}\text{NO}_3^-$ subplot
O_{L+F+H}	FL	89.8 (13.6)	81.4 (2.1)	78.7 (3.3)	72.9 (3.6)
	Ocl.I	0.6 ^{ab} (0.3)	0.5 ^a (0.1)	0.3 ^b (0.1)	1.8 ^c (0.2)
	Ocl.II	2.8 (2.3)	1.4 (0.6)	0.9 ^a (0.2)	4.0 ^b (1.2)
	Ocl.III	0.0 ^a (0.0)	1.1 ^b (0.5)	0.2 ^c (0.05)	3.4 ^{bc} (3.1)
	DF	0.0 ^a (0.0)	0.4 ^b (0.1)	0.1 ^c (0.02)	0.0 ^d (0.0)
	sum	93.2	84.8	80.2	82.1
0-5 cm	FL	n.d.	20.1 (5.2)	20.8 (2.6)	35.8 (5.6)
	Ocl.I	n.d.	2.1 (0.8)	9.5 (5.4)	2.3 (0.5)
	Ocl.II	n.d.	4.6 (1.7)	14.9 ^a (1.4)	7.1 ^b (0.9)
	Ocl.III	n.d.	13.1 (4.5)	22.0 (3.7)	12.0 (2.8)
	DF	n.d.	35.5 (10.5)	26.8 (7.1)	7.1 (3.9)
	sum		75.3	94.0	64.4
5-10 cm	FL	n.d.	22.9 (6.5)	33.2 (9.7)	27.9 (7.5)
	Ocl.I	n.d.	2.4 (0.4)	2.6 (0.5)	3.6 (1.2)
	Ocl.II	n.d.	4.3 (0.4)	4.7 (1.7)	5.9 (1.0)
	Ocl.III	n.d.	10.9 (3.0)	14.6 (7.8)	7.3 (1.0)
	DF	n.d.	63.7 (19.8)	34.9 (20.2)	38.3 (6.2)
	sum		104.1	90.2	83.1

FL = free light fraction ($d < 1.6 \text{ g cm}^{-3}$), Ocl. = occluded fraction (Ocl. I $d < 1.6 \text{ g cm}^{-3}$, Ocl. II $d = 1.6-1.8 \text{ g cm}^{-3}$, Ocl. III $d = 1.8-2.0 \text{ g cm}^{-3}$),

DF = dense fraction ($d > 2.0 \text{ g cm}^{-3}$), n.d. = not determined.

Different letters show significant difference for each plot between the two ^{15}N tracers as well as for each ^{15}N tracer between the clean rain and the roof control plot (Mann-Whitney U Test, $p \leq 0.05$)

5 Discussion

5.1 ^{15}N tracer experiment

5.1.1 Natural ^{15}N abundance

The natural ^{15}N abundances of the tree compartments in the roof control and the clean rain plot (Table 4.1, Table 4.7) fall within the range of those reported from other studies (-5 to +4‰) (Gebauer and Schulze 1991, Nadelhoffer and Fry 1994, Emmett et al. 1998a). Low $\delta^{15}\text{N}$ values in the tree compartments in the two roofed plots are ultimately caused by isotopic fractionation against ^{15}N during N mineralization and tree uptake (Nadelhoffer and Fry 1994). In the roof control plot, the bole bark and bole wood were ^{15}N depleted relative to the current year needles, reflecting that N in the bole bark and bole wood may preferentially originate from compounds recycled from senescing compartments (Gebauer and Schulze 1991). The natural ^{15}N abundance of the current year needles in the roof control plot varied between those of the live fine roots in both the upper and deeper soil layers, indicating that not only the live fine roots in the upper soil but also those in the deeper soil provide considerable N to the needles. Corresponding to increased natural ^{15}N abundance of the soil with depth in the roof control and the clean rain plot (see below), the natural ^{15}N abundance of the live fine roots in the two roofed plots which assimilate N from the soil increased also with soil depth. In the same layers in each roofed plot, the natural ^{15}N abundance of the live fine roots was always lower than that of the soil due to isotopic fractionation during mineralization and uptake.

Compared to the tree compartments, the soil in the two roofed plots was enriched in ^{15}N . The natural ^{15}N abundance of the organic layer was low, caused mainly by return of the ^{15}N -depleted needle and root litter onto the soil surface (Emmett et al. 1998a). When fractionation against ^{15}N occurs, either through the mineralization-tree uptake pathway, or via the continuous leaching of nitrate produced by nitrification throughout the soil profile, the remaining N in the soil is gradually enriched in ^{15}N (Nadelhoffer and Fry 1994). Hoegberg (1997) reported another possible explanation for ^{15}N -enrichment with soil depth. Norway spruce can form symbiosis with ecto-mycorrhizal fungi which are enriched in ^{15}N caused by fractionation during metabolic processes or resulted from selective retention of specific N compounds. Fungi N are important precursors of recalcitrant N in the soil. Accumulation of the ^{15}N -enriched recalcitrant N with soil depth might contribute to the increased ^{15}N abundance of the soil.

In the throughfall water in the roof control plot, NH_4^+ was strongly ^{15}N enriched relative to NO_3^- (Table 4.2). The high ^{15}N enrichment of NH_4^+ was probably caused by isotopic fractionation during nitrification, which occurred during the

collection and re-sprinkling of the throughfall water. In the soil solution in the roof control plot, the negative $\delta^{15}\text{N}$ value of nitrate indicated that nitrate in the soil solution was derived more from ^{15}N -depleted nitrate deposition than from ^{15}N -enriched ammonium deposition. DON in the soil solution in the two roofed plots originated from the throughfall water, root exudates, microbial metabolites and products of litter composition (Smolander et al. 2001) and the positive $\delta^{15}\text{N}$ value of DON might also result from these sources.

5.1.2 ^{15}N recoveries

The Solling site is characterized by equivalent deposition of atmospheric ammonium and nitrate (Table 3.1). In the roof control plot, the two ^{15}N -labelled sub-plots have received the same amount of labelled N applied as $^{15}\text{NH}_4\text{NO}_3$ or $\text{NH}_4^{15}\text{NO}_3$ in a period of over 3 years. In the clean rain plot, different amounts of $^{15}\text{NH}_4\text{NO}_3$ and $\text{NH}_4^{15}\text{NO}_3$ were separately added in the period of over 3 years after 10-years of reduction of atmospheric deposition. This experimental design offered opportunities to trace the fate of atmospheric N, and to provide insights into the distribution of atmospheric ammonium and nitrate within this Norway spruce forest ecosystem under both ambient and long-term reduced atmospheric deposition conditions.

In this ^{15}N tracer study, coarse roots were not sampled. The role of the coarse roots alone in retaining N input have not been reported so far. However, Melin et al. (1983) and Buchmann et al. (1996) found that less than 7% of ^{15}N were recovered in roots (≤ 30 mm) of an old Scots pine and less than 4% in roots (< 10 mm) of a young Norway spruce forest, respectively. Schleppi et al. (1999) reported that 13% of ^{15}N was found together in roots and litter of an old Norway spruce forest. Higher ^{15}N recoveries (16 to 22%) were found by Gundersen (1998) in roots of an old Norway spruce forest. In the present spruce forest ecosystem, the high ^{15}N recoveries in the roof control and the clean rain plot indicated that the coarse roots may play a minor role in retaining N input.

5.1.2.1 Under ambient atmospheric deposition (the roof control plot)

5.1.2.1.1 Soil

As in other studies (Buchmann et al. 1996, Koopmans et al. 1996, Nadelhoffer et al. 1999a, 2004, Gebauer et al. 2000), under ambient atmospheric deposition the largest proportion of atmospheric N was retained in the soil of the Norway spruce forest at Solling (Table 4.6). Furthermore, the results showed a very high retention of atmospheric ammonium and a low retention of atmospheric nitrate in the organic layer in the roof control plot. Corre and Lamersdorf (2004) verified that microbes assimilated less NO_3^- than NH_4^+ and that the abiotic NO_3^- immobilization was low in the organic layer of this Norway spruce forest ecosystem under

ambient atmospheric deposition. As a result, atmospheric nitrate was highly mobile in the roof control plot and transported to deeper soil layers. The considerable vertical transport of atmospheric nitrate, as indicated by high ^{15}N abundance of NO_3^- in the soil solution at deeper depths in the $^{15}\text{NO}_3^-$ -labelled subplot of the roof control plot (Fig. 4.6), resulted in a four-time greater retention of atmospheric nitrate than that of atmospheric ammonium in the mineral soil in the roof control plot (Table 4.6). In comparison with the results of the roof control plot, similar high retention of atmospheric ammonium (46-63%) but much higher retention of atmospheric nitrate (46-74%) in the organic layer was reported in other ^{15}N studies (Buchmann et al. 1996, Nadelhoffer et al. 1999a, Table 1.1). The difference in nitrate retention could be attributed to the lower atmospheric N deposition at those study sites ($\leq 12 \text{ kg ha}^{-1} \text{ yr}^{-1}$, as compared to $> 30 \text{ kg ha}^{-1} \text{ yr}^{-1}$ in the roof control plot). Under lower atmospheric N deposition, the supply of atmospheric ammonium in the organic layer may not meet the N demand of microbes, which led to increased microbial uptake of atmospheric nitrate. Moreover, the abiotic nitrate immobilization in the organic layer may increase under lower N deposition (Corre and Lamersdorf 2004).

5.1.2.1.2 Tree

Trees are the second important sink for atmospheric N under ambient atmospheric deposition. In the roof control plot, more than 30% of atmospheric N was found in the trees. A similar result was reported by Koopmans et al. (1996) in a N-saturated Douglas fir forest at Speuld in the Netherlands, in which 29% of atmospheric ammonium was recovered in trees. Buchmann et al. (1996) and Nadelhoffer et al. (1999a) found, however, a noticeably lower proportion ($\leq 10\%$) of atmospheric ammonium and nitrate in the Norway spruce forest in Fichtelgebirge and in a red pine forest at Harvard Forest, respectively. The different recovery in trees was mainly due to the difference in atmospheric N deposition among these study sites. At sites with low atmospheric N deposition (Buchmann et al. 1996, Nadelhoffer et al. 1999a), trees seemed to be less competitive than microbes, whereas the availability of atmospheric N for trees appeared to increase at sites with high atmospheric N deposition (Koopmans et al. 1996, the present study). The relationship between the N application rate and N consuming processes (the proportion of applied N) was demonstrated by Nõmmik (1990) in a Scott pine forest: N uptake by trees and loss by leaching and/or denitrification increased with elevated N application while N immobilization in soil decreased.

Among the tree compartments, the largest proportion of the assimilated atmospheric N was retained in the needles under ambient atmospheric deposition. The ^{15}N recovery in the needles showed a decreasing trend with increasing needle ages in the roof control plot, which may be mainly due to the needle biomass difference between the different age classes (Table 4.3). The ^{15}N signal in the nee-

dles that grew before ^{15}N addition (Fig. 4.1) indicated a retranslocation of the newly assimilated atmospheric N into the older needles.

The woody tissues (twigs, branches and boles) are the second largest sink in the trees for atmospheric N under ambient atmospheric deposition. Like the needles, atmospheric N was not only assimilated to the new woody tissues, but also retranslocated to the old ones. The retranslocation of ^{15}N among tree rings was also reported by Hart and Classen (2003) in ponderosa pine trees, in which the $\delta^{15}\text{N}$ value reached the maximum in the ring formed one year after ^{15}N addition and decreased bidirectionally toward younger and older tree rings. Although the bark and wood of the twigs and branches showed similar $\delta^{15}\text{N}$ excess value as the corresponding needles in the roof control plot, they accounted only for a small proportion of atmospheric N as the smallest N pool in the trees. In contrast to the needles, the bole bark and bole wood were a larger N pool but retained a smaller proportion of atmospheric N in the roof control plot, indicating that the assimilated atmospheric N was preferentially transported to the needles.

Under ambient atmospheric deposition, the live fine roots accounted for a large proportion of atmospheric N. Compared with the live fine roots in the upper mineral soil, a higher recovery of atmospheric ammonium was found in those in the organic layer ($p = 0.06$) in the roof control plot due to the higher $\delta^{15}\text{N}$ excess ($p = 0.06$) combined with significantly higher biomass. Because of energetic advantage in utilizing ammonium (Gutschick 1981), the recovery of atmospheric ammonium in the live fine roots in the organic layer tended to be higher than that of atmospheric nitrate in the roof control plot. The difference was not statistically significant, probably due to the high spatial variability caused by the small sample size ($n \leq 4$). From another root sampling applied in the same subplots and the same year (2004) but with larger sample size ($n = 5$), significant higher recovery of atmospheric ammonium (3.0%) than nitrate (1.4%) in the live and dead fine roots in the organic layer was found in the roof control plot. In the deeper soil, atmospheric nitrate was the major available N source for the fine roots under ambient atmospheric deposition, indicated by the higher $\delta^{15}\text{N}$ excess of the live fine roots after $^{15}\text{NO}_3^-$ addition than after $^{15}\text{NH}_4^+$ addition in the roof control plot (Fig. 4.4). Consequently, the higher recovery of atmospheric nitrate than ammonium was found in the live fine roots in the deeper soil in the roof control plot ($p = 0.06$). Although the recovery of atmospheric ammonium and nitrate in the live fine roots differed with soil depth, the total recovery of the two N species in the live fine roots was equal in the roof control plot.

5.1.2.1.3 Leaching

Consistent with the higher retention efficiency of the soil for atmospheric ammonium under ambient atmospheric deposition, a larger proportion of atmospheric nitrate than ammonium was exported as nitrate below root zone. The sink strength of nitrate leaching has been reported from several studies (Koopmans et

al. 1996, Gundersen 1998, Tietema et al. 1998, Nadelhoffer et al. 1999b, Schleppi et al. 1999, Table 1.1). In accordance with the result in the roof control plot in which nitrate leaching comprised 3% of atmospheric ammonium, Nadelhoffer et al. (1999b) reported that 5% of ^{15}N -ammonium leached as nitrate during 2 years of ^{15}N addition to the forest at West Bear Brook Watershed in Maine, USA. In the N-saturated Douglas fir forest at Speuld in the Netherlands, however, Koopmans et al. (1996) found a much larger proportion (32%) of atmospheric ammonium in the nitrate leachate. The higher nitrate leaching at Speuld was caused by lower C/N ratio of organic layer (21, as compared to 25 in the roof control plot) combined with higher N deposition ($44 \text{ kg ha}^{-1} \text{ yr}^{-1}$). The lower C/N ratio indicates more active nitrification as well as lower retention capacity of the soil for deposited and internally generated nitrate (Emmett et al. 1998b).

DON leaching is a negligible sink for atmospheric N under ambient atmospheric deposition. This result is consistent with the finding by Perakis and Hedin (2001) that < 2% of ^{15}N -ammonium and ^{15}N -nitrate were respectively recovered in extractable NH_4^+ and DON pools in an old mixed-angiosperm forest in Chile. Because inorganic N in the throughfall water was transformed to organic N by the assimilation of tree and microbe, the negligible ^{15}N recovery in DON leachate in the roof control plot suggested that almost all of the assimilated inorganic N was either recycled within the spruce forest ecosystem or exported as nitrate leachate under ambient atmospheric deposition.

5.1.2.2 Under long-term reduced atmospheric deposition (the clean rain plot)

5.1.2.2.1 Soil

Similar to under ambient atmospheric deposition, under long-term reduced atmospheric deposition, soil was the largest sink for atmospheric N (Table 4.14). In the clean rain plot, the recovery of atmospheric ammonium in the total soil profile was not different from that of atmospheric nitrate. However, the organic layer seemed to account for a larger proportion of atmospheric ammonium than atmospheric nitrate, although the difference was not significant. Conversely, the recovery of atmospheric ammonium in the mineral soil was only 0.7% and much lower than that of atmospheric nitrate (30.7%). This suggested that almost all atmospheric ammonium in the soil was retained in the organic layer, while a large proportion of atmospheric nitrate was still transported to the deeper soil under long-term reduced atmospheric deposition. Buchmann et al. (1996) reported similar recovery of $^{15}\text{NH}_4^+$ and $^{15}\text{NO}_3^-$ in the soil of the Norway spruce forest in the Fichtelgebirge with a similar atmospheric N deposition rate ($12 \text{ kg ha}^{-1} \text{ yr}^{-1}$), with the exception that a higher recovery of $^{15}\text{NH}_4^+$ (24%) was found in the mineral soil.

The retention of atmospheric N in the soil was influenced by long-term reduced atmospheric deposition (Table 4.14, Fig. 5.1). Although the organic layer

and the mineral soil together retained the same proportion of atmospheric ammonium in the clean rain plot as in the roof control plot, the distribution of the recovered atmospheric ammonium in soil layers was different between the two roofed plots. The recovery of atmospheric ammonium in the organic layer had a slight increase in the clean rain plot, resulting in a lower recovery of atmospheric ammonium in the mineral soil in the clean rain plot than in the roof control plot. Long-term reduced atmospheric deposition had a greater influence on the retention of atmospheric nitrate in the soil. The recovery of atmospheric nitrate in the soil amounted to 42% in the roof control plot and increased significantly to 68% in the clean rain plot, driven by an obvious increase of the recovery in the organic layer from 8% in the roof control plot to 37% in the clean rain plot. The mineral soil accounted for about one third of atmospheric nitrate, and the recovery was not different between the clean rain and the roof control plot. It indicated that the mineral soil was an important and a relatively stable sink for atmospheric nitrate. Therefore, in such forest ecosystem, the organic layer was the key compartment for indicating and controlling the change in retention efficiency of the soil for atmospheric nitrate under changed atmospheric deposition.

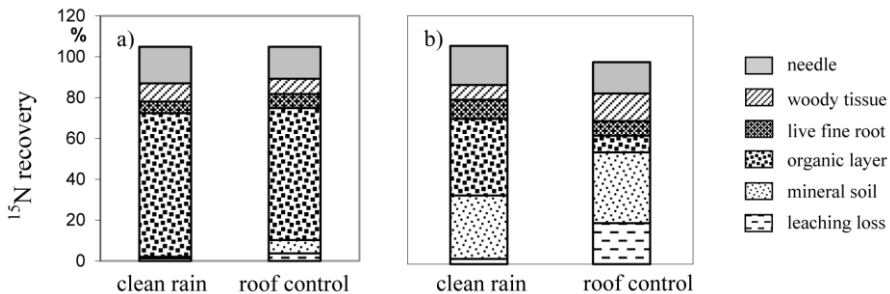


Fig. 5.1. Percent recovery of a) $^{15}\text{NH}_4^+$; b) $^{15}\text{NO}_3^-$ in the spruce forest ecosystem compartments in the clean rain and the roof control plot.

Compared to the roof control plot, the lower recovery of atmospheric ammonium in the mineral soil and the obviously higher recovery of atmospheric nitrate in the organic layer in the clean rain plot could be explained by the N transformation processes reported by Corre and Lamersdorf (2004) in the same Norway spruce forest. They found that microbial immobilization of ammonium was enhanced and abiotic nitrate immobilization increased in the organic layer in the clean rain plot. Moreover, gross nitrification was undetectable in the clean rain plot. The enhanced microbial immobilization of ammonium in the organic layer in the clean rain plot enabled atmospheric ammonium to have less opportunity to leach to the deeper soil. The undetectable gross nitrification suggested that nitrate in the soil originated from atmospheric nitrate. Consequently, the increased abiotic nitrate

immobilization in the organic layer in the clean rain plot led to a higher proportion of atmospheric nitrate retained in this layer.

The retention efficiency of the soil for N input under changed N input conditions was reported in other ^{15}N tracer studies and yielded different results. In agreement with this present study, Koopmans et al. (1996) found a higher recovery of $^{15}\text{NH}_4^+$ in the organic layer under reduced atmospheric N deposition in the Douglas fir forest at Speuld in the Netherlands. Tietema et al. (1998) and Gundersen (1998) reported higher recoveries of ^{15}N ($^{15}\text{NH}_4^+$, $^{15}\text{NO}_3^-$ or $^{15}\text{NO}_3^-$) in the organic layer and constant recoveries of ^{15}N in the mineral soil under lower N inputs in two European spruce forests. Perakis et al. (2005) found a relative constant recovery of $^{15}\text{NH}_4^+$ in a temperate forest soil in Chile under N fertilization of up to $160 \text{ kg ha}^{-1} \text{ yr}^{-1}$. Nevertheless, Nadelhoffer et al. (1999a) reported a higher recovery of $^{15}\text{NO}_3^-$ in the mineral soil in a fertilized plot than in a control plot in the red pine forest at Harvard Forest. They attributed the higher recovery of $^{15}\text{NO}_3^-$ in the mineral soil to a possibly lower proportion of $^{15}\text{NO}_3^-$ immobilized by microbes in the organic layer in the fertilized plot. In addition, Nadelhoffer et al. (1999a) found the differences in the recovery of $^{15}\text{NH}_4^+$ vs. $^{15}\text{NO}_3^-$ in the control and the fertilized plot. In the control plot, a lower recovery of $^{15}\text{NH}_4^+$ than $^{15}\text{NO}_3^-$ was shown in the organic layer, whereas the recoveries of the two ^{15}N tracers were not different in the mineral soil. In the fertilized plot, a higher recovery of $^{15}\text{NH}_4^+$ than $^{15}\text{NO}_3^-$ was observed in the organic layer, whereas the opposite pattern was found in the mineral soil. The present study showed, however, consistent trends in the recovery of $^{15}\text{NH}_4^+$ vs. $^{15}\text{NO}_3^-$ in the clean rain and the roof control plot, i.e. higher recovery of $^{15}\text{NH}_4^+$ than $^{15}\text{NO}_3^-$ in the organic layer and lower recovery of $^{15}\text{NH}_4^+$ than $^{15}\text{NO}_3^-$ in the mineral soil. This indicated that the retention efficiency of the organic layer for ammonium and nitrate input may be different between the red pine forest and the Norway spruce forest under changed N input conditions. In the red pine forest at Harvard Forest, the retention efficiency of the organic layer for nitrate input was higher than that for ammonium input in the control plot, while this retention capacity for nitrate input may reach saturation in the fertilized plot (Nadelhoffer et al. 1999a, 2004). In the Norway spruce forest at Solling (the present study), the organic layer had a higher retention efficiency for atmospheric ammonium than for atmospheric nitrate in both the clean rain and the roof control plot, leading to greater transport of atmospheric nitrate than ammonium to the mineral soil in the two plots.

5.1.2.2.2 Tree

Under long-term reduced atmospheric deposition, trees were the second important sink for atmospheric N, accounting for more than 32% of the added ^{15}N . The distribution of atmospheric N in tree compartments under long-term reduced atmospheric deposition showed similar patterns as that under ambient atmospheric deposition. Among the tree compartments, needles retained the largest proportion of atmospheric N in the clean rain plot, followed by the woody tissues and the live fine roots. The assimilated atmospheric N in above ground tree tissues was not only used to produce new tissues but also retranslocated to older tissues. In the live fine roots in the 10-40 cm mineral soil layer, the recovery of atmospheric nitrate was slightly higher than that of atmospheric ammonium in the clean rain plot. This retention pattern was consistent with that found in the soil, where a clearly higher recovery of atmospheric nitrate than ammonium was found in the mineral soil in the clean rain plot. The similar retention pattern in the live fine roots and the soil demonstrated the high mobility of atmospheric nitrate to the deeper soil under long-term reduced atmospheric deposition. In general, the retention efficiency of the trees for atmospheric ammonium did not differ from that for atmospheric nitrate under long-term reduced atmospheric deposition.

The retention efficiency of the trees for atmospheric N was not significantly affected by long-term reduced atmospheric deposition, with the exception that the retention efficiency of the live fine roots in different soil layers showed small differences. The recovery of atmospheric ammonium in the live fine roots in the 10-40 cm mineral soil layer tended to be lower in the clean rain plot than in the roof control plot, whereas the recovery of atmospheric nitrate in the live fine roots in the organic layer tended to be higher in the clean rain plot than in the roof control plot. These retention patterns in the live fine roots were consistent with those in the soil, and may reflect the leaching loss of atmospheric N under long-term reduced atmospheric deposition. Compared to the roof control plot, the lower recovery of atmospheric ammonium in the deeper soil and in the live fine roots in deeper soil layer in the clean rain plot indicated a lower proportion of atmospheric ammonium was transported to deeper soil depths and may leach out under long-term reduced atmospheric deposition. The recovery of atmospheric nitrate in the mineral soil was constant, and that in the live fine roots in the mineral soil was not different between the clean rain and the roof control plot. The higher recovery of atmospheric nitrate in the organic layer and in the live fine roots in this layer in the clean rain plot could enable a lower proportion of atmospheric nitrate to leach out under long-term reduced atmospheric deposition.

The same retention efficiency of the trees for atmospheric N under long-term reduced atmospheric deposition as under ambient atmospheric deposition, may be attributed to enhanced microbial immobilization of ammonium as well as faster turnover of ammonium and microbial N pools in the clean rain plot (Corre and

Lamersdorf 2004). ^{15}N recovery in a pool is a function of initial uptake, residence time, subsequent inputs from and losses to other ecosystem pools (Nadelhoffer et al. 2004). The enhanced microbial immobilization of ammonium and faster turnover of ammonium and microbial N pools could enable more atmospheric N to be transferred from microbial pool to the trees in a shorter time. As a result, the retention efficiency of the trees for atmospheric N may remain constant under long-term reduced atmospheric deposition.

Compared to the present study, in which the recovery of ^{15}N in the trees was not significantly influenced by long-term reduced atmospheric deposition, a similar result was also reported by Koopmans et al. (1996) in the Douglas fir forest at Speuld. They demonstrated that the recovery of $^{15}\text{NH}_4^+$ in trees did not change significantly under reduced atmospheric N deposition. Gundersen (1998), Tietema et al. (1998) and Nadelhoffer et al. (1999a) found different results in N fertilization experiments. Higher recoveries of ^{15}N tracers in trees with increased N inputs were found in a Norway spruce forest at Klosterhede (Gundersen 1998) and in the red pine forest at Harvard Forest in Massachusetts (Nadelhoffer et al. 1999), while a lower recovery of $^{15}\text{NO}_3^-$ with increased N input was reported in Sitka spruce trees at Aber (Tietema et al. 1998). The different results in the N fertilization experiments could be explained by different N inputs to the forests. In these N fertilization experiments, N input to the forests in Massachusetts and at Klosterhede increased from 8 to 58 $\text{kg ha}^{-1} \text{ yr}^{-1}$ and from 20 to 55 $\text{kg ha}^{-1} \text{ yr}^{-1}$, respectively, while N input to the forest at Aber increased from 50 to 90 $\text{kg ha}^{-1} \text{ yr}^{-1}$. The lower initial N input and N fertilization rate in Massachusetts and at Klosterhede enabled the trees to further assimilate available N. At Aber, the high initial N input may have already far exceeded the demand of the trees, as indicated by a large proportion of N input in leachate (35%, see Table 1.1). Therefore, the trees at Aber retained a smaller proportion of N input after N fertilization with a higher fertilization rate. Simultaneously, a larger proportion of N input (50%) was leached out.

In the present study, the recovery of atmospheric ammonium in the trees was not different from that of atmospheric nitrate under ambient and long-term reduced atmospheric deposition. Perakis and Hedin (2001) reported similar recovery of $^{15}\text{NH}_4^+$ and $^{15}\text{NO}_3^-$ in fine roots in a mixed-angiosperm forest in Chile. However, higher recoveries of $^{15}\text{NO}_3^-$ than $^{15}\text{NH}_4^+$ in trees were found in two European Norway spruce forests (Buchmann et al. 1996, Providoli et al. 2005) and in the red pine forest at Harvard Forest in USA (Nadelhoffer et al. 1999a). Nadelhoffer et al. (1999a) attributed the higher recovery of $^{15}\text{NO}_3^-$ than $^{15}\text{NH}_4^+$ in the trees to tree species preference for nitrate, to greater competition between tree roots and soil microbes for ammonium or to more rapid movement of nitrate to root surfaces.

5.1.2.2.3 Leaching

Leaching loss accounted for a small proportion of atmospheric N under long-term reduced atmospheric deposition. Due to high retention of atmospheric ammonium and nitrate in the forest ecosystem, no atmospheric ammonium was detected in the nitrate leachate, and only 2% of atmospheric nitrate was exported as nitrate leachate below root zone in the clean rain plot. At a similar atmospheric N deposition rate ($12 \text{ kg N ha}^{-1} \text{ yr}^{-1}$), low recoveries of $^{15}\text{NH}_4^+$ and $^{15}\text{NO}_3^-$ in the nitrate leachate (0.2% and 2.3%, respectively) were also found in the Norway spruce forest in Switzerland (Providoli et al. 2005).

Long-term reduced atmospheric deposition decreased the leaching loss of atmospheric N as nitrate. Although almost all atmospheric ammonium was retained in the forest ecosystem in the roof control plot, the retention efficiency of the forest ecosystem still increased slightly in the clean rain plot. As a result, no atmospheric ammonium was exported as nitrate leachate in the clean rain plot. The leaching loss of atmospheric nitrate decreased drastically under long-term reduced atmospheric deposition from 19.2% in the roof control plot to 2.0% in the clean rain plot. Since trees and the mineral soil were stable sinks for atmospheric nitrate, the drastic decrease in leaching loss of atmospheric nitrate was driven by a strongly increased retention efficiency of the organic layer. The retention efficiency of the organic layer controlled, thus, the leaching loss of atmospheric nitrate. The influence of changed N inputs on the recovery of ^{15}N in the nitrate leachate was reported in several studies. In the Douglas fir forest at Speuld, the recovery of $^{15}\text{NH}_4^+$ in nitrate leachate decreased drastically from 32% to 2% under reduced atmospheric N deposition (Koopmans et al. 1996). Gundersen (1998) and Tietema et al. (1998) found increased recoveries of ^{15}N in nitrate leachate with increased N inputs in two European spruce forests, respectively.

The recovery of atmospheric N in the DON leachate was very low in the clean rain plot. As gross nitrification was not detected in the clean rain plot (Corre and Lamersdorf 2004), the low recovery of atmospheric N in the DON leachate suggested that almost all assimilated atmospheric N was recycled within the forest ecosystem under long-term reduced nitrogen deposition. The low recovery of atmospheric N in the DON leachate was independent of the amounts and forms of atmospheric N deposition, indicating that export of atmospheric ammonium and nitrate as DON leachate was small and relative stable.

5.2 Density fractionation experiment

5.2.1 Preparation of density solution

It was time-consuming to prepare the SPT (sodium polytungstate) solutions for the density fractionation experiments, as the volume of SPT solution varied with the amount of added SPT. In the small preliminary experiment, the volume change of SPT solution was found to be linearly correlated with the amount of added SPT (Fig. 4.7). Based on the linear correlation, the amount of SPT and the volume of water needed for an expected volume of SPT solution with an expected density could be calculated (equation 3.6, 3.7). The calculated amount of SPT and the volume of water were tested during the density fractionation experiment. It was found that the density of SPT solution was slightly lower and the volume of the solution slightly higher than that expected, respectively, after the addition of the calculated amount of SPT and volume of water (data not shown). The density of SPT solution did not need to be further adjusted, when only the calculated amount of SPT was used and water was added to the level marked in the container. It suggested that the constant k may not be exact enough, due to the inaccurate estimate of volume of the solution in the measuring cylinder. In spite of this shortcoming, the constant k and the related equations gave directions, and greatly reduced the time needed to prepare the SPT solution. Therefore, the constant k and the related equations, especially equation 3.6, could be considered as useful tools in preparing an expected volume of SPT solution with an expected density.

5.2.2 Comparison of two aggregate-disrupting methods

Sonification seemed to provide more energy to disrupt aggregates than 16-h shaking with glass beads. Compared to 16-h shaking, sonification destroyed the association between organic matter and mineral particles to a greater extent. As a consequence, more organic matter with less mineral particles was released from the aggregates and accumulated in the lighter Ocl. I fraction (Table 4.15). As the mineral particles had a low C and N concentration, less mineral particles in the Ocl. I fraction after sonification resulted in the slightly higher C and N concentration of this fraction. The higher yield of the Ocl. I fraction combined with the slightly higher C and N concentration led to a larger contribution of the Ocl. I fraction to soil OC and total soil N after sonification than after shaking. SOM in the heavier Ocl. III fraction had a close association with mineral particles (Golchin et al. 1994b). Properties of this fraction were, thus, not significantly influenced by the two different aggregate-disrupting methods, except that the C/N ratio was lower after sonification than after shaking. Different trends were showed in the properties of the Ocl. II fraction with a medium density after using the two aggregate-

disrupting methods in different soil layers. The Ocl. II fraction from the organic layer had higher C and N concentration after sonification than after shaking, while that from the 0-5 cm mineral soil layer had significantly lower C concentration after sonification than after shaking. A higher C concentration may result from a lower mineral content and/or a more advanced degree of SOM decomposition (Golchin et al. 1994a). The different aggregate-disrupting methods were unlikely to cause the difference in degree of SOM decomposition. The different C and N concentration of the Ocl. II fraction after using the two aggregate-disrupting methods in the measured soil layers, indicated a different mineral content in this fraction. The mineral content in the Ocl. II fraction from the organic layer was lower after sonification than after shaking. Conversely, the mineral content in the Ocl. II fraction from the 0-5 cm mineral soil layer was higher after sonification than after shaking. The DF with the highest density accumulated the mineral particles, which remained after the release of SOM (Golchin et al. 1994b). In the organic layer, fewer mineral particles were associated with organic matter in the occluded fractions after sonification. More mineral particles were, therefore, retained and accumulated in the DF after sonification. The DF had a higher mineral content, resulting in a significantly lower C and N concentration after sonification than after shaking. The significantly lower C concentration of the DF after sonification was the main cause of a significantly smaller contribution of this fraction to soil OC. The C/N ratio of the DF from the organic layer was obviously lower after sonification than after shaking, attributing probably to the higher mineral content in this fraction after sonification. Microbial biomass and products, which had a low C/N ratio, were absorbed to the surfaces of the mineral particles during the decomposition of SOM (Golchin et al. 1994b). The higher mineral content with associated microbial biomass and products in the DF could lead to the lower C/N ratio. In the organic layer and the 0-5 cm mineral soil layer, soil OC and N were not completely recovered in the separated density fractions after using the two aggregate-disrupting methods. This phenomenon was common in density fractionation experiments, and may be explained by the loss of soluble OC and N with the SPT solution during the density fractionation procedure (Compton and Boone 2002, Rovira and Vallejo 2003).

In both the organic layer and the 0-5 cm mineral soil layer, natural ^{15}N abundance increased from the FL fraction to the occluded fractions after using the two aggregate-disrupting methods, indicating an increased degree of decomposition. After using the two aggregate-disrupting methods, the natural ^{15}N abundances of the occluded fractions and the DF from the different soil layers showed different trends. The $\delta^{15}\text{N}$ values of the occluded fractions and the DF from the organic layer were obviously higher after sonification than after shaking, while the $\delta^{15}\text{N}$ values of these fractions from the 0-5 cm mineral soil layer were not significantly different after using the two methods. It was not clear why the stronger isotopic fractionation against ^{15}N after sonification than after shaking occurred in the frac-

tions from the organic layer, but not in those from the 0-5 cm mineral soil layer. The higher $\delta^{15}\text{N}$ values of the occluded fractions and the DF from the organic layer combined with incomplete recovery of soil N, might indicate that more ^{14}N was lost with the SPT solution after sonification than after shaking. The preferential loss of ^{14}N with the SPT solution during density fractionation was evidenced by Crow et al. (2007) in a conifer forest soil.

Generally, properties of soil density fractions showed only few significant differences after using the two different aggregate-disrupting methods. It demonstrated that sonification and 16-h shaking may have no significant difference in aggregate-disruption.

5.2.3 Distribution of OC and N in soil density fractions

The organic layer consisted mostly of undecomposed litter. The FL fraction had, therefore, a predominant contribution to the soil dry weight, soil OC and total soil N (Table 4.17). The occluded fractions and the DF played only a small role. The C/N ratio of the occluded fractions was lower than that of the FL fraction, indicating an increased degree of decomposition. The C/N ratio was lowest in the DF, due to microbial biomass and products adsorbed on the mineral surface (Golchin et al. 1994b). These results were in accordance with those reported by Rovira and Vallejo (2003). They found 89% of OC and 85% of N in the FL fraction from the O_H layer, respectively; the C/N ratio was highest in the FL fraction and lowest in the DF.

Compared to the roof control plot, the occluded fractions from the organic layer showed a smaller contribution to the soil dry weight, soil OC and total soil N in the clean rain plot. It suggested that relative less SOM was accumulated in the occluded fractions in the clean rain plot than in the roof control plot. The organic matter in the occluded fractions has higher stability than that in the FL fraction, attributing to the higher recalcitrance and spatial inaccessibility caused by the occlusion (von Lützow et al. 2007). The accumulation of relative less SOM in the occluded fractions from the organic layer in the clean rain plot indicated that SOM in the organic layer had a lower stability in the clean rain plot. As the occlude fractions from the organic layer made only a small contribution to SOM, the difference in the stability of SOM between the clean rain and the roof control plot may not be great. This was consistent with slightly increased gross N mineralization in the organic layer in the clean rain plot compared to the roof control plot (Corre and Lamersdorf 2004). Swanston et al. (2004) concluded that long-term elevated N could increase SOM stability. They attributed the increased SOM stability in the organic layer to increased recalcitrance of the SOM, but did not preclude the effect of elevated N on specific microbial species, functional species groups or enzymes.

Krosshavn et al. (1992) reported that the C content of organic matter increased with increasing decomposition in spruce forest soil. In the present study, although decomposition of organic matter was stronger in the clean rain plot, C concentrations of the occluded fractions from the organic layer were significantly lower in the clean rain plot than in the roof control. One possible explanation was an underestimation of the C concentration caused by the formation of CaPT. Rovira and Vallejo (2003) noted that CaPT could increase the weight of a fraction, resulting in a decreased C concentration, especially for the occluded fractions with small amounts. In the present study site, the Ca content in the organic layer was higher in the clean rain plot (2.7 g kg^{-1}) than in the roof control plot (2.4 g kg^{-1} , Heinrichs et al. 1986, see also Corre and Lamersdorf 2004). More CaPT may form in the clean rain plot, as evidenced by the high recovery of soil dry weight which was more than 100%. Combined with the smaller amount of the occluded fractions, C concentrations of these fractions may be underestimated in the clean rain plot. Similarly, N concentrations of the occluded fractions might be also underestimated in the clean rain plot. The C and N concentration of total soil decreased with increasing soil depth (Table 4.4). In the roof control plot, C and N concentrations of the density fractions followed the same pattern as the total soil. However, C and N concentrations of the occluded fractions from the organic layer were lower than those from the 0-5 cm mineral soil layer in the clean rain plot. This supported the idea that C and N concentrations of the occluded fractions from the organic layer were probably underestimated in the clean rain plot.

In the mineral soil layers, the DF played the most important role. The DF made the largest contribution to soil dry weight, soil OC and total soil N (Table 4.18, Table 4.19). Its contribution to soil OC, especially to total soil N, became predominant in the 5-10 cm mineral soil layer. The increased contribution of the DF to soil OC with soil depth, especially to total soil N, was also found in mediterranean forest soils (Rovira and Vallejo 2003). The distribution of soil OC and total soil N in the density fractions from the mineral soil layers in the present study was comparable to that reported in other studies, in which the same density fractionation procedure was applied. Golchin et al. (1994a, b) demonstrated similar results from five virgin soils. Rovira and Vallejo (2003) and John et al. (2005) (see also Helfrich et al. 2006) showed, however, a higher contribution of the FL fraction to soil OC and total soil N. They found that the FL fraction from A horizon accounted for 58% of soil OC and 50% of total soil N in the mediterranean forest soils, and 34% of soil OC and 28% of total soil N in a Norway spruce forest soil, respectively.

Like the occluded fractions from the organic layer, those from the mineral soil layers made generally a smaller contribution to soil dry weight, soil OC and total soil N in the clean rain plot than in the roof control plot, indicating lower accumulation and stability of SOM in the clean rain plot. Swanston et al. (2004) reported two different stabilization mechanisms of SOM for light fractions (LF,

$d < 1.65\text{g cm}^{-3}$) and heavy fractions (HF) stimulated by elevated N. In the LF, elevated N may cause greater incorporation of N to the Klason lignin fraction, leading to increasing recalcitrance of SOM. In the HF, elevated N may inhibit the mechanisms of the degradation of complex molecules. Besides the two stabilization mechanisms, another possible mechanism was the interaction of SOM with Al. In the present study site, the Al concentration in the soil solution in upper mineral soil depth was lower in the clean rain plot than in the roof control plot (Bredemeier et al. 1998b, Lamersdorf and Borken 2004). The interaction between SOM and Al was probably lower in the clean rain plot than in the roof control plot, resulting in lower stability of SOM in the clean rain plot.

In the upper mineral soil, the higher C and N concentrations of the occlude fractions in the clean rain plot than in the roof control plot may result from more advanced decomposition and lower mineral content in the clean rain plot. The FL fraction consisted mainly of relative fresh and undecomposed plant debris (Golchin et al. 1994a, Helfrich et al. 2006). The lower C and N concentration of the FL fraction from the mineral soil layer in the clean rain plot suggested that this fraction may have a higher mineral content in the clean rain plot than in the roof control plot.

5.2.4 Recovery of soil ^{15}N

Recovery of soil ^{15}N in the density fractionation experiment reflected the distribution of atmospheric N retained in the soil in different density fractions. Since density fractions differ from each other in stability, the incorporation of atmospheric N in different density fractions may demonstrate the stability of atmospheric N retained in the soil. In most cases, the total recoveries of soil ^{15}N in the density fractions ranged from 64% to 94%. The incomplete recovery of soil ^{15}N in the density fractions may be due to loss of soil ^{15}N through the incorporation in dissolved organic matter and subsequent loss with the SPT solution (Compton and Boone 2002).

In the clean rain and the roof control plot, the FL fraction was a predominant sink for atmospheric N retained in the organic layer, while the occluded fractions and the DF accounted for less than 10% of atmospheric N in this layer (Table 4.20, Fig. 5.2). As the FL fraction represents an active pool with low stability, and the occluded fractions and the DF contribute intermediate and passive pools with high stability (von Lützwow et al. 2007), high recovery of atmospheric N in the FL fraction and low recovery in the occluded fractions and the DF from the organic layer indicated that atmospheric N retained in the organic layer may be mainly active and have a low stability. The stability of atmospheric N in the organic layer was little different between atmospheric N forms as well as between the two roofed plots. In the clean rain and the roof control plot, smaller proportions of atmospheric ammonium than nitrate in the organic layer were incorporated into

the occluded fractions and the DF, suggesting possibly lower stability of atmospheric ammonium in the organic layer in the two plots. Compared to the roof control plot, smaller proportions of atmospheric N in the organic layer were recovered in the occluded fractions in the clean rain plot, indicating that the stability of atmospheric N in the organic layer may be lower in the clean rain plot.

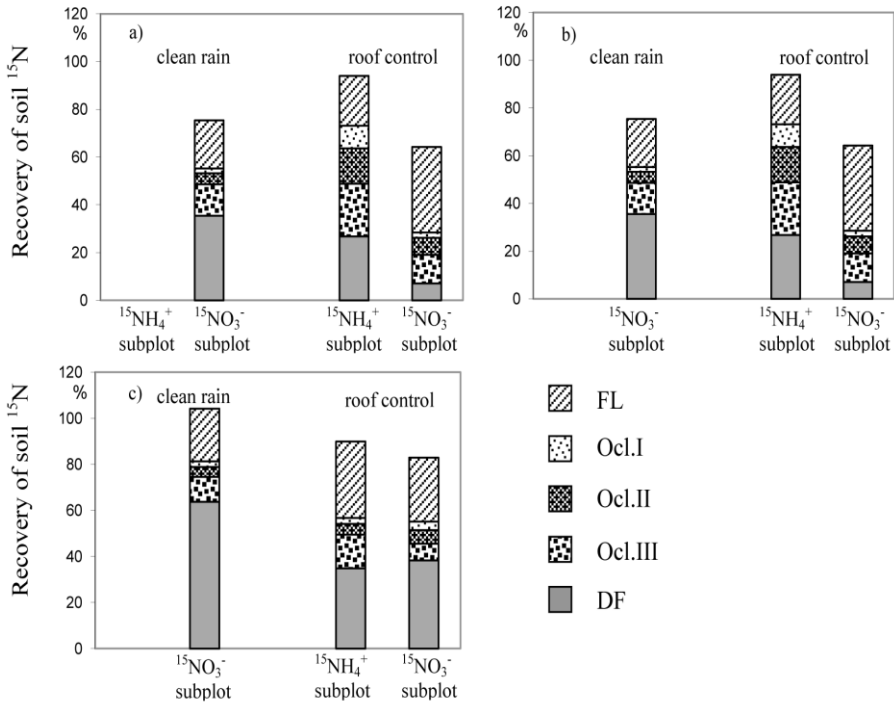


Fig. 5.2. Percent recovery of soil ^{15}N in density fractions from a) the organic layer; b) the 0-5 cm mineral soil layer; c) the 5-10 cm mineral soil layer in the clean rain and the roof control plot after $^{15}\text{NH}_4^+$ and $^{15}\text{NO}_3^-$ addition.

Compared to the organic layer, the FL fraction was a much smaller sink for atmospheric N retained in the mineral soil layers, whereas the occluded fractions and the DF were larger sinks. The DF had the highest stability and accounted for larger proportions of atmospheric N in the 5-10 cm mineral layer than in the 0-5 cm mineral soil layer. This suggested that the stability of atmospheric N in the soil may increase with soil depth. Atmospheric N forms and long-term reduced atmospheric N deposition seemed to have greater influences on the stability of atmospheric N in the 0-5 cm mineral soil layer than that in the organic layer. In the roof control plot, the tendency to a lower recovery of atmospheric ammonium

than nitrate in the FL fraction combined with higher recoveries of atmospheric ammonium than nitrate in the occluded fractions and the DF from the 0-5 cm mineral soil layer demonstrated that atmospheric ammonium was probably more stable than atmospheric nitrate in this layer. However, it should be noted that the total recovery of atmospheric ammonium (94%) was higher than that of atmospheric nitrate (64%) in the density fractions from the 0-5 cm mineral soil layer. Therefore, the stability of atmospheric ammonium might be less different from that of atmospheric nitrate in the 0-5 cm mineral soil layer. Long-term reduced atmospheric deposition tended to increase the stability of atmospheric nitrate in the 0-5 cm mineral soil layer, as indicated by the trend to a higher recovery of atmospheric nitrate in the DF in the clean rain plot than in the roof control plot. In the deeper mineral soil layer (5-10 cm), the stability of atmospheric N was influenced neither by atmospheric N forms nor by long-term reduced atmospheric deposition.

The results from the mineral soil layers in the present study were different from those reported by Compton and Boone (2002). They found that the LF (corresponding to the FL in the present study) accounted for a higher proportion of $^{15}\text{NH}_4^+$ and $^{15}\text{NO}_3^-$ (17-39%) than the HF (corresponding to the occluded fractions and the DF in the present study, < 5%) after 18h incubation in 0-15 cm mineral soil layer, and concluded that the LF was a strong short-term sink for N. In the present study, in which $^{15}\text{NH}_4^+$ and $^{15}\text{NO}_3^-$ had been added for over 3 years, the recoveries of soil ^{15}N in the FL fraction from the mineral soil layers were less than or approximately equal to those in the occluded fractions and the DF. It suggested that the roles of the density fractions in incorporation of added N may vary with time.

Atmospheric N was incorporated into the soil through biotic (microbial) and abiotic immobilization (Johnson 1992, Aber et al. 1998, Berntson and Aber 2000). Mechanisms for abiotic ammonium immobilization include condensation reaction with phenolic compound and fixation on clay minerals (Nömmik and Vahtras 1982, Davidson et al. 1991, Johnson et al. 2000). Abiotic nitrate immobilization is thought to occur via the reaction of NO_2^- with soil organic matter (Smith and Chalk 1980, Azhar et al. 1986, Thorn and Mikita 2000). These mechanisms could not be clearly distinguished. In the organic layer, low recovery of atmospheric N in the occluded fractions and the DF indicated that microbial and abiotic N immobilization occurred mainly in the undecomposed plant debris. The organic matter in the DF was mainly of microbial origin (Golchin et al. 1994b, 1995). Although the proportion of microbial biomass in the FL fraction and the occluded fractions were unknown, high recovery of atmospheric nitrate in the DF from the mineral soil layers suggested that microbial immobilization may play an important role in incorporation of atmospheric nitrate in mineral soil.

6 Conclusion

In the present study, $^{15}\text{NH}_4^+$ and $^{15}\text{NO}_3^-$ had been added to a typical central European Norway spruce forest for over 3 years after a 10-year reduction of atmospheric deposition. The distribution of ^{15}N in different spruce forest ecosystem compartments was followed under ambient and long-term reduced atmospheric deposition. In addition, the distributions of soil ^{15}N in different density fractions were compared under the two atmospheric deposition conditions. The results reflected the influence of long-term reduced atmospheric deposition on the partitioning of atmospheric N within the spruce forest ecosystem as well as on the partitioning of atmospheric N in SOM pools.

Influence of long-term reduced atmospheric deposition on the partitioning of atmospheric N within the spruce forest ecosystem

The soil was the largest sink for atmospheric N under ambient and long-term reduced atmospheric deposition. Trees had a high contribution to the retention of atmospheric N and the retention efficiency of the trees was independent of the amount and inorganic N forms of atmospheric N deposition. Long-term reduced atmospheric deposition influenced mainly the partitioning of atmospheric nitrate. The mineral soil was an important and a constant sink for atmospheric nitrate, while the retention efficiency of the organic layer controlled the leaching loss of atmospheric nitrate. Under ambient atmospheric deposition, the partitioning of atmospheric ammonium and nitrate differed from each other in the soil and the nitrate leachate. A higher proportion of atmospheric ammonium than nitrate was retained in the soil and conversely a lower proportion of atmospheric ammonium than nitrate losses by the nitrate leachate. Long-term reduced atmospheric deposition lessened the differences in the partitioning of atmospheric ammonium and nitrate. The similarity in the partitioning of atmospheric N between the present study, in which $^{15}\text{NH}_4^+$ and $^{15}\text{NO}_3^-$ had been separately applied for over 3 years after a 10-year reduction of atmospheric deposition, and the study at Speuld, in which $^{15}\text{NH}_4^+$ had been added for one year after a 3-year reduction of atmospheric ammonium deposition, may conclude that the short-term and long-term response of forest ecosystems to the reduced atmospheric N deposition does not seem to differ greatly.

Influence of long-term reduced atmospheric deposition on the partitioning of atmospheric N in SOM pools

SOM pools played different roles in incorporation of atmospheric N retained in different soil layers. Atmospheric N retained in the organic layer was incorporated predominantly into the less stable SOM pool (FL fraction). The contribution of the stable SOM pool (DF) to incorporation of atmospheric N in the soil increased

with soil depth. The stability of atmospheric N in the soil increased, thus, with soil depth. N forms and long-term reduced atmospheric deposition influenced mainly the stability of atmospheric N in the most upper mineral soil layer (0-5 cm). Under ambient atmospheric deposition, atmospheric ammonium in the 0-5 cm mineral soil layer may be more stable than atmospheric nitrate. Long-term reduced atmospheric deposition increased the stability of atmospheric nitrate in the 0-5 cm mineral soil layer.

7 Summary

In the past century, anthropogenic activities have increased N input drastically to terrestrial ecosystems and influenced the global N cycle. Especially temperate forest ecosystems are affected in their productivity, species composition, soil chemistry and water quality. N input to forest ecosystems is retained in trees and soil. Excessive N is leached out or released as gases. The retention of N input in soils is mainly influenced by the stability of soil organic matter (SOM). In central Europe and North America, many forests have been subjected to N saturation, i.e. excessive N appeared as nitrate in the leachate below the rooting zone. To improve N-saturated forest ecosystems, reduction of atmospheric N emission and consequent atmospheric N deposition is proposed to be the only practical long-term solution. Therefore, it is necessary to know how N-saturated forest ecosystems respond to reduced atmospheric N deposition. The main objective of the present study was to evaluate how long-term reduced atmospheric N deposition influences the partitioning of atmospheric ammonium and nitrate in a Norway spruce forest ecosystem. Two main experiments were conducted in the study: a ^{15}N tracer field and a density fractionation laboratory experiment. The aims were to 1) evaluate how long-term reduced atmospheric N deposition influences N retention in trees and soil, as well as N loss by leaching and 2) evaluate how long-term reduced atmospheric N deposition influences the partitioning of atmospheric N retained in the soil in different SOM pools.

The study was conducted in a currently 75-year-old Norway spruce forest on the Solling plateau in central Germany. Atmospheric deposition was manipulated through roof constructions below the canopy of the spruce forest. A roof control plot received nearly unchanged ambient atmospheric N deposition of $30 \text{ kg ha}^{-1} \text{ yr}^{-1}$ (sum of ammonium and nitrate), while a clean rain plot received reduced atmospheric N deposition to about $10 \text{ kg ha}^{-1} \text{ yr}^{-1}$. Simultaneously, annual atmospheric deposition of dissolved organic nitrogen (DON), sulphate and proton in the clean rain plot were reduced by 27%, 53% and 77%, respectively, compared to the roof control plot. Besides the two roofed plots, an ambient control plot without a roof served as a non-manipulated reference. After 10-year reduction of atmospheric N deposition, small amounts of highly labelled $^{15}\text{NH}_4\text{NO}_3$ and $\text{NH}_4^{15}\text{NO}_3$ had been separately and continuously added to one half of the clean rain and the roof control plot for over 3 years. In the ^{15}N tracer experiment, tree compartments (needles, twigs and branches, boles and fine roots), different soil layers (organic layer, 0-5, 5-10, 10-20, 20-30, 30-40, 40-60 cm mineral soil layer) and leachates at different soil depth (0, 10, 40, 100 cm mineral soil depth) were sampled in each ^{15}N -labelled subplot and the ambient control plot to analyze the C, N concentrations and ^{15}N abundances. In the density fractionation experiment, the organic layer and the upper two mineral soil layers in each ^{15}N -labelled subplot

were separated into five density fractions, respectively: the Free Light fraction (FL, $d < 1.6 \text{ g cm}^{-3}$); three occluded fractions (Ocl. I, Ocl. II and Ocl. III, $d < 1.6 \text{ g cm}^{-3}$, $d = 1.6\text{-}1.8 \text{ g cm}^{-3}$ and $d = 1.8\text{-}2.0 \text{ g cm}^{-3}$, respectively) and the Dense fraction (DF, $d > 2.0 \text{ g cm}^{-3}$). The organic C and total N concentration as well as the ^{15}N abundance of each density fraction were analyzed. In addition, in a preliminary density fractionation experiment two aggregate-disrupting methods (sonification and 16-h shaking with glass beads) were used for the density fractionation of the organic layer and the 0-5 cm mineral soil layer in the ambient control plot. In the preliminary experiment, different amounts of a density agent (sodium polytungstate, SPT) were added to a volume of water to derive equations for preparation of solutions of a range of densities.

Results from the ^{15}N tracer experiment demonstrated that the soil was the largest sink for atmospheric N in the clean rain and the roof control plot. Seventy-one percent of added $^{15}\text{NH}_4^+$ was retained in the soil in the two plots. The organic layer retained the largest proportion of added $^{15}\text{NH}_4^+$, accounting for 70% in the clean rain plot and 65% in the roof control plot. The recovery of added $^{15}\text{NO}_3^-$ in the soil increased significantly from 42% in the roof control plot to 68% in the clean rain plot, mainly due to an increase in the organic layer from 8% to 37%. The mineral soil was an important and a constant sink for atmospheric nitrate, retaining 31-34% of added $^{15}\text{NO}_3^-$ in the two plots. Trees had a high contribution to the retention of atmospheric N, accounting for 30-36% of added $^{15}\text{NH}_4^+$ and $^{15}\text{NO}_3^-$ in the clean rain and the roof control plot. The recovery of added ^{15}N in the trees was affected neither by long-term reduced atmospheric N deposition nor by the forms of the ^{15}N tracers. Among tree compartments, the largest proportion of added ^{15}N was retained in needles (15-19%), followed by woody tissues (7-13%) and live fine roots (6-9%). In the roof control plot, NO_3^- leaching accounted for 3% of added $^{15}\text{NH}_4^+$ and 19% of added $^{15}\text{NO}_3^-$. The recoveries of added $^{15}\text{NH}_4^+$ and $^{15}\text{NO}_3^-$ in the NO_3^- leachate decreased to 0% and 2% in the clean rain plot, respectively. In the two plots, only less than 2% of added $^{15}\text{NH}_4^+$ and $^{15}\text{NO}_3^-$ were found in the DON leachate. These results suggested that long-term reduced atmospheric N deposition influences mainly the partitioning of atmospheric nitrate and lessens differences between the partitioning of atmospheric ammonium and nitrate in forest ecosystems.

In the preliminary density fractionation experiment, the volume change of SPT solution was found to be closely correlated with the amount of added SPT ($y = 0.1863x$, $r^2 = 0.9993$). Based on the linear correlation, the amount of SPT and the volume of water needed for a SPT solution with an expected volume and an expected density could be calculated, and thus reduced largely the time in preparing SPT solution. In the ambient control plot, only the Ocl. I fraction from the 0-5 cm mineral soil layer had a greater contribution to total soil N after sonification (10%) than after 16-h shaking (2%). It demonstrated that the two methods may have no significant difference in the degree of aggregate-disruption.

Results from the density fractionation experiment showed that the FL fraction was a predominant sink for atmospheric N retained in the organic layer. Ninety percent of soil $^{15}\text{NH}_4^+$ and 81% of soil $^{15}\text{NO}_3^-$ were found in the FL fraction in the clean rain plot. The recovery of soil $^{15}\text{NH}_4^+$ and $^{15}\text{NO}_3^-$ in the FL fraction was 79% and 73% in the roof control plot, respectively. Recoveries of atmospheric N retained in the 0-5 cm mineral soil layer in density fractions were influenced by N forms and long-term reduced atmospheric N deposition. In the roof control plot, the FL fraction from the 0-5 cm mineral soil layer accounted for a larger proportion of soil $^{15}\text{NO}_3^-$ (36%) than soil $^{15}\text{NH}_4^+$ (21%). The recovery of soil $^{15}\text{NH}_4^+$ in the occlude fractions was conversely higher (46%) than that of soil $^{15}\text{NO}_3^-$ (21%). The DF had a greater contribution to the retention of soil $^{15}\text{NH}_4^+$ (27%) than to that of soil $^{15}\text{NO}_3^-$ (7%). In the clean rain plot, the FL fraction, the occluded fractions and the DF from the 0-5 cm mineral soil layer retained 20%, 20% and 35% of soil $^{15}\text{NO}_3^-$, respectively. In the 5-10 cm mineral soil layer, the retention of atmospheric N in density fractions was affected neither by N forms nor by long-term reduced atmospheric N deposition. The recovery of soil $^{15}\text{NH}_4^+$ and $^{15}\text{NO}_3^-$ in the FL fraction, the occluded fractions and the DF fraction was 23-33%, 17-22% and 35-64% in the clean rain and the roof control plot, respectively. These results indicated that the stability of atmospheric N retained in the soil increases with soil depth. Atmospheric ammonium retained in the most upper mineral soil layer is more stable than atmospheric nitrate under ambient atmospheric N deposition. Long-term reduced atmospheric N deposition increases mainly the stability of atmospheric nitrate retained in the most upper mineral soil layer.

8 Zusammenfassung

Anthropogene Aktivitäten haben im letzten Jahrhundert zur deutlichen Veränderung des weltweiten Stickstoffkreislaufs sowie zur drastischen Steigerung der Stickstoffeinträge in zahlreichen terrestrischen Ökosystemen geführt. Nachgewiesene Folgen für Waldökosysteme der gemäßigten Zonen sind u.a. die Veränderung der Produktivität, die Beeinflussung von Bodenchemie und Sickerwasserqualität sowie eine Veränderung der Zusammensetzung von Pflanzengesellschaften. Der in Waldökosysteme eingetragene Stickstoff kann entweder von der Waldvegetation direkt aufgenommen oder von Böden und Bodenmikroorganismen absorbiert bzw. immobilisiert werden. Überschüssiger Stickstoff wird als Nitrat mit dem Sickerwasser ausgewaschen oder verlässt gasförmig das System. Die Rate der Festlegung des Stickstoffeintrags im Boden wird primär von der Stabilität der vorhandenen organischen Bodensubstanz beeinflusst. Insgesamt unterliegen in Zentraleuropa und Nordamerika bereits viele Wälder einer N-Sättigung, d. h. der im Überschuss vorhandene Stickstoff erscheint als Nitrat in der Bodenlösung unterhalb des Hauptwurzelsraums. Zur langfristigen Minderung dieser Problematik wird gefordert, die Stickstoffemissionen und damit auch die Stickstoffeinträge deutlich zu reduzieren. Dabei ist es von grundlegender Bedeutung zu wissen, wie bereits N-gesättigte Waldökosysteme auf einen langfristig reduzierten atmosphärischen Stickstoffeintrag reagieren. Das Hauptanliegen der vorliegenden Arbeit war es daher zu klären, wie eine längerfristig applizierte Reduktion des Stickstoffeintrags die Verteilung von deponiertem Ammonium und Nitrat in einem typischen Fichtenwaldökosystem beeinflusst. Dazu wurden zwei Hauptversuche durchgeführt, i) ein ^{15}N -Tracerversuch im Feld und ii) Laboruntersuchungen zur Charakterisierung der organischen Bodensubstanz mittels Dichtefraktionierung. Die wesentlichen Fragestellungen lauteten: 1.) Wie beeinflusst eine längerfristige Reduktion des Stickstoffeintrags die Verteilung von deponiertem Stickstoff in wesentlichen Kompartimenten von Bäumen, Böden und hinsichtlich der Auswaschung, und 2.) Welche Veränderungen ergeben sich bezüglich der Verteilung des im Boden festgelegten Stickstoffs auf unterschiedliche Pools der organischen Bodensubstanz.

Die vorliegende Arbeit wurde in einem heute 75-jährigen Fichtenreinbestand im Solling durchgeführt. Die atmosphärischen Einträge wurden durch eine Dachkonstruktion unterhalb des Kronendaches dauerhaft manipuliert. Dabei erhielt die Variante „Dach-Kontroll“-Fläche den nahezu unveränderten atmosphärischen Stickstoffeintrag der Umgebung mit Raten von $30 \text{ kg ha}^{-1} \text{ yr}^{-1}$ (Summe des Ammoniums und Nitrats), während die so genannte „Clean-Rain“-Fläche einen reduzierten atmosphärischen Stickstoffeintrag mit ca. $10 \text{ kg ha}^{-1} \text{ yr}^{-1}$ erhielt. Gleichzeitig wurden die jährlichen atmosphärischen Einträge von organisch gelöstem N (DON), Sulfat und Protonen auf der „Clean Rain“-Fläche im Vergleich zur „Dach-Kontroll“-Fläche jeweils um 27 %, 53 % und bzw. 77 % reduziert. Außer den

beiden Dach-Flächen diente eine Kontrollfläche ohne Dach als eine nicht-manipulierte Referenz. Nach 10-jähriger Reduktion des atmosphärischen Stickstoffeintrags wurden geringe Menge von hoch markiertem $^{15}\text{NH}_4\text{NO}_3$ und $\text{NH}_4^{15}\text{NO}_3$ getrennt in je einer Hälfte der „Clean-Rain“- und der „Dach-Kontroll“-Fläche für mehr als drei Jahre kontinuierlich zugegeben. Im Rahmen dieses ^{15}N -Tracerversuchs wurden Proben von Baumkompartimenten (Nadeln, Äste, Stammholz und -rinde, Feinwurzeln), verschiedenen Bodenhorizonten (organische Auflage, 0-5, 5-10, 10-20, 20-30, 30-40, 40-60 cm Mineralbodenhorizont) und vom Sickerwasser aus unterschiedlichen Bodentiefen (0, 10, 40, 100 cm Mineralbodentiefe) in jeder ^{15}N -markierten Teilfläche und in der Kontrollfläche genommen und bezüglich der C- und N-Konzentrationen sowie der ^{15}N -Abundanzen analysiert. Im Versuch zur Dichtefraktionierung wurden die organische Auflage und die oberen zwei Mineralbodenhorizonte in jeder ^{15}N -markierten Teilfläche jeweils in fünf Dichtefraktionen getrennt. Folgende Fraktionen wurden ausgeschieden: 1.) die „Freie leichte Fraktion“ (FL, $d < 1.6 \text{ g cm}^{-3}$), 2.) – 4.) drei „Okkludierte Fraktionen“ (Ocl. I, Ocl. II und Ocl. III, $d < 1.6 \text{ g cm}^{-3}$, $d = 1.6-1.8 \text{ g cm}^{-3}$ und $d = 1.8-2.0 \text{ g cm}^{-3}$) und 5.) die „Dichte Fraktion“ (DF, $d > 2.0 \text{ g cm}^{-3}$). In diesen Fraktionen wurden jeweils die organischen C-Gehalte, die N-Gesamtgehalte sowie die ^{15}N Abundanzen bestimmt. Zusätzlich wurden in einem Vorversuch die Aggregate mit zwei unterschiedlichen Analysemethoden (Ultraschall *versus* 16-h Schütteln mit Glasperle) zerstört. Untersucht wurden dabei die organische Auflage und der obere Mineralboden (0-5 cm) der ambienten Kontrollfläche. Weiterhin wurden Gleichungen für die Herstellung der Dichtelösung abgeleitet, indem unterschiedliche Verdünnungen des Dichtemittels (Natriumpolywolframat, SPT) eingesetzt wurden.

Die Ergebnisse aus dem ^{15}N -Tracerversuch zeigen, dass der Boden die größte Senke für eingetragenen atmosphärischen Stickstoff sowohl für die „Clean Rain“- als auch für die „Dach-Kontroll“-Fläche bildet. Im Betrachtungszeitraum wurden im Mittel 71 % des zugegebenen $^{15}\text{NH}_4^+$ im Boden in den zwei Flächen festgelegt. Mit 70 % auf der „Clean-Rain“-Fläche und 65 % auf der „Dach-Kontroll“-Fläche wurde in der organischen Auflage jeweils der größte Anteil des zugegebenen $^{15}\text{NH}_4^+$ gebunden. Die Wiederfindung des zugegebenen $^{15}\text{NO}_3^-$ im Boden stieg signifikant von 42 % auf der „Dach-Kontroll“-Fläche bis auf 68 % auf der „Clean-Rain“-Fläche an, wobei die Steigerung der Nitrat-Wiederfindung auf der „Clean-Rain“-Fläche hauptsächlich auf die Zunahme der Wiederfindung in der organischen Auflage zurückzuführen war (Steigerung von 8 auf 37 %). Dagegen wurden im Mineralboden unabhängig von den Behandlungen zwischen 31 und 34 % des eingetragenen Nitrats festgelegt. Die Waldbäume selbst lieferten einen relativ großen Beitrag zur Festlegung des eingetragenen Stickstoffs, nämlich 30-36 % des zugegebenen $^{15}\text{NH}_4^+$ und $^{15}\text{NO}_3^-$ auf der „Clean-Rain“- und der „Dach-Kontroll“-Fläche. Insgesamt wurde die Wiederfindung des zugegebenen ^{15}N in den Bäumen weder vom längerfristig reduzierten atmosphärischen Stickstoffein-

trag noch von den Formen des ^{15}N Tracers beeinflusst. Zwischen den Baumkompartimenten wurde der größte Anteil vom zugegebenen ^{15}N in den Nadeln festgelegt (15-19 %). Im verholzten Gewebe lag die Festlegung zwischen 7 und 13 %, in den lebenden Feinwurzeln zwischen 6 und 9 %. Die Nitratauswaschung trug zu 3 % zur Wiederfindung vom zugegebenen $^{15}\text{NH}_4^+$ und 19 % vom zugegebenen $^{15}\text{NO}_3^-$ auf der „Dach-Kontroll“-Fläche bei. Die Wiederfindung des zugegebenen $^{15}\text{NH}_4^+$ und $^{15}\text{NO}_3^-$ in der Nitratauswaschung sank jeweils auf 0 % und 2 % auf der „Clean-Rain“-Fläche. Auf beiden Flächen wurde jeweils nur weniger als 2 % des zugegebenen $^{15}\text{NH}_4^+$ und $^{15}\text{NO}_3^-$ in der Auswaschung der organisch gebundenen N-Fraktion (DON) wiedergefunden. Die Ergebnisse weisen darauf hin, dass sich der längerfristig reduzierte atmosphärische Stickstoffeintrag hauptsächlich auf die Verteilung des eingetragenen Nitrats auswirkt. Damit verringern sich insgesamt die Unterschiede zwischen der Verteilung von deponiertem Ammonium und Nitrat in wesentlichen Kompartimenten des untersuchten Fichtenwaldökosystems.

Hinsichtlich der Dichtefraktionierung ergaben sich folgende wesentliche Ergebnisse: In dem Vorversuch konnte gezeigt werden, dass die Volumenänderung der SPT-Lösung eine enge Korrelation mit der Menge des zugegebenen SPT aufweist ($y = 0.1863x$, $r^2 = 0.9993$). Damit konnten die Menge des SPT und das Volumen des Wassers für eine SPT-Lösung mit einem bestimmten Volumen und einer bestimmten Dichte kalkuliert werden. Dadurch reduzierte sich der Zeitaufwand bei der Herstellung der SPT-Lösung erheblich. Hinsichtlich der zwei verwendeten Methoden zur Zerstörung der Aggregate ergaben sich insgesamt keine signifikanten Unterschiede. Lediglich die Fraktion Ocl. I des oberen Mineralbodens zeigte nach der Ultraschallbehandlung einen signifikant größeren Beitrag bezüglich des N-Gesamtgehalts, im Vergleich zur Schüttelbehandlung.

Die Ergebnisse der Hauptuntersuchungen zur Dichtefraktionierung ergaben, dass das in der organischen Auflage festgelegte atmosphärische Ammonium und Nitrat vorwiegend in der FL-Fraktion wiederzufinden war. Auf der „Clean-Rain“-Fläche wurden 90 % des im Boden festgelegten $^{15}\text{NH}_4^+$ und 81 % des im Boden festgelegten $^{15}\text{NO}_3^-$ in der FL-Fraktion der organischen Auflage wiedergefunden. Auf der „Dach-Kontroll“-Fläche lag der entsprechende Wert für $^{15}\text{NH}_4^+$ bei 79 % und für $^{15}\text{NO}_3^-$ bei 73 %. Im oberen Mineralboden (0-5 cm) wurde die Wiederfindung des im Boden festgelegten atmosphärischen N in den Dichtefractionen sowohl von der N-Form als auch von der Eintragsreduktion beeinflusst. So wurden auf der „Dach-Kontroll“-Fläche 36 % des im Boden festgelegten $^{15}\text{NO}_3^-$ und nur 21 % des im Boden festgelegten $^{15}\text{NH}_4^+$ in der FL-Fraktion wiedergefunden. In den okkludierten Fraktionen dagegen lag die Wiederfindung des im Boden festgelegten $^{15}\text{NH}_4^+$ mit 46 % über der des im Boden festgelegten $^{15}\text{NO}_3^-$ (21 %). Auch für die DF-Fraktion des oberen Mineralbodens der „Dach-Kontroll“-Fläche wurde eine höhere Wiederfindung für das im Boden festgelegte $^{15}\text{NH}_4^+$ (27 %) als für das $^{15}\text{NO}_3^-$ (7 %) analysiert. Auf der „Clean-Rain“-Fläche ergab sich für die FL-,

die okkludierte und die DF-Fraktion eine Wiederfindung von jeweils 20 %, 20 % und 35 % für das im oberen Mineralboden festgelegte $^{15}\text{NO}_3^-$. In 5-10 cm Bodentiefe hatten die N-Form und die Eintragsreduktion keinen Einfluss auf die Wiederfindungen des im Boden festgelegten atmosphärischen N in den Dichtefraktionen. Die Wiederfindungen des im Boden festgelegten $^{15}\text{NH}_4^+$ und $^{15}\text{NO}_3^-$ auf beiden Untersuchungsflächen in der FL-, in den okkludierten und in der DF-Fraktion lagen jeweils bei 23-33 %, 17-22 % und 35-64 %. Die Ergebnisse weisen darauf hin, dass die Stabilität des im Boden festgelegten atmosphärischen N mit der Bodentiefe zunimmt. Dabei zeigt sich unter Stickstoffeinträgen aus der umgebenden Atmosphäre für das im Mineraloberboden festgelegte Ammonium eine größere Stabilität als für das Nitrat. Der längerfristig reduzierte atmosphärische Stickstoffeintrag steigert hauptsächlich die Stabilität des im Mineraloberboden festgelegten atmosphärischen Nitrats.

9 References

- Aber, J.D., Nadelhoffer, K.J., Steudler, P., Melillo, J.M., 1989. Nitrogen saturation in northern forest ecosystems. *BioScience* 39, 378-386
- Aber, J.D., Magill, A., Boone, R., 1993. Plant and soil responses to chronic nitrogen additions at the Harvard Forest, Massachusetts. *Ecological Application* 3, 156-166
- Aber, J., McDowell, W., Nadelhoffer, K., Magill, A., Berntson, G., Kamakea, M., McNulty, S., Currie, W., Rustad, L., Fernandez, I., 1998. Nitrogen saturation in temperate forest ecosystems: hypotheses revisited. *BioScience* 48, 921-934
- Ågren, G.I., Bosatta, E., 1988. Nitrogen saturation of terrestrial ecosystems. *Environmental Pollution* 54, 185-197
- Alewell, C., Manderscheid, B., Gerstberger, P., Matzner, E., 2000. Effects of reduced atmospheric deposition on soil solution chemistry and elemental contents of spruce needles in NE-Bavaria, Germany. *Journal of Plant Nutrition and Soil Science* 163, 509-516
- Azhar, E.S., Verhie, M., Proot, M., Sandra, P., Verstraete, W., 1986. Binding of nitrite-N on polyphenols during nitrification. *Plant and Soil* 94, 369-382
- Balesdent, J., Pétraud, J.-P., Feller, C. 1991. Effects des ultrasons sur la distribution granulométrique des matières organiques des sols. *Sci. Sol* 59, 95-106.
- Berg, B., Matzner, E., 1997. Effect of N deposition on decomposition of plant litter and soil organic matter in forest ecosystems. *Environmental Reviews* 5, 1-25
- Berntson, G.M., Aber, J.D., 2000. Fast nitrate immobilization in N saturated temperate forest soils. *Soil Biology and Biochemistry* 32, 151-156
- Binkley, D., Hart, S.C., 1989. The components of nitrogen availability assessments in forest soils. In: Stewart, B.A. (Ed.) *Advances in Soil Sciences* 10, 57-112
- Blanck, K., Lamersdorf, N., Bredemeier, M., 1993. Bodenchemie und Stoffhaushalt auf den Dachfläche in Solling. *Forstarchiv* 64, 164-172
- Bobbink, R., Hornung, M., Roelofs, J.G.M., 1998. The effects of air-borne nitrogen pollutants on species diversity in natural and semi-natural European vegetation. *Journal of Ecology* 86, 717-738
- Borken, W., Matzner, E., 2004. Nitrate leaching in German forest soils: An analysis of long-term monitoring sites. *Journal of Plant Nutrition and Soil Science* 167, 277-283
- Boxman, A.W., Van Dam, D., Van Dijk, H. F.G., Hogervorst, R.F., Koopmans, C.J., 1995. Ecosystem responses to reduced nitrogen and sulphur inputs into two coniferous forest stands in the Netherlands. *Forest Ecology and Management* 71, 7-29

- Bredemeier, M., Blanck, K., Lamersdorf, N., Wiedey, G.A., 1995. Response of soil water chemistry to experimental 'clean rain' in the NITRIX roof experiment at Solling, Germany. *Forest Ecology and Management* 71, 31-44
- Bredemeier, M., Blanck, K., Xu, Y.-J., Tietema, A., Boxman, A.W., Emmett, B., Moldan, F., Gundersen, P., Schleppei, P., Wright, R.F., 1998a. Input-output budgets at the NITREX sites. *Forest Ecology and Management* 101, 57-64
- Bredemeier, M., Blanck, K., Dohrenbusch, A., Lamersdorf, N., Meyer, A.C., Murach, D., Parth, A., Xu, Y.-J., 1998b. The solling roof project – site characteristics, experiments and results. *Forest Ecology and Management* 101, 281-293
- Brumme, R., Beese, F., 1992. Effects of Liming and Nitrogen Fertilization on Emissions of CO₂ and N₂O from a Temperate Forest. *Journal of Geophysical Research-Atmospheres* 97 (D12), 12851-12858
- Buchmann, N., Gebauer, G., Schulze, E.D., 1996. Partitioning of ¹⁵N-labeled ammonium and nitrate among soil, litter, below- and above-ground biomass of trees and understory in a 15-year-old *Picea abies* plantation. *Biogeochemistry* 33, 1-23
- Butterbach-Bahl, K., Gasche, R., Huber, C.H., Kreutzer, K., Papen, H., 1998. Impact of N-input by wet deposition on N-trace gas fluxes and CH₄-oxidation in spruce forest ecosystems of the temperate zone in Europe. *Atmospheric Environment* 32, 559-564
- Cabrera, M.L., Beare, M.H., 1993. Alkaline persulfate oxidation for determining total nitrogen in microbial biomass extracts. *Soil Science Society of American Journal* 57, 1007-1012
- Christensen, B.T., 1992. Physical fractionation of soil and organic matter in primary particle size and density separates. *Advances in Agronomy* 20, 1-90
- Compton, J.E., Boone, R.D., 2002. Soil nitrogen transformations and the role of light fraction organic matter in forest soils. *Soil Biology and Biochemistry* 34, 933-943
- Corre, M., Beese, F., Brumme, R., 2003. Soil nitrogen cycle in high nitrogen deposition forest: changes under nitrogen saturation and liming. *Ecological Application* 13, 287-298
- Corre, M.D., Lamersdorf, N.P., 2004. Reversal of nitrogen saturation after long-term deposition reduction: impact on soil nitrogen cycling. *Ecology* 85, 3090-3104
- Crow, S.E., Swanston, C.W., Lajtha, K., Brooks, J.R., Keirstead, H., 2007. Density fractionation of forest soils: methodological questions and interpretation of incubation results and turnover time in an ecosystem context. *Biogeochemistry* 85, 69-90
- Davidson, E.A., Hart, S.C., Shanks, C.A., Firestone, M.K., 1991. Measuring gross nitrogen mineralization, immobilization, and nitrification by ¹⁵N isotopic pool dilution in intact soil cores. *Journal of Soil Science* 42, 335-349

- Dise, N.B., Wright, R.F., (Editors) 1992. The NITREX project (NITROgen saturation Experiment) Ecosystems Research. Report 2, Commission of the European Communities, Brussel, pp 101
- Dohrenbusch, A., Grote, R., Fritz, H.W., 1993. Struktur und Wachstum eines Fichtenbestandes unter experimenteller Manipulation der Stoffeinträge. *Forstarchiv* 64, 172-177
- Dohrenbusch, A., Jaehne, S., Fritz, H.W., 2002. Vitality and nutrient level of Norway spruce trees under changed environmental conditions. In: Dohrenbusch, A., Bartsch, N. (Eds.) *Forest Development Succession, Environmental Stress and Forest Management: Case studies*. Springer, Berlin Heidelberg, 93-108
- Emmett, B.A., Brittain, S.A., Hughes, S., Kennedy, V., 1995. Nitrogen additions (NaNO_3 and NH_4NO_3) at Aber forest, Wales: I. Response of trees and soil nitrogen transformations. *Forest Ecology and Management* 71, 61-74
- Emmett, A., Kjonaas, O.J., Gundersen, P., Koopmans, C., Tietema, A., Selp, D., 1998a. Natural abundance of ^{15}N in forests across a nitrogen deposition gradient. *Forest Ecology and Management* 101, 9-18
- Emmett, B.A., Boxman, D., Bredemeier, M., Gundersen, P., Kjonaas, O.J., Moldan, F., Schleppi, P., Tietema, A., Wright, R.F., 1998b. Predicting the effects of atmospheric nitrogen deposition in conifer stands: evidence from the NITREX ecosystem-scale experiments. *Ecosystems* 1, 352-360
- Emmett, B.A., 1999. The impact of nitrogen on forest soils and feedbacks on tree growth. *Water, Air and Soil Pollution* 116, 65-74
- FAO STAT, 2000. FAO statistical Databases. <http://apps.fao.org>.
- Feddes, R.A., Kowalik, P.J., Neuman, S.P., Bresler, P., 1976. Finite and finite element simulation of field water uptake by plants. *Hydrological Sciences Bulletin* 21, 81-98
- Federer, C.A., Hornbeck, J.W., Tritton L.M., Martin, C.W., Pierce, R.S., Smith, C.T., 1989. Long-term depletion of calcium and other nutrients in eastern U.S. forests. *Environmental Management* 13, 593-601
- Fenn, M.E., Poth, M.A., Aber, J.D., Baron, J.S., Bormann, B.T., Johnson, D.W., Lemly, A.D., McNulty, S.G., Ryan, D.E., Stottleyer, R., 1998. Nitrogen excess in North American ecosystems: Predisposing factors, ecosystem responses, and management strategies. *Ecological Applications* 8, 706-733
- Galloway, J.N., Schlesinger, W.H., Levy II, H., Michaels, A., Schnoor, J.L., 1995. Nitrogen fixation: Anthropogenic enhancement – environmental response. *Global Biogeochemical Cycles* 9, 235-252
- Galloway, J.N., Cowling, E.B., 2002. Reactive nitrogen and the world: 200 years of change. *Ambio* 31, 64-71
- Garten Jr., C.T., Van Miegroet, H., 1994. Relationships between soil nitrogen dynamics and natural ^{15}N abundance in plant foliage from Great Smoky Mountains National Park. *Canadian Journal of Forest Research* 24, 1636-1645

- Gebauer, G., Schulze, E.D., 1991. Carbon and nitrogen isotope ratios in different compartments of a healthy and a declining *Picea abies* forest in the Fichtelgebirge, NE Bavaria. *Oecologia* 87, 198-207
- Gebauer, G., Zeller, B., Schmidt, G., May, C., Buchmann, N., Colin-Belgrand, M., Dambrine, E., Martin, F., Schulze, E.-D., Bottner, P., 2000. The fate of ^{15}N -labelled nitrogen inputs to coniferous and broadleaf forests. *Ecological Studies* 142, 144-170
- Golchin, A., Oades, J.M., Skjemstad, J.O., Clarke, P., 1994a. Study of Free and Occluded Particulate Organic Matter in Soils by Solid state ^{13}C CP/MAS NMR Spectroscopy and Scanning Electron Microscopy. *Soil Biology and Biochemistry* 32, 285-309
- Golchin, A., Oades, J.M., Skjemstad, J.O., Clarke, P., 1994b. Soil Structure and Carbon Cycling. *Soil Biology and Biochemistry* 32, 1043-68
- Golchin, A., Oades, J.M., Skjemstad, J.O., Clarke, P., 1995. Structural and dynamic properties of soil organic matter as reflected by ^{13}C natural abundance, pyrolysis mass spectrometry and solid-state ^{13}C NMR spectroscopy in density fractions of an Oxisol under forest and pasture. *Australian Journal of Soil Research* 33, 59-76
- Gundersen, P., 1998. Effects of enhance nitrogen deposition in a spruce forest at Klosterhede, Denmark, examined by moderate NH_4NO_3 addition. *Forest Ecology and Management* 101, 251-268
- Gundersen, P., Boxman, A.W., Lamersdorf, N., Moldan, F., Andersen, B.R., 1998. Experimental manipulation of forest ecosystems: lessons from large roof experiments. *Forest Ecology and Management* 101, 339-352
- Gutschick, V.P., 1981. Evolved strategies in nitrogen acquisition by plants. *American Naturalist* 118, 607-637
- Hart, S.C., Firestone, M.K., Paul, E.A., Smith, J.L., 1993. Flow and fate of soil nitrogen in an annual grassland and a young mixed-conifer forest. *Soil Biology and Biochemistry* 25, 431-442
- Hart, S.C., Stark, J.M., Davidson, E.A., Firestone, M.K., 1994. Nitrogen mineralization, immobilization and nitrification. In: Weaver, R.W., et al. (Eds.) *Methods of Soil Analysis, Part 2. Microbiological and Biochemical Properties: Soil Science Society of America Book Series No. 5*, Soil Science Society of America, Madison, WI, 985-1018
- Hart, S.C., Classen, A.T., 2003. Potential for assessing long-term dynamics in soil nitrogen availability from variations in $\delta^{15}\text{N}$ of tree rings. *Isotopes in Environmental and Health Studies* 39, 15-28
- Heinrichs, H., Brumsack, H.-J., Lofffield, N., Koenig, N., 1986. Verbessertes Druckaufschlusssystem für biologische anorganische Materialien. *Zeitschrift für Pflanzenernährung und Bodenkunde* 149, 350-353

- Helfrich, M., Ludwig, B., Buurman, P., Flessa, H., 2006. Effect of land use on the composition of soil organic matter in density and aggregate fractions as revealed by solid-state ^{13}C NMR spectroscopy. *Geoderma* 136, 331-341
- Heupel, G.M., 1989. Bodenkartierung der Sollingversuchsflächen Abt. 257. Univer. Manuskript, Institut für Bodenkunde und Waldernährung Göttingen
- Hoegberg, P., 1997. Tansley Review No.95: ^{15}N natural abundance in soil-plant systems. *New Phytologist* 137, 179-203
- Holland, E.A., Dentener, F.J., Braswell, B.H., Sulzman, J.M., 1999. Contemporary and pre-industrial global reactive nitrogen budgets. *Biogeochemistry* 46, 7-43
- Jachne, S., 2000. Auswirkungen eines Entsauerungs- und Austrocknungsversuchs auf Vitalität und Wachstum eines Fichtenaltbestandes (Dachprojekt im Solling). Dissertation. University Göttingen
- Jenkinson, D.S., 1981. The fate of plant and animal residues in soil. In Greenland, D.J., Hayes, M.H.B. (Eds.) *The chemistry of soil processes*. John Wiley and Sons Ltd. Chichester, 505-562
- Johannisson, C., 1996. ^{15}N abundance as an indicator of N-saturation of coniferous forest. Ph.D. thesis, SLU, Umeå, Sweden
- John, B., Yamashita, T., Ludwig, B., Flessa, B., 2005. Storage of organic carbon in aggregate and density fractions of silty soils under different types of land use. *Geoderma* 128, 63-79
- Johnson, D.W., 1992. Nitrogen retention in forest soils. *Journal of Environmental Quality* 21, 1-12
- Johnson, D.W., Cheng, W., Burke, I.C., 2000. Biotic and abiotic nitrogen retention in a variety of forest soils. *Soil Science Society of America Journal* 64, 1503-1514
- Kauppi, P.E., Mielikäinen, K., Kuusela, K., 1992. Biomass and carbon budget of European forests, 1971 to 1990. *Science* 256, 70-74
- Knigge, W., Schulz, H., 1966. *Grundriss der Forstbenutzung – Entstehung, Eigenschaften, Verwertung und Verwendung des Holzes und anderer Forstprodukte*. Paul Parey, Hamburg und Berlin
- Kögel-Knabner, I., Ekschmitt, K., Flessa, H., Guggenberger, G., Matzner, E., Marschner, B., von Lütow, M., 2008. An integrative approach of organic matter stabilization in temperate soils: Linking chemistry, physics, and biology. *Journal of Plant Nutrition and Soil Science* 171, 5-13
- Koopmans, C.J., Tietema, A., Boxman, A.W., 1996. The fate of ^{15}N enriched throughfall in two coniferous forest stands at different nitrogen deposition levels. *Biogeochemistry* 34, 19-44
- Krosshavn, M., Southon, T.E., Steinnes, E., 1992. The influence of vegetational origin and degree of humification of organic soils on their chemical composition determined by solid-state ^{13}C NMR. *Journal of Soil Science* 43, 485-493

- Lamersdorf, N., Beier, C., Blank, K., Bredemeier, M., Cummins, T., Farrell, E.P., Kreutzer, K., Rasmussen, L., Ryan, M., Weis, W., and Xu, Y.-J., 1998. Effect of drought experiments using roof installations on acidification/nitrification of soils. *Forest Ecology and Management* 101, 95-109
- Lamersdorf, N., Borcken, W., 2004. Clean rain promotes fine root growth and soil respiration in a Norway spruce forest. *Global Change Biology* 10, 1-12
- Lawrence, G.B., David, M.B., Shortle, W.C., 1995. A new mechanism of calcium loss in forest-floor soils. *Nature* 378, 162-165
- Lelieveld, J., Dentener, F., 2000. What controls tropospheric ozone? *Journal of Geophysical Research* 105, 3531-3551
- Levy II, H., Klonecki, A.A., Kasibhatla, P.S., 1999. Simulated tropospheric NO_x: Its evaluation, global distribution and individual source contributions. *Journal of Geophysical Research* 104, 26 279-26 3606
- Likens, G.E., Driscoll, C.T., Buso, D.C., 1996. Long-term effects of acid rain: response and recovery of a forest ecosystem. *Science* 272, 244-246
- MacDonald, J.A., Dise, N.B., Matzner, E., Armbruster, M., Gundersen, P., Forsius, M., 2002. Nitrogen input together with ecosystem nitrogen enrichment predict nitrate leaching from European forest. *Global Change Biology* 8, 1028-1033
- Magill, A.H., Aber, J.D., Currie, W.S., Nadelhoffer, K.J., Martin, M.E., McDowell, W.H., Melillo, J.M., Steudler, P., 2004. Ecosystem response to 15 years of chronic nitrogen additions at the Harvard Forest LTER, Massachusetts, USA. *Forest Ecology and Management* 196, 7-28
- Manderscheid, B., Matzner, E., Meiwes, K.J., Xu, Y.-J., 1995. Long-term development of element budgets in a Norway spruce (*Picea abies* (L.) Karst.) forest of the German Solling area. *Water, Air and Soil Pollution* 79, 3-18
- Matson, P., Lohse, K.A., Hall, S.J., 2002. The globalization of nitrogen deposition: consequences for terrestrial ecosystems. *Ambio* 31, 113-119
- Matzner, E., Murach, D., 1995. Soil changes induced by air pollutant deposition and their implication for forests in central Europe. *Water, Air and Soil Pollution* 85, 63-76
- Matzner, E., 2004. Biogeochemistry of forested catchments in a changing environment: a German case study. *Ecological Studies* 172, Springer, Berlin.
- McNulty, S.G., Aber, J.D., McLellan, T.M., Katt, S.M., 1990. Nitrogen cycling in high elevation forests of the northeastern US in relation to nitrogen deposition. *Ambio* 19, 38-40
- McNulty, S.G., Aber, J.D., Boone, R.D., 1991. Spatial changes in forest floor and foliar chemistry of spruce-fir forests across New England. *Biogeochemistry* 14, 13-29
- McNulty, S.G., Aber, J.D., Newman, S.D., 1996. Nitrogen saturation in a high elevation New England spruce-fir stand. *Forest Ecology and Management* 84, 109-121

- Meesenburg, H., Meiwes, K.J., Rademacher, P., 1995. Long term trends in atmospheric deposition and seepage output in northwest German forest ecosystems. *Water, Air and Soil Pollution* 85, 611-616
- Meesenburg, H., Merino, A., Meiwes, K.J., Beese, F.O., 2004. Effects of long-term application of ammonium sulphate on nitrogen fluxes in a beech ecosystem at Solling, Germany. *Water, Air and Soil Pollution, Focus* 4, 415-426
- Melin, J., Nömmik, H., Lohm, U., Flower-Ellis, J., 1983. Fertilizer nitrogen budget in a Scots pine ecosystem attained by using root-isolated plots and ^{15}N tracer technique. *Plant and Soil* 74, 249-263
- Moldan, F., Hultberg, H., Nyström, U., Wright, R.F., 1995. Nitrogen saturation at Gårdsjön, southwest Sweden, induced by experimental addition of ammonium nitrate. *Forest Ecology and Management* 71, 89-98
- Monteith, J.J., Unsworth, J.L., 1990. *Principles of environmental physics*. Arnold, Paris
- Müller-Using, B., Rademacher, P., Buß, B., Auth, A., 2004. Bioelementenzug bei der Holznutzung in Rein- und Mischbeständen aus Buche und Fichte. Indikatoren und Strategien für eine nachhaltige, multifunktionelle Waldnutzung - Fallstudie Waldlandschaft Solling. Abschlussbericht 1999-2003 zum BMBF-Verbundforschungsvorhaben. Teil 2: Ausführliche Teilvorhabenberichte. Forschungszentrum Waldökosystem der Universität Göttingen, 81-109
- Nadelhoffer, K.J., Fry, B., 1994. Nitrogen isotope studies in forest ecosystems. In: Lajtha, K., Michener, R.H. (Eds.) *Stable isotopes in ecology and environmental science*. Blackwell Scientific Publications, Oxford, 22-44
- Nadelhoffer, K.J., Downs, M.R., Fry, B., Aber, J.D., Magill, A.H., Melillo J.M., 1995. The fate of ^{15}N -labelled nitrate additions to a northern hardwood forest in eastern Maine, USA. *Oecologia* 103, 292-301
- Nadelhoffer, K.J., Downs, M.R., Fry, B., 1999a. Sinks for ^{15}N -enriched additions to an oak forest and a red pine plantation. *Ecological Application* 9, 72-86.
- Nadelhoffer, K., Downs, M., Fry, B., Magill, A., Aber, J., 1999b. Controls on N retention and exports in a forested watershed. *Environmental Monitoring and Assessment* 55, 187-210
- Nadelhoffer, K.J., Colman, B.P., Currie, W.S., Magill, A., Aber, J.D., 2004. Decadal-scale fates of ^{15}N tracers added to oak and pine stands under ambient and elevated N inputs at the Harvard Forest (USA). *Forest Ecology and Management* 196, 89-107
- Nihlgård, B., 1985. The ammonium hypothesis: an additional explanation to the forest decline in Europe. *Ambio* 14, 2-8
- Nohrstedt, H-Ö, Sikström, U., Ring, E., Näsholm, T., Högberg, P., Persson, T., 1996. Nitrate in soil water in three Norway spruce stands in southwest Sweden as related to N-deposition and soil, stand and foliage properties. *Canadian Journal of Forest Research* 26, 836-848

- Nõmmik, H., Vahtras, K., 1982. Retention and fixation of ammonium and ammonia in soils. In: Stevenson, F.J. (Eds.) Nitrogen in agricultural soils. American Society of Agronomy, Madison, WI, 123-171
- Nõmmik, H., 1990. Application of ^{15}N as a tracer in studying fertiliser nitrogen transformations and recovery in coniferous ecosystems. In: Harrison, A.F., Ineson, P., Heal, O.W. (Eds.) Nutrient cycling in terrestrial ecosystems – field methods, application and interpretation. Elsevier Science Publishers LTD, London, 276-290
- Perakis, S.S., Hedin, L.O., 2001. Fluxes and fates of nitrogen in soil of an unpolluted old-growth temperate forest, Southern Chile. *Ecology* 82, 2245-2260
- Perakis, S.S., Compton, J.E., Hedin, L.O., 2005. Nitrogen retention across a gradient of ^{15}N additions to an unpolluted temperate forest soil in Chile. *Ecology* 86, 96-105
- Poirier, N., Sohi, S.P., John, L., Gaunt, J.L., Mahieuc, N., Randall, E.W., Powlson, D.S., Evershed, R.P., 2005. The chemical composition of measurable soil organic matter pools. *Organic Geochemistry* 36, 1174-1189
- Providoli, I., Bugmann, H., Siegwolf, R., Buchmann, N., Schleppei, P., 2005. Flow of deposited inorganic N in two Gleysol-dominated mountain catchments traced with $^{15}\text{NO}_3^-$ and $^{15}\text{NH}_4^+$. *Biogeochemistry* 76, 453-475
- Puhe, J., Ulrich, B., 2001. Global climate change and human impacts on forest ecosystems - Postglacial development, present situation, and future trends in Central Europe. *Ecological Studies* 143. Springer, Berlin
- Richards, L.A., 1931. Capillary conduction of liquids through porous mediums. *Physics* 1, 318-333
- Rovira, P., Vallejo, V.R., 2003. Physical protection and biochemical quality of organic matter in Mediterranean calcareous forest soils: a density fractionation approach. *Soil Biology and Biochemistry* 35, 245-261
- Sah, S.P., Lamersdorf, N., Brumme, R., 2008. Natural abundance of ^{15}N of a spruce forest ecosystem under acid rain and manipulated clean rain field conditions. *Journal of forest science* 54, 377-387
- Schleppei, P., Bucher-Wallin, L., Siegwolf, R., Saurer, M., Muller, N., Bucher, J.B., 1999. Simulation of increased nitrogen deposition to a montane forest ecosystem: partitioning of the added ^{15}N . *Water, Air and Soil Pollution* 116, 129-134
- Schmidt, J., Seiler, W., Conrad, R., 1988. Emission of nitrous oxide from temperate forest soils into the atmosphere. *Journal of Atmospheric Chemistry* 6, 95-115
- Schulze, E.D., 1989. Air pollution and forest decline in a spruce (*Picea abies*) forest. *Science* 244, 776-783
- Seitzinger, S.P., Kroeze, C., 1998. Global distribution of nitrous oxide production and N inputs in freshwater and coastal marine ecosystems. *Global Biogeochemistry Cycles* 12, 93-113

- Smil, V., 1999. Nitrogen in crop production: An account of global flows. *Global Biogeochemistry Cycles* 13, 647-662
- Smil, V., 2002. *Energy at the Crossroads*. The MIT Press, Cambridge, MA, pp 360
- Smith, C.J., Chalk, F.E., 1980. Gaseous nitrogen evolution during nitrification of ammonia fertilizer and nitrite transformations in soil. *Soil Science Society of America Journal* 44, 277-282
- Smolander, A., Kitunen, V., Mälkönen, E., 2001. Dissolved soil organic nitrogen and carbon in a Norway spruce stand and an adjacent clear-cut. *Biology and Fertility of Soils* 33, 190-196
- Sollins, P., Homann, P., Caldwell, B.A., 1996. Stabilisation and destabilisation of soil organic matter: mechanisms and controls. *Geoderma* 74, 65-105
- Spiecker, H., 1999. Overview of recent growth trends in European forest. *Water, Air and Soil Pollution* 116, 33-46
- Stark, J.M., Hart, S.C., 1996. Diffusion technique for preparing salt solutions, Kjeldahl digests, and persulfate digests for nitrogen-15 analysis. *Soil Science Society of American Journal* 60, 1846-1855
- Swanston, C., Homann, P.S., Caldwell, B.A., Myrold, D.D., Ganio, L., Sollins, P., 2004. Long-term effects of elevated nitrogen on forest soil organic matter stability. *Biogeochemistry* 70, 227-250
- Tamm, C.O., 1989. Comparative and experimental approaches to the study of acid deposition effects on soils as substrate for forest growth. *Ambio* 18, 184-191.
- Thorn, K.A., Mikita, M.A., 2000. Nitrite fixation by humic substances: nitrogen-15 nuclear magnetic resonance evidence for potential intermediates of chemodenitrification. *Soil Science Society of America Journal* 64, 568-582
- Tietema, A., Emmett, B.A., Gundersen, P., Kjonaas, O.J., Koopmans, C., 1998. The fate of ¹⁵N-labelled nitrogen deposition in coniferous forest ecosystems. *Forest Ecology and Management* 101, 19-27
- Van Aardenne, J.A., Dentener, F.J., Olivier, J.G.J., Goldewijk, C.G.M.K., Lelieveld, J., 2001. A 1 degree x 1 degree resolution dataset of historical anthropogenic trace gas emissions for the period 1890-1990. *Global Biogeochemical Cycles* 15, 909-928
- Van Breemen, N., van Dijk, H.F.G., 1988. Ecosystem effects of atmospheric deposition of nitrogen in the Netherlands. *Environmental Pollution* 54, 249-274
- Van Dijk, H.F.G., Roelofs, J.G.M., 1988. Effects of excessive ammonium deposition on the nutritional-status and condition of pine needles. *Physiologia plantarum* 73, 494-501
- Van Egmond, K., Bresser, T., Bouwman, L., 2002. The European nitrogen case. *Ambio* 31, 72-78.

- Vitousek, P., Matson, P., 1984. Mechanisms of nitrogen retention in forest ecosystems: a field experiment. *Science* 225, 51-52
- Vitousek, P., Matson, P., 1985. Disturbance, nitrogen availability, and nitrogen losses in an intensively managed loblolly pine plantation. *Ecology* 66, 1360-1376
- von Lützow, M., Kögel-Knabner, I., Ekschmitt, K., Matzner, E., Guggenberger, G., Marschner, B., Flessa, H., 2006. Stabilization of organic matter in temperate soils: mechanisms and their relevance under different soil conditions – a review. *European Journal of Soil Science* 57, 426-445
- von Lützow, M., Kögel-Knabner, I., Ekschmitt, K., Flessa, H., Guggenberger, G., Matzner, E., Marschner, B., 2007. SOM fractionation methods: Relevance to functional pools and to stabilization mechanisms. *Soil Biology and Biochemistry* 39, 2183-2207
- Wright, R.F., van Breemen, N., 1995. The NITREX project: an introduction. *Forest Ecology and Management* 71, 1-5.
- Wright, R.F., Rasmussen, L., 1998. Introduction to the NITREX and EXMAN projects. *Forest Ecology and Management* 101, 1-7
- Xu, Y.-J., Blanck, K., Bredemeier, M., Lamersdorf, N.P., 1998. Hydrochemical input-output budgets for a clean rain and drought experiment at Solling. *Forest Ecology and Management* 101, 295-306

10 Appendix

Table 10.1. C and N concentration of the organic layer and mineral soil layers in the ambient control plot, the clean rain and the roof control plot based on oven-dried level.

Soil layer	plot	C%	N%
O _{L+F+H}	ambient control	42.6	1.7
	clean rain	42.4	1.5
	roof control	37.4	1.5
0-5 cm	ambient control	7.5	0.2
	clean rain	8.3	0.3
	roof control	5.8	0.3
5-10 cm	ambient control	3.8	0.2
	clean rain	3.3	0.2
	roof control	3.9	0.2

Table 10.2. The relationship between the amounts of SPT added to 150 g water and the volume change of solution.

SPT (g)	volume of solution (ml)	corrected volume of solution (ml)	Δ vol. (ml)
0	152.0	150.0	0.0
25.05	157.0	154.9	4.9
50.09	162.0	159.9	9.9
75.17	167.0	164.8	14.8
100.17	171.0	168.8	18.8
125.17	176.0	173.7	23.7
150.16	180.0	177.6	27.6
175.18	184.5	182.1	32.1
200.25	190.0	187.5	37.5
225.31	194.5	191.9	41.9
244.29	198.0	195.4	45.4

Table 10.3. $\delta^{15}\text{N}$ excess (‰) of density fractions from the organic layer and the mineral soil layers in the clean rain and the roof control plot after $^{15}\text{NH}_4^+$ and $^{15}\text{NO}_3^-$ addition.

soil layer	fraction	clean rain		roof control	
		$^{15}\text{NH}_4^+$ subplot	$^{15}\text{NO}_3^-$ subplot	$^{15}\text{NH}_4^+$ subplot	$^{15}\text{NO}_3^-$ subplot
$\text{O}_{\text{L+FH}}$	FL	3.5	33.4	14.0	5.7
	Ocl.I	6.9	20.6	11.9	6.0
	Ocl. II	2.4	12.7	9.9	3.3
	Ocl. III	0.0	8.0	6.5	0.2
	DF	2.4	12.0	6.7	0.7
0-5 cm	FL		14.2	10.1	21.6
	Ocl.I		10.2	8.5	5.1
	Ocl. II		7.2	6.1	4.1
	Ocl. III		4.0	4.4	2.8
	DF		2.1	2.3	0.8
5-10 cm	FL		18.4	18.1	43.6
	Ocl.I		7.5	31.9	32.4
	Ocl. II		4.2	9.1	12.3
	Ocl. III		3.7	5.7	6.5
	DF		1.9	3.7	4.1

FL = free light fraction ($d < 1.6 \text{ g cm}^{-3}$), Ocl. = occluded fraction (Ocl. I $d < 1.6 \text{ g cm}^{-3}$, Ocl. II $d = 1.6-1.8 \text{ g cm}^{-3}$, Ocl. III $d = 1.8-2.0 \text{ g cm}^{-3}$), DF = dense fraction ($d > 2.0 \text{ g cm}^{-3}$).

Lebenslauf

Familiennamen: Feng
Vorname: Zhuo
Geburtsdatum: 07.08.1972
Geburtsort: Hunan, V.R.China
Staatsangehörigkeit: China

09.1989-06.1993 Studium der Forstwissenschaft an der Forstwissenschaftlichen Universität Mitte-Süd
Bachelor-Abschluss

07.1993-11.1997 Tätigkeit bei der Forstverwaltung Hainan für Technologie Popularisierung

12.1997-03.1999 Tätigkeit im GTZ-Projekt Büro (Hainan) für Waldbau und Soziale Forstwirtschaft

04.1999-09.1999 Besuch eines Sprachkurses am Goethe-Institut in Göttingen

10.1999-03.2002 Studium der Forstwirtschaft in den Tropen und Subtropen an der Universität Göttingen
Magister-Abschluss

08.2002-06.2009 Promotion an der Fakultät für Forstwissenschaft und Waldökologie der Universität Göttingen

In the past century, anthropogenic activities have increased N input drastically to terrestrial ecosystems and influenced the global N cycle. Especially temperate forest ecosystems are affected in their productivity, species composition, soil chemistry and water quality. N input to forest ecosystems is retained in trees and soil. Excessive N is leached out or released as gases. The retention of N input in soils is mainly influenced by the stability of soil organic matter (SOM). Many forests in central Europe and North America have been subjected to N saturation, i.e. excessive N appeared as nitrate in the leachate below the rooting zone. Reduction of atmospheric N emission and consequent atmospheric N deposition is proposed to be the only practical long-term solution to improve N-saturated forest ecosystems. However, responses of N-saturated forest ecosystems to reduced atmospheric N deposition have been seldom investigated. In the present study, atmospheric deposition was manipulated through roof constructions below the canopy of a mature Norway spruce forest on the Solling plateau in central Germany. A ^{15}N tracer field and a density fractionation laboratory experiment were conducted in the present study to investigate the influence of long-term reduced atmospheric N deposition on the partitioning of atmospheric N in different forest ecosystem compartments as well as on the partitioning of atmospheric N retained in the soil in different SOM pools.